Journal of
*Experimental and Theoretical Analyses*

MDPI

*Review*

# Integrated Experimental–Theoretical and Data-Driven Multiphysics Analysis of Material Properties in Coatings, Pretreatments, Interfaces, and Artificial Intelligence-Assisted Reliability for Medical and Biomedical Devices

**Marshall Shuai Yang [1,*] and Chengqian Xian [2,*]**

[1] Department of Chemistry, Western University, London, ON N6A 5B7, Canada
[2] Department of Statistical and Actuarial Sciences, Western University, London, ON N6A 5B7, Canada
* Correspondence: marshall.yang@uwo.ca (M.S.Y.); cxian3@uwo.ca (C.X.)

**Abstract**

Surface engineering strongly influences the performance, reliability, and safety of medical and biomedical devices, yet failures often originate at interfaces rather than in bulk materials alone. This review addresses the fragmented evidence base linking coating selection, interphase design, qualification testing, advanced characterization, and data-driven durability analysis. The objective is to provide an integrative, failure-mode-based framework for implants, reusable instruments, inhalation systems, diagnostics, wearables, and implantable electronics. A narrative synthesis of the peer-reviewed literature in coatings, biomaterials, electrochemistry, reliability, standards, and materials informatics was conducted, with qualitative tables used only when protocols were too heterogeneous for numerical pooling. The review compares physical vapor deposition (PVD), chemical and plasma-enhanced chemical vapor deposition (CVD/PECVD), atomic layer deposition (ALD), sol–gel/organically modified silica (ORMOSIL) hybrids, plasma polymers, parylene, bioactive or antimicrobial surfaces, and electronic encapsulation strategies. The main finding is that no universally superior coating exists; reliable performance depends on matching architecture and characterization to the dominant failure pathway, substrate compliance, geometry, sterilization or physiologic exposure, and the standards-constrained endpoint. The review further shows how electrochemical diagnostics, interfacial mechanics, multiphysics models, survival/reliability statistics, and carefully governed AI workflows can be combined to support service-life prediction and decision-oriented qualification.

**Keywords:** coatings; pretreatments; adhesion; characterization; thin film; sterilization; reliability

Check for updates

Academic Editor: Marco Rossi

Received: 1 March 2026
Revised: 1 June 2026
Accepted: 4 June 2026
Published: 15 June 2026

**Copyright:** © 2026 by the authors. Licensee MDPI, Basel, Switzerland. This article is an open access article distributed under the terms and conditions of the Creative Commons Attribution (CC BY) license.

## 1. Introduction

Medical and biomedical devices rely on engineered surfaces and interfaces, where material properties often determine system performance. Coatings, primers, hybrid layers, inorganic films, and encapsulants influence resistance to corrosion, humidity, wear, chemical exposure, sterilization, and mechanical fatigue [1]. Unlike general industrial parts, medical devices endure repeated sterilization cycles [2], exposure to bodily fluids, aggressive cleaning agents, condensation from inhalation vapor, electromechanical vibration, and long-term implant conditions [3]. These challenges require a detailed understanding of the microstructure, chemistry, mechanical behavior, dielectric response, and environmental stability of both the coating and the interphase. Because modern devices combine polymers,

metals, thin films, flexible electronics, and multi-material assemblies, material selection must be linked to predictive models of interfacial behavior and degradation.

### 1.1. The Clinical Imperative

Advanced coatings and interface engineering are driven by persistent clinical and reliability challenges. In implantable devices, surface degradation, poor osseointegration, and wear can lead to loosening or failure, potentially requiring invasive revision surgery. Two major threats to long-term success are infection [4], often associated with biofilm formation [5], and adverse host responses, such as chronic inflammation or fibrous encapsulation [6,7]. Many structural substrates (e.g., stainless steel or titanium alloys) are mechanically suitable but biologically inert; coatings and specially designed surface architectures are therefore used to promote stable tissue-implant bonding, control protein adsorption and cell attachment, and add antimicrobial or drug-delivery functions while maintaining mechanical integrity [6].

### 1.2. Distinguishing Between Medical and Biomedical Device Environments

In this review, "medical devices" broadly refer to instruments and systems used for diagnosis, monitoring, or treatment whose primary action is not achieved through chemical means within the body (e.g., surgical tools, diagnostic cartridges, inhalation systems, and wearable sensors). For these systems, surface durability, sterilizability, condensation control, and chemical resistance often take precedence [2]. "Biomedical devices" refer to systems with greater biological integration and longer in vivo exposure (e.g., orthopedic and dental implants, implantable sensors, and long-term catheters), where bioactivity, osseointegration, tribocorrosion resistance, and biofouling control are key design considerations [8,9]. Many modern products span both categories, such as implantable electronics and long-term biosensors, making an integrated, surface- and interface-focused reliability framework increasingly important.

### 1.3. Organization of the Review

The review is structured to connect (i) material classes and surface chemistries, (ii) coating and encapsulation technologies, (iii) pretreatments, adhesion mechanisms, and failure modes, (iv) characterization methods (mechanical, microstructural, chemical, dielectric, and electrochemical), and (v) multiphysics and data-driven approaches for prediction and optimization.

### 1.4. Literature Search and Compilation Methodology

This article was compiled as an integrative narrative review rather than a formal systematic review. Keyword combinations included medical device coating, biomedical coating, implant coating, pretreatment, adhesion, interphase, sterilization, electrochemical characterization, tribocorrosion, barrier encapsulation, parylene, atomic layer deposition (ALD), plasma-enhanced chemical vapor deposition (PECVD), sol–gel, plasma polymer, multiphysics modeling, machine learning, artificial intelligence, reliability, and service life. Most of the literature was selected from 2010 to 2026; earlier mechanistic papers and foundational standards were retained as needed to interpret coating behavior, electrochemistry, adhesion mechanics, or qualification logic.

Because the literature spans implants, reusable instruments, electronics packaging, and surface-functional biomaterials, the review was organized around failure questions rather than a single device class. Priority was given to peer-reviewed studies and standards that linked processing to measurable interfacial, chemical, microstructural, electrochemical, mechanical, dielectric, or biological endpoints in realistic environments, such as physiologic media, humidity, cleaning and sterilization cycles, wear, or electrical bias. Exclusions

included papers focused solely on device-level clinical workflow, pharmacology without surface/interface relevance, or biological mechanisms not connected to material-surface behavior. Standards and standard-like documents were included when they constrained endpoint definitions, test conditions, terminology, or risk-management logic.

When both general materials-methods sources and medical or biomedical sources were available, medical and biomedical literature was prioritized in the cited evidence; broader non-biomedical references were retained only when they provided foundational mechanics, electrochemical methods, statistics, reliability, standards, or process-physics support not adequately covered by domain-specific sources.

The qualitative comparison tables were compiled as literature syntheses rather than as meta-analytic rankings: the symbol assignments summarize recurring directional trends across the cited sources and are not intended to imply universally transferable quantitative performance. This approach broadens applicability but also imposes limits. Evidence density is uneven across device classes, protocols are heterogeneous, and direct numerical pooling is often unjustified; accordingly, the review emphasizes mechanism-based interpretation and qualification logic rather than pooled effect estimates.

### *1.5. Purpose and Objective of This Review*

Surface-engineered medical and biomedical devices operate at the intersection of (i) complex environments, including physiologic fluids, disinfectants/cleaners, lubricants, and sterilants; (ii) heterogeneous assemblies comprising metals, polymers, ceramics, adhesives, and electronics; and (iii) regulated performance standards that emphasize safety, reliability, and verification. The literature is extensive yet fragmented across application areas. Implant-focused studies often highlight bioactivity, tribology, corrosion/tribocorrosion, and osseointegration, whereas medical electronics and instruments focus on barrier integrity, dielectric stability, and manufacturable encapsulation methods. High-quality reviews are available for hard, wear-resistant coatings such as diamond-like carbon (DLC) [10], parylene-based biomedical coatings and their functionalization [11], and atomic layer deposition (ALD) as a basis for conformal ultrathin oxide barriers [12]. Still, cross-domain guidance linking coating choices to standards-based qualification, failure physics, and manufacturable process windows remains limited.

#### 1.5.1. What Prior Reviews Cover: Metallic Implants, Load-Bearing Tribology, and Bioactivity

For load-bearing metallic implants (e.g., Ti alloys, cobalt-chromium (CoCr) alloys, and stainless steels), the main themes in the literature include (a) reducing wear and ion leaching through hard coatings such as titanium nitride (TiN), chromium nitride (CrN), and diamond-like carbon (DLC); (b) degradation driven by electrochemical and tribocorrosion processes in protein-rich electrolytes; and (c) bioactive or osteogenic surface designs, including hydroxyapatite, bioactive glass, anodic oxides, and $TiO_2$ nanotube architectures. The reviews highlight that the combination of wear and corrosion can be the primary cause of in vivo degradation, making tribocorrosion testing and coating durability essential for performance claims [3]. More broadly, the implant surface-engineering literature increasingly supports multifunctional strategies that balance osseointegration, mechanical durability, and infection prevention within manufacturable coating systems.

#### 1.5.2. What Prior Reviews Include: Infection Control, Antifouling, and Blood Compatibility

A growing body of research focuses on device-associated infections and biofilms. Clinical and microbiologic reviews indicate that biofilm formation on implanted devices can lead to persistent infections and revision surgeries, prompting surface strategies that either kill microbes at the interface or reduce initial adhesion and conditioning-film formation [5].

From a materials perspective, the literature includes contact-killing coatings (e.g., quaternary ammonium or cationic chemistries), release-based systems (antibiotics, antiseptics, metal ions), and anti-adhesive or antifouling surfaces that form stable hydration layers. However, translating these approaches is often limited by coating durability under wear and sterilization, as well as by the need to maintain biocompatibility under International Organization for Standardization (ISO) 10993-1 [13] and to meet risk-managed performance claims under ISO 14971 [14].

Table 1 synthesizes these challenges in infection control, antifouling, osseointegration, tribocorrosion, and smart surfaces by distinguishing material root causes, clinical implications, and design or verification actions. Materials and biological assays are included in the table only as verification methods; detailed method selection is summarized later in Table 9.

**Table 1.** Major challenges and solution strategies for next-generation biomedical surfaces. The table highlights design actions and device-relevant verification endpoints. Analytical methods are listed only when they verify a design claim; detailed method selection is summarized separately in Table 9. Abbreviations: FE, finite element; FTIR, Fourier-transform infrared spectroscopy; ML, machine learning; SEM, scanning electron microscopy; Ti, titanium; ToF-SIMS, time-of-flight secondary ion mass spectrometry; XPS, X-ray photoelectron spectroscopy.

| Challenge | Root Cause | Implication | Design and Verification Focus |
| --- | --- | --- | --- |
| Antifouling stability | Hydration-layer collapse, degrafting, or fouling reduces low-fouling performance [15]. | Conditioning-film formation can progress to biofilm-related device infection [6]. | Use anchored or crosslinked hydrated chemistries [15]. After aging, verify protein adsorption, bacterial adhesion, or biofilm behavior with device-relevant assays [6]. Confirm surface chemistry claims [16]. |
| Antimicrobial efficacy and safety | Active agents can deplete or release at subtherapeutic levels [17]. Silver nanoparticles can create cytotoxicity/genotoxicity concerns [18]. | Biofilms can cause chronic infection and revision risk [5]. | Use controlled release for short high-risk windows [17]. Use contact-active or antimicrobial-peptide coatings for sustained surfaces [19]. Verify antimicrobial activity, release kinetics, cytotoxicity, extractables/leachables, and surface-bound chemistry by XPS/FTIR/ToF-SIMS when chemistry claims are made [16,20]. |
| Osseointegration versus bacterial retention | Micro/nano-roughness and porous oxides can support bone integration but may also increase bacterial retention [21]. | Poor integration can cause loosening; bacterial colonization can cause persistent infection [6]. | Use multifunctional Ti surfaces that combine osteogenic topography with infection-control chemistry [22]. Verify bone-cell response, bacterial adhesion, ion release, coating adhesion after aging, and topography/chemistry stability with imaging as needed [21]. |
| Wear, corrosion, and tribocorrosion | Combined wear-corrosion can dominate in load-bearing implants [3]. Hard coatings reduce wear but can fail due to stress, defects, or delamination [23]. | Wear debris, ion release, delamination, and fretting/tribocorrosion can limit implant lifetime. | Use graded or multilayer hard coatings and adhesion layers. Verify with combined wear-corrosion testing rather than dry wear alone [3]. Use post-test SEM/XPS and ion release analysis to identify wear-through, oxide damage, and corrosion products [24,25]. |

**Table 1.** *Cont.*

| Challenge | Root Cause | Implication | Design and Verification Focus |
| --- | --- | --- | --- |
| Smart and data-driven design | Responsive additives can introduce drift or mechanical trade-offs; sparse datasets can overfit. | Failure can appear as loss of response, uncontrolled release, delamination, or unreliable service-life prediction. | Use ML to prioritize antifouling candidates when descriptors are defined [26]. Use impedance-based ML only when features are linked to degradation [27]. Validate FE-derived surrogate models before optimization [28]. Use surface analyses and biological assay outputs as traceable features rather than unverified model inputs [29]. |

#### 1.5.3. What Prior Reviews Cover: Thin-Film Encapsulation for Implantable and Wearable Electronics

Parallel streams of literature address encapsulation and packaging for implantable and wearable electronics. Parylene C remains a benchmark conformal coating for its biocompatibility and processability, and dedicated reviews summarize approaches to enhance parylene's barrier properties, surface chemistry, and anti-infection performance [11]. However, long-term reliability issues, such as moisture permeation, loss of interfacial adhesion, and defect-driven leakage, have driven the development of hybrid stacks that combine organic toughness with inorganic diffusion barriers. Atomic layer deposition (ALD) [12] is widely recognized for producing conformal ultrathin oxides with precise thickness control [30] and is a core component of multilayer barrier designs used in both electronics and emerging biomedical encapsulation applications.

#### 1.5.4. Persistent Gap: Connecting Standards-Based Qualifications, Failure Physics, and Data-Driven Design

A major gap is not merely the lack of additional coating studies but the absence of a common evidentiary chain linking coating architecture to failure physics, standards-based qualification, and model-supported decision-making. In many subfields, processing, characterization, electrochemistry, and biological testing are still reported as parallel work packages rather than as a single integrated argument. As a result, a coating may appear promising based on coupon-scale barrier metrics yet remain weakly justified with respect to delamination, defect statistics, sterilization damage, tribocorrosion, or device-level risk control.

This disconnect is especially evident where standards-based endpoints and mechanistic interpretation should converge. Electrochemical evaluation is commonly used to measure corrosion potential, barrier breakdown, and ion release behavior using complementary methods such as open circuit monitoring, polarization tests [31], galvanic/noise monitoring, transient holds, and localized probes [24,32,33]. However, these datasets are still too rarely explicitly linked to mechanical failure modes, sterilization-driven aging, or design-of-experiments logic. Meanwhile, machine learning [26,28] and physics-informed modeling [34] are beginning to accelerate materials discovery and process optimization across broader fields of materials science and biomedical coatings. Yet adoption in biomedical coating qualification remains limited unless the features, endpoints, and uncertainty statements can be traced back to realistic failure questions.

This review consolidates coating technologies, including physical vapor deposition (PVD), chemical vapor deposition (CVD), atomic layer deposition (ALD), sol–gel, and plasma–polymer approaches, along with surface pretreatments, coupling chemistries, application-driven failure modes, and qualification testing, into a unified engineering

narrative covering both medical devices (instruments, sensors, reusable systems) and biomedical devices (implants and long-term tissue-contacting systems). It provides an evidence-based decision framework, grounded in current literature and standards, to support reliable material selection, process design, and reliability assessment across device classes.

### *1.6. Medical vs. Biomedical Comparison*

Although medical and biomedical devices share many materials and coating technologies, their primary reliability factors differ because the exposure environment, tissue contact duration, sterilization route [2], mechanical loading [3], and electrical operating conditions [11] vary across device classes [13,14].

When evidence is compared across device classes and highly variable protocols, the synthesis should specify the search scope, eligibility criteria, and the major sources of heterogeneity. When quantitative pooling is not justified, it is better to explain why studies are not directly comparable than to over-interpret isolated single-study results [35].

For many medical devices, including diagnostic platforms, reusable instruments, inhalers, and wearables, the main surface- and interface-reliability challenges include repeated cleaning, disinfection, and sterilization/reprocessing [2,36,37], humid or condensing environments and biofluid/sweat exposure [38,39], mechanical deformation and motion-related loading in wearable or portable systems, and dielectric or leakage-current stability for embedded electronics and patient-contacting electrical systems [30,40,41].

For many biomedical devices, including long-term implants and implantable sensors, continuous or prolonged exposure to physiological fluids can drive tribocorrosion and wear-corrosion coupling in load-bearing metallic implants [3], fretting or mechanically assisted interfacial degradation at modular or contacting interfaces [3], biofilm formation and biofouling on implanted-device surfaces [5], biologically mediated degradation or adverse host response at the tissue–material interface [6], and mechanical fatigue or adhesion loss under long-term cyclic service. As a result, biomedical coatings often prioritize bioactivity and osseointegration [7], antimicrobial or anti-infective performance [6], and antifouling control through stable hydration layers or low-fouling surface chemistries [15]. By contrast, many non-implantable medical-device coatings emphasize chemical resistance, sterilization durability, and protection of embedded electronics. The growing use of implantable sensors and wearable or miniaturized electronics makes hybrid requirements increasingly common, so coating selection often must combine biological performance with dielectric stability, moisture-barrier integrity, and long-term encapsulation reliability [30,40,41].

### *1.7. Scope*

This review covers:

- Material systems such as metals/alloys, polymers, ceramics, and electronic materials.
- Coating and thin film technologies (PVD, CVD/PECVD, ALD, sol–gel/ORMOSIL hybrids, plasma polymers, and bioactive/functional coatings).
- Pretreatments and primers (both inorganic and organic) that promote strong adhesion to metals and polymers.
- Adhesion mechanisms, interphase chemistry, and multi-material interface engineering (including graded and hybrid stacks).
- Failure modes under service conditions (mechanical, chemical, electrochemical, environmental, and dielectric).
- Characterization approaches include mechanical, microstructural, chemical, dielectric, thermal/environmental, and electrochemical methods, with guidance on selecting methods based on failure mode and endpoint.

- Standards and regulatory frameworks that influence qualification and verification (e.g., ISO 10993-1 [13], ISO 14971 [14], ISO 13485 [42], the International Electrotechnical Commission (IEC) 60601-1 [43], ISO 11135 [44], ISO 11137-1 [8], and ISO 17665 [9], and the IPC conformal coating document IPC-CC-830C [45]) are referenced when they constrain material selection, sterilization compatibility, electrical safety, quality system evidence, and reliability requirements.
- Multiphysics and data-driven modeling, including AI-assisted reliability and optimization.

And excludes:

- Device-level design, clinical pathways, and detailed biological mechanisms extend beyond material-surface interactions.

### *1.8. Unique Material-Property Requirements*

Medical and biomedical materials are subjected to combinations of environmental and operational loads that are uncommon in traditional engineering systems. Qualification, therefore, involves assessing not only the fundamental coating properties but also the stability of the coating-substrate interface under combined humidity, thermal, mechanical, chemical, and electrical conditions.

- Humidity, condensation, and biological fluids (water uptake, swelling, hydrolysis, ionic transport).
- Chemical disinfectants and sterilants (e.g., alcohols, oxidizers, and detergents) can cause residue-induced stress cracking in polymers.
- Sterilization processes include autoclaving, ethylene oxide (EtO), hydrogen peroxide ($H_2O_2$) plasma, and gamma irradiation.
- Mechanical cycling, impact, and vibration (including electromechanical actuation in inhalation and diagnostic modules).
- Temperature fluctuations and thermal gradients lead to residual stress, buckling, and cracking.
- Long-term aging (such as physical aging in polymers, corrosion or tribocorrosion in metals, and dielectric drift in encapsulants).
- Electrical loading in sensors and electronics, including leakage current, dielectric breakdown, and corrosion under bias.

These stressors rarely act in isolation. For example, moisture uptake can plasticize polymers while reducing dielectric resistance [46]; sterilization cycles can accelerate hydrothermal aging and trigger residual-stress-driven cracking in brittle inorganic films [47]; and mechanical flexing can create microcracks that provide rapid diffusion pathways for water and ions [48].

Material property assessment must therefore include (i) adhesion and mechanical mismatch, (ii) permeability and water uptake, (iii) residual stress and fracture resistance in thin films, (iv) electrochemical stability of metals and conductive pathways, and (v) sterilization durability of both structural and electronic protection layers. Table 2 summarizes typical sterilization compatibility trends for representative polymer coating systems.

**Table 2.** Sterilization resistance of representative polymer coating systems. Ratings are qualitative directional estimates based on the literature on polymer sterilization, aging, and coating reliability. Legend for qualitative ratings: ●●●●● = excellent compatibility; ●●●● = very good; ●●● = moderate; ●● = limited; ○-● = mixed outcomes depending on formulation and cycle conditions. Symbols represent directional literature syntheses, not pooled quantitative rankings. Abbreviations: ABS, acrylonitrile–butadiene–styrene; ALD, atomic layer deposition; EtO, ethylene oxide; PC, polycarbonate; PEEK, polyether ether ketone; PI, polyimide; $SiO_x$, silicon oxide or silicon oxide-like barrier; TPU, thermoplastic polyurethane.

| Material + Coating | Autoclave [9,49] | Gamma [8] | EtO [44] | Plasma/Low-Temperature Oxidative Sterilization [37,50] | Notes |
|---|---|---|---|---|---|
| PC + $SiO_x$ | ●●● | ●●●● | ●●●●● | ●●●● | PC can be sensitive to residual stress, environmental stress cracking, and aging/sterilization history [2,49,51]. |
| ABS + sol–gel | ●● | ●●● | ●●●●● | ●●● | Sol–gel coatings can be brittle if too thick; cure, residual porosity, and aging conditions affect durability [49,51,52]. |
| PI + ALD | ●●●●● | ●●●●● | ●●●●● | ●●●●● | PI and ALD-based dielectric stacks are relevant for stable electronic encapsulation [41,53]. |
| PEEK + hybrid ALD | ●●●●● | ●●●●● | ●●●●● | ●●●● | PEEK has strong thermal and chemical stability; hybrid ALD stacks can improve barrier reliability [41,53]. |
| TPU + plasma polymer | ○-● | ●● | ●●●● | ●●● | TPU performance is formulation-dependent; softening, swelling, and interfacial aging should be verified after conditioning [2,49]. |

## 2. Material Systems

Medical and biomedical devices often integrate multiple materials, including metals, polymers, ceramics, and electronics, so the relevant "material system" is typically an engineered stack rather than a single substrate. Because each material has distinct surface chemistry and failure modes, coating choices must account for substrate compatibility (Table 3), polymer/film modulus mismatch, primer selection, and failure-mode mitigation, as discussed in later sections.

**Table 3.** Coating–metal compatibility for representative biomedical metals. Ratings are qualitative starting points rather than universal rankings because compatibility depends on surface preparation, native oxide or passive-film chemistry, coating thickness, residual stress, geometry, sterilization history, corrosion/tribocorrosion environment, and biological endpoint. Legend: ●●●●● = excellent compatibility or adhesion with appropriate preparation; ●●●● = good; ●●● = moderate; ●● = limited. Abbreviations: 316L, low-carbon austenitic stainless steel; 316LVM, vacuum-melted medical-grade 316L stainless steel; ALD, atomic layer deposition; CoCr, cobalt–chromium alloy; CVD, chemical vapor deposition; MAO, microarc oxidation; Mg, magnesium; PECVD, plasma-enhanced chemical vapor deposition; PVD, physical vapor deposition; SS, stainless steel; Ti, titanium; Ti6Al4V, titanium–6 aluminum–4 vanadium alloy; Zn, zinc.

| Metal Substrate | PVD | PECVD/CVD | ALD | Sol–gel/MAO | Notes |
|---|---|---|---|---|---|
| Ti/Ti6Al4V | ●●●●● | ●●●● | ●●●●● | ●●●● | Oxide-forming Ti alloys generally support strong adhesion and are widely used with orthopedic surface-engineering strategies [54]. Hard coatings are relevant when wear and tribocorrosion are controlling risks [3]. Bioceramic or oxide-based coatings are useful when osseointegration is the primary endpoint [55]. |
| 316L/316LVM SS | ●●●● | ●●●● | ●●●● | ●●● | Stainless steels require careful activation, passivation control, and residue management because corrosion resistance depends on a stable passive film [56]. Electropolishing is especially relevant for stents and fine metallic components [57]. |
| CoCr alloys | ●●●●● | ●●●● | ●●●● | ●●● | CoCr alloys are strong candidates for hard wear-resistant coatings in joint-contact applications [23]. Because wear and corrosion can interact, tribocorrosion and ion release endpoints should be checked rather than relying on dry wear alone [54]. |
| Nitinol | ●●●● | ●●●● | ●●●● | ●●● | Nitinol compatibility is controlled by surface oxide stability and nickel-release risk, so surface modification should be verified with chemistry and ion release testing [54]. |
| Mg alloys | ●● | ●●● | ●●● | ●●●● | Mg is highly reactive, so conversion layers, sol–gel barriers, and MAO-type approaches are often more suitable than hard line-of-sight coatings [58]. Degradation models are useful because Mg performance depends strongly on local corrosion kinetics [34]. |
| Zn-based biodegradable alloys | ●● | ●●● | ●●● | ●●● | Zn-based biomaterials should be treated separately from Mg because their degradation kinetics and biological design space differ [59]. For additively manufactured Zn biomaterials, surface finishing and corrosion control remain important qualification issues [59]. |

### 2.1. Metals/Alloys

Common metallic substrates include 316L stainless steel, titanium and titanium alloys (e.g., Ti6Al4V), cobalt-chromium alloys, nickel-titanium (Nitinol), and, for bioresorbable concepts, magnesium alloys [24,56]. Metals form native oxides that influence surface energy, corrosion resistance, and bonding to coupling agents [56,60]. Stainless steel offers excellent manufacturability but limited inherent bioactivity; therefore, surface finishing, passivation control [61], PVD coatings [62], sol–gel hybrids [61], anodic or microarc-oxidized layers [63], and bioactive ceramic topcoats [55] are used to improve corrosion resistance, wear behavior, or tissue integration depending on the device endpoint [56]. Nitinol requires specific attention to nickel release and oxide stability [25], while magnesium alloys require barrier or conversion-layer strategies to manage rapid biodegradation, hydrogen evolution, and local alkalization [64,65]. Overall, reviews of metallic implants indicate that surface engineering and coatings must balance corrosion resistance, ion release control, mechanical durability, and biocompatibility, rather than optimizing any single property alone [54].

Beyond 316L, so-called high-performance stainless steels (HPSS) have been developed for aggressive chloride environments by increasing Cr and Mo and, in many grades, adding N. These alloying additions raise the pitting resistance equivalent number (PREN), commonly expressed as PREN = %Cr + 3.3(%Mo) + 16(%N), and enhance resistance to localized corrosion (pitting or crevice attack) and stress corrosion cracking. HPSS includes high-alloy austenitic and duplex families. While not routinely used for all implants, they are relevant for biomedical components and tools where chloride-driven pitting resistance is essential [64].

Beyond magnesium, zinc-based biodegradable metals are also emerging because their degradation kinetics can be more moderate and clinically manageable for certain temporary implants [66]. This makes surface finishing, barrier design, and corrosion monitoring especially important for future biodegradable-device concepts, even when the final device does not use a conventional long-life protective coating.

### 2.2. Polymers

Polymers are widely used for housings, fluidic components, adhesives, and flexible structures, including acrylonitrile–butadiene–styrene (ABS), polyamide (PA), polyimide (PI), polycarbonate (PC), polyether ether ketone (PEEK), thermoplastic polyurethane (TPU), polydimethylsiloxane (PDMS), and cyclic olefin copolymers (COC/COP). Polymer reliability is often governed by surface energy, moisture absorption, and resistance to solvents or sterilants. For instance, PA can absorb moisture and swell, PC may be prone to stress cracking, and low-surface-energy materials like PEEK typically require strong activation methods (e.g., plasma) and specially designed primers to ensure durable adhesion. Because polymers generally have a lower modulus than inorganic films, a mismatch in modulus and flexural stress can cause cracking or delamination (Table 4). Graded or hybrid interlayers are used to address this issue.

**Table 4.** Representative elastic modulus mismatch and qualitative failure risk for stiff inorganic/hard coatings on polymer substrates. Modulus values are approximate ranges compiled from polymer mechanical-property studies and the thin-film/coating nanoindentation literature; risk assignments are based on thin-film cracking, buckling, and delamination mechanics for stiff films on compliant substrates. Abbreviations: ABS, acrylonitrile–butadiene–styrene; ALD, atomic layer deposition; $Al_2O_3$, aluminum oxide/alumina; DLC, diamond-like carbon; E, elastic modulus; ORMOSIL, organically modified silicate; PA, polyamide; PC, polycarbonate; PECVD, plasma-enhanced chemical vapor deposition; PEEK, polyether ether ketone; PI, polyimide; $SiN_x$, silicon nitride-like film; $SiO_x$, silicon oxide-like film; TiN, titanium nitride.

| Polymer Substrate | Polymer E, GPa | Representative Stiff Coating | Coating E, GPa | Mismatch Risk | Main Failure Concern | Preferred Mitigation |
|---|---|---|---|---|---|---|
| ABS | ~1.8–2.5 [67] | DLC or TiN hard coating | DLC~60–250; TiN~100–600 [68] | High | Channel cracking, buckling, or delamination under bending or humidity aging [69] | Use plasma activation, flexible primer, or graded interlayer before hard coating [70]. |
| PA | ~1.5–3.5 [71] | ALD $Al_2O_3$ or other ALD oxide | ~150–250 [72] | High | Moisture-assisted swelling, debonding, and oxide cracking | Pre-dry the polymer; use plasma/silane activation and ultrathin or multilayer ALD rather than a thick brittle oxide [73]. |
| PC | ~2.3–2.5 [74] | PECVD $SiO_x$ or $SiN_x$ | ~50–90 [75] | Moderate | Crazing, channel cracks, or stress-driven film damage [76] | Use low-stress PECVD recipes and validate after thermal/humidity cycling [77]. |
| PI | ~2.5–3.0 [78,79] | ALD oxide or inorganic encapsulation layer | ~120–250 | Moderate | Microcracking during flexure or thermal cycling | Keep oxide layers ultrathin; use organic–inorganic multilayers for strain accommodation [53]. |
| PEEK, unfilled | ~3.6–4.0 [78] | Hybrid sol–gel or ORMOSIL-type coating | ~5–30 [80] | Moderate–High | Delamination, decohesion, or hydrolytic weakening | Use compliant hybrid sol–gel chemistry, surface activation, and controlled cure/thickness [52]. |

### *2.3. Ceramics and Inorganic Films*

Ceramics and inorganic thin films (e.g., alumina, titania, silica, silicon nitride, and other nitride/oxide dielectrics) serve as wear surfaces, diffusion barriers, and electrical insulators. Their high modulus and brittleness confer excellent hardness and barrier performance but also increase the risk of fracture on compliant polymer substrates unless thickness, residual stress, and interlayers are carefully controlled [23,77].

### 2.4. Hybrid Organic–Inorganic Materials

Hybrid organic–inorganic materials, especially sol–gel/ORMOSIL systems, enable adjustable combinations of hardness, flexibility, and chemical properties. They are commonly used as adhesion-promoting and barrier layers on metals and polymers and can also serve as carriers for functional additives (e.g., antimicrobial agents) when compatibility and leaching are controlled [81].

### 2.5. Electronics Materials

Electronics introduce additional material constraints, including copper conductors, gold finishes, solder joints, conductive adhesives, and polyimide flex circuits. In this context, coating systems must preserve dielectric integrity, prevent corrosion and dendritic growth under bias, and maintain adhesion during thermal cycling and vibration. These requirements lead to the use of conformal encapsulation strategies (Section 3.8) and the selection of electrochemical or dielectric diagnostics based on the primary failure mode (Section 4.5) [40].

## 3. Coating Technologies and Functional Architectures

Coatings on medical and biomedical devices serve two broad roles: first, to delay transport, corrosion, wear, or electrical leakage, as illustrated by tribocorrosion-resistant implant coatings [3], wear-resistant hard coatings for joint-contact applications [23], and ALD/polymer encapsulation for implantable electronics [41]. Second, coatings can impart biological or functional behavior, including osseointegration via bioactive ceramic or oxide surfaces [6,55], antimicrobial or anti-infective activity [6,82], antifouling performance through hydrated, low-fouling surfaces [15], and sensing or electronic protection in implantable/wearable systems [40]. In practice, these roles are not independent. The same architecture that improves barrier properties can increase residual stress or reduce flexibility in stiff film/polymer systems [83], alter protein adsorption and biological response [15], or complicate sterilization compatibility and post-aging adhesion [2]. Reliable systems are therefore rarely single films; they are engineered stacks that combine adhesion-promoting interlayers [84], dense inorganic barriers [41], and compliant organic topcoats or multilayers [40] to manage modulus mismatch, defect tolerance, and aging pathways (Figure 1).

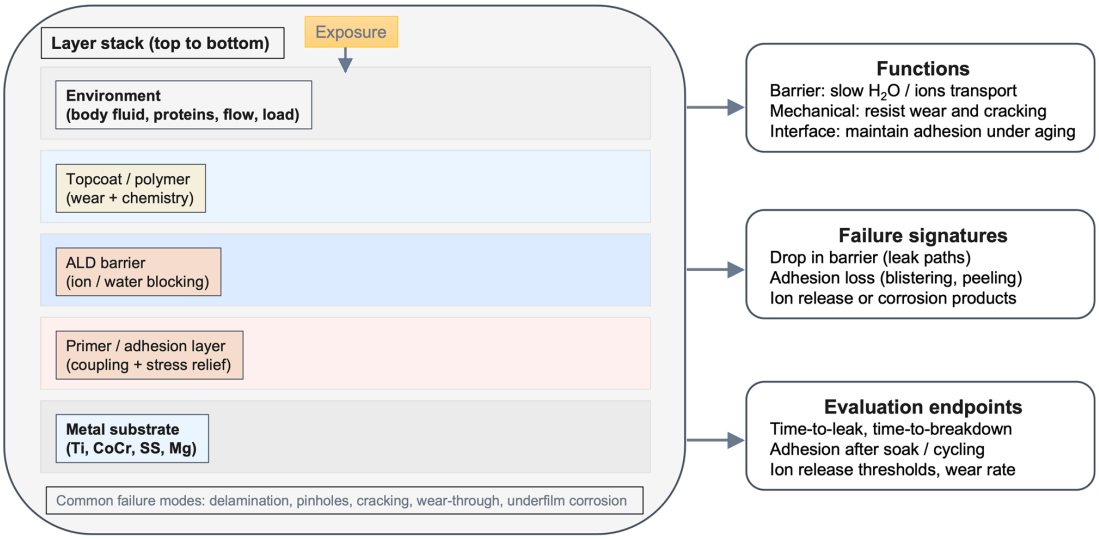



**Figure 1.** Schematic of a layered architecture (from environment to substrate) showing layer functions, failure modes, and evaluation endpoints. Abbreviations in the schematic include Ti (titanium), CoCr (cobalt-chromium), SS (stainless steel), and Mg (magnesium).

The appropriate technology is therefore determined less by its best planar-coupon result than by the combination of substrate class, geometry, dominant failure mode, and the rigor with which the process can be controlled during manufacturing. Hard PVD nitrides and diamond-like carbon (DLC) remain strong options for load-bearing metallic components where wear, debris generation, tribocorrosion, and ion release dominate [3]. PVD implant coatings and joint wear-coating studies further support their use when mechanical wear resistance is the primary endpoint [62]. Atomic layer deposition (ALD) and hybrid ALD-organic stacks are better suited to implantable or wearable electronics, where conformality, pinhole tolerance, moisture-barrier performance, and dielectric leakage control are critical [41]. ALD/polymer barrier studies also support using inorganic–organic stacks rather than relying on a single brittle oxide layer [30]. Sol–gel or organically modified silicate (ORMOSIL) systems are often advantageous for low-temperature barrier or primer functions on polymers and oxide-forming metals [81]. Sol–gel corrosion-barrier studies further support their use when low-temperature processing and interfacial chemistry are important [52]. Plasma polymers are usually most effective as interlayers that tune adhesion and surface chemistry rather than as standalone, long-duration barriers [84]. Parylene and related conformal polymers are attractive for complex assemblies, but long-term humid or implanted service commonly requires inorganic reinforcement when moisture ingress, rather than handling robustness alone, controls failure [40].

The principal advantages, limitations, and mitigation strategies for the major coating, pretreatment, and encapsulation methods are summarized in Table 5.

**Table 5.** Advantages and limitations of major coating, pretreatment, and encapsulation techniques (a compiled qualitative synthesis based primarily on biomedical and medical device sources). Abbreviations: MAO, microarc oxidation; EP, electropolishing; PEP/EPP, plasma or electrolytic plasma polishing; AM, additive manufacturing.

| Method/Technique | Key Advantages | Key Limitations/Failure Sensitivities | Design Notes and Common Mitigations |
| --- | --- | --- | --- |
| PVD (TiN/CrN/DLC) | High hardness/wear resistance [10]; thin films preserve tolerances [62]; wide material design space (multilayers, graded stacks) [23]. | Line-of-sight coverage [62]; residual stress and modulus mismatch can cause cracking/delamination [69]; adhesion is sensitive to surface preparation [85]. | Use adhesion layers (Ti/Cr), stress-graded stacks, and compliant primers on polymers [10]; validate defect statistics [62]; plasma treatment [70]. |
| PECVD/CVD ($SiO_x$/$SiN_x$, fluorocarbons) | Conformal dielectric/barrier films [40]; tunable stress and dielectric properties [11]; PECVD enables lower temperatures [86]; $SiN_x$ cracking [87]. | Plasma damage/charging on polymers [40]; hydrogen/porosity can increase permeability [11]. | Use low-damage recipes, stress control, and multilayer designs [40]; verify with dielectric + humidity/bias testing [41]; parylene coatings [11]; $SiO_x$ barriers [76]. |
| ALD ($Al_2O_3$/$TiO_2$/$HfO_2$) | Excellent conformality and thickness control [41]; low defect density [12]; ideal for hybrid organic–inorganic stacks [88]. | Slow throughput [88]; brittle films crack under flexure; some oxides hydrolyze without capping [89]; nucleation issues on polymers [88]. | Use ALD/polymer multilayers for strain accommodation and defect decoupling [89,90]. Add capping or multilayer protection for moisture-sensitive oxides [89]. Verify conformality, leakage, and batch uniformity [41,91]. |

**Table 5.** *Cont.*

| Method/Technique | Key Advantages | Key Limitations/Failure Sensitivities | Design Notes and Common Mitigations |
|---|---|---|---|
| Sol–gel/ORMOSIL | Low-temperature, scalable, modular chemistry (hydrophobicity, inhibitors, bioactive phases) [81]; can act as interphase/topcoat [52,92]. | Shrinkage cracking if thick [81]; residual porosity increases water uptake [55]; hydrolytic aging can change properties over time [52,80,92]. | Control thickness and cure [81]; use coupling agents [52]; consider hybrid stacks and post-treatments to densify networks [73,80,92]. |
| Plasma polymer interlayers | Solvent-free functionalization improves wet adhesion [84]; a compliant interlayer reduces stress concentration in brittle films [70,77]. | Chemistry variability and aging [84]; typically thin and not a standalone long-term barrier [70]; requires rigorous process control [93]. | Use as an adhesion/gradient layer in stacks [84]; characterize chemistry and validate long-term wet adhesion [70,93]. |
| Parylene encapsulation | Highly conformal polymer dielectric [40]; mature process history in electronics [11]; good biocompatibility record. | Moisture/ion permeability over long duration [40]; adhesion can be weak without activation [11]; defects at edges/particles dominate [53]. | Use adhesion promoters and plasma pretreatments [40]; reinforce with ALD/PECVD layers for long-term barrier performance [11,45]. |
| Conformal coatings (acrylic/urethane/silicone/epoxy) | Scalable, repairable/inspectable in manufacturing [45]; mechanical compliance [94]; broad materials library. | Permeability and solvent sensitivity vary [45]; some chemistries soften or crack under sterilization cycling and thickness variation [94]. | Match chemistry to the sterilization method [45]; control cure and cleanliness [94]; combine with inorganic layers for enhanced barrier performance. |
| Conversion coatings (anodization/MAO/phosphate) | Strong mechanical anchoring [58]; can host bioactive/antimicrobial agents [83]; improves adhesion on oxide-forming metals. | Porosity can be a transport pathway [58]; roughness can reduce fatigue or increase fretting [83]; process variability can affect fatigue and fretting. | Seal porous layers with overcoats [58]; optimize surface roughness [83]; qualify with fatigue and corrosion/tribocorrosion testing when relevant. |
| Primers/coupling agents (silanes, epoxies, urethanes) | Covalent bridging and improved wet adhesion [95]; modulus-matching interphases [73]; enable robust multilayer integration [95,96]. | Sensitive to humidity/contamination and cure [95]; added process steps increase variability [73]; some primers hydrolyze in water [96]. | Control hydrolysis/cure [95]; minimize time-to-coat after activation [73]; validate post-sterilization adhesion and aging behavior [73,96]. |
| Electropolishing (EP) and passivation | Produces smooth, bright surfaces; removes micro-burrs and machining marks [97]. Can improve corrosion resistance via defect reduction and more stable passivation; improves cleanability. Widely used for biomedical instruments and stents [98]. | Electrolytes can be hazardous; requires robust rinsing/neutralization and residue control. Current distribution causes edge effects; non-uniformity risk on sharp features. Material removal affects tolerances [97]; process qualification is required. | Control current, voltage, time, electrolyte, fixturing, and rinsing [98,99]; verify roughness, residues, dimensions, and corrosion [97]. |

**Table 5.** *Cont.*

| Method/Technique | Key Advantages | Key Limitations/Failure Sensitivities | Design Notes and Common Mitigations |
| --- | --- | --- | --- |
| Plasma electrolytic polishing (PEP/EPP; "plasma polishing") | High-efficiency finishing can achieve ultra-smooth surfaces (e.g., Ra < 0.1 μm) and polish complex geometries [100]. Uses aqueous salt electrolytes in many implementations; reduced mechanical damage versus abrasive polishing [101]. Applicable to stainless steels, Ti alloys [102], and AM parts [100,103,104]. | High-voltage equipment and sensitive process window (voltage, conductivity, temperature, hydrodynamics) [103]. Limited to conductive materials; field concentration can cause non-uniformity [100]. Electrolyte management and regulatory validation can be challenging [103]. | Optimize voltage, temperature, conductivity, agitation, and fixture design [103]; validate roughness, chemistry, corrosion, fatigue, and cleanliness [100]. |

### *3.1. Physical Vapor Deposition (PVD) Coatings (TiN, CrN, DLC)*

Physical vapor deposition (PVD) hard coatings, including titanium nitride (TiN), chromium nitride (CrN), zirconium nitride (ZrN), and diamond-like carbon (DLC), are widely used as surface-engineering coatings for biomedical implants because they can improve hardness, friction, wear resistance, corrosion resistance, and biocompatibility [62]. TiN coatings on CoCrMo and Ti6Al4V implant alloys have been shown to reduce wear and metallic ion release under simulated joint-wear conditions [105]. DLC coatings are particularly attractive for biomedical applications because their tribological and mechanical properties can be tailored by adjusting bonding configuration, especially the $sp^2/sp^3$ ratio, hydrogen content, and dopants, allowing trade-offs among hardness, residual stress, friction, and interfacial adhesion [10]. However, PVD coatings may fail due to cracking, delamination, coating defects, and corrosion-assisted damage, particularly when defects expose the metallic substrate to physiological environments [106]. Therefore, performance claims should be supported by tribocorrosion-relevant testing and failure-mode analysis rather than by dry wear testing alone [107].

Recent PVD research trends include graded or multilayer architectures, such as Ti/TiN, Cr/CrN, CrN/TiN, CrN/ZrN, and other nanolaminate systems, to improve coating hardness, adhesion, wear resistance, and corrosion resistance [108]. Ion-assisted deposition and substrate biasing are also used to increase coating density and modify morphology, roughness, hardness, and corrosion response [109]. Duplex designs that combine diffusion-modified or engineered interlayers with a hard topcoat are used to improve load support, toughness, and tribocorrosion performance [110]. These architectures can reduce pinhole-driven corrosion pathways, but coating defects or mechanical damage may still expose the metallic substrate and initiate localized corrosion [106]. Because coated medical devices may undergo sterilization before clinical use, moist-heat/autoclave exposure should be considered during qualification, as it can alter surface topography or chemistry [111]. In joint or articulating applications, performance should be verified using electrochemical or tribocorrosion testing in physiologically relevant media such as Ringer's solution, simulated body fluid, or protein-containing serum rather than dry wear testing alone [110].

Advantages:

- DLC coatings offer high hardness, low friction, and enhanced wear resistance for biomedical components [112].
- TiN coatings on CoCrMo and Ti6Al4V can reduce wear and suppress detectable metal ion release under simulated orthopedic wear conditions [105].

- PVD coatings can modify medical-device surface properties without altering the biomechanical properties of the substrate [113].
- Thin-film PVD coatings enable low-dimensional surface functionalization at thicknesses ranging from the angstrom to the micrometer scale [114].
- Multilayer nitride PVD coatings can be used to tailor hardness, wear resistance, corrosion resistance, and biological response on Ti6Al4V [108].
- DLC bonding structure, hydrogen content, and dopants can be adjusted to tailor hardness, friction, residual stress, and adhesion [112].
- Dry, vacuum-based PVD processing avoids liquid coating baths and can reduce concerns about wet-process residue compared with solution-based coatings [115].

Limitations and trade-offs:

- Line-of-sight deposition can cause shadowing in complex geometries, resulting in undercoated regions, pinholes, or local coating discontinuities [116].
- Coating defects or mechanical damage can expose the substrate, thereby creating localized corrosion pathways [106].
- High residual stress and elastic mismatch [115] can promote cracking or delamination, especially on flexible or bending substrates [117].
- Adhesion depends strongly on surface preparation, oxide chemistry, plasma activation, and interlayer design [118].
- PVD processing can be limited by equipment cost, batch size, deposition rate, cycle time, and throughput constraints [103].

### *3.2. Chemical Vapor Deposition (CVD)/Plasma-Enhanced Chemical Vapor Deposition (PECVD) Barrier and Dielectric Coatings ($SiO_x$, $SiN_x$, Fluorocarbon Films)*

Chemical vapor deposition (CVD) and plasma-enhanced chemical vapor deposition (PECVD) are used to deposit oxide, nitride, and fluorocarbon thin films, including $SiO_x$, $SiN_x$, and fluorinated coatings, for barrier, dielectric, and surface-functionalization applications [12]. Compared with line-of-sight deposition methods, these processes provide improved coverage on moderately complex three-dimensional surfaces, making them useful for medical devices, electronics, packaging, and microfabricated components [12,22]. PECVD is particularly useful for polymer substrates because it enables deposition at relatively low temperatures [12]. However, film stress, plasma exposure, hydrogen incorporation, and defect density must be carefully controlled to prevent cracking, crazing, embrittlement, leakage, or barrier degradation [62,97]. Common mitigation strategies include low-stress recipes, thin-film or multilayer architectures, optimized plasma power, substrate-temperature control, and adhesion-promoting primers or interlayers [97].

Advantages:

- CVD and PECVD can provide more conformal coverage than line-of-sight methods, enabling coating of moderately complex three-dimensional geometries [119].
- Precursor chemistry and plasma parameters can be adjusted to tune film density, stress, dielectric behavior, and surface energy [120].
- PECVD allows lower-temperature deposition, improving compatibility with polymers, sensors, and electronics packaging [120].
- $SiO_x$, $SiN_x$, and related inorganic thin films are well suited for dielectric and moisture-barrier applications when defects and stress are controlled [90].
- Fluorocarbon PECVD films can provide low-surface-energy coatings for hydrophobicity, anti-fouling behavior, or surface-energy control [120].

Limitations and trade-offs:

- Plasma exposure can damage polymer surfaces, alter their chemistry, cause charge trapping, or contribute to embrittlement if the process is overly aggressive [120].
- Hydrogen incorporation, microvoids, or porous film structures can increase permeability and reduce long-term barrier reliability [121].
- Intrinsic or thermal stress can cause buckling, crazing, or microcracking, especially during humidity or thermal cycling [62].
- Thin inorganic barrier films can lose integrity if cracks, pinholes, or interfacial defects form during handling, bending, or environmental exposure [105].
- Precursor gases, plasma byproducts, and chamber residues require appropriate safety controls, contamination control, and process qualification [77].

### *3.3. Atomic Layer Deposition (ALD) Ultrathin Barriers*

Atomic layer deposition (ALD) produces ultrathin oxide and dielectric films via sequential, self-limiting gas–surface reactions, enabling Å-level thickness control and excellent conformality on complex 3D and high-aspect-ratio features [122]. These characteristics make ALD well-suited for diffusion barriers, corrosion passivation, and dielectric layers in implantable electronics, sensors, and stimulation devices [41].

For medical and biomedical devices, common ALD materials include $Al_2O_3$, $TiO_2$, and $HfO_2$. These films can reduce moisture and ionic permeation, but their performance is highly sensitive to defects: particles, pinholes, edge defects, microcracks, or hydrolysis-prone oxides can create localized leakage or corrosion pathways even when the average thickness appears adequate [123].

ALD barrier performance should therefore be evaluated using representative replicate structures and clearly defined part locations. Thickness, conformality, leakage, and barrier uniformity should be reported with run-to-run or batch-to-batch variation, preferably as mean ± standard deviation or as median [interquartile range] [91]. When temperature, precursor dose, plasma exposure, oxidant dose, or purge time is varied, designed experiments or response surface methods are preferred over one-factor-at-a-time screening because they capture parameter interactions more efficiently [91].

For polymer substrates and electronic assemblies, ALD is often most reliable when integrated into a multilayer or hybrid stack. Thin inorganic ALD layers provide low permeability, while polymer layers or organic interlayers help absorb strain, decouple defects, and improve durability under humidity, bending, and thermal cycling [90]. Parylene–ALD or polymer–oxide hybrid structures are therefore commonly used when long-term encapsulation stability is required [119].

Case study:

Jeong et al. demonstrated multilayer ALD-based hermetic encapsulation for wireless implantable microelectronic chiplets, showing that conformal nanolaminates and multilayer stacks can reduce pinhole-driven leakage paths and improve long-term stability in soak and accelerated aging tests [41]. A practical caution is that excellent planar barrier metrics alone do not establish implant-grade hermeticity. Lifetime claims are strongest when accelerated soak data are paired with physical failure readouts, such as leakage-current drift, ion release, localized failure imaging, post-aging adhesion, or electrical-function monitoring.

Advantages:

- ALD provides exceptional conformality and Å-level thickness control for ultrathin barriers on complex microfeatures [122].
- Self-limiting growth enables uniform nanolaminates, graded stacks, and tailored dielectric or barrier performance [12].
- Low-temperature ALD can be compatible with polymers and with temperature-sensitive electronics [124].

- ALD layers are useful in hybrid organic–inorganic stacks because they can decouple defects and improve moisture-barrier reliability [90].

Limitations and trade-offs:

- Slow growth rates and long cycle times can reduce throughput and increase costs for thick or multilayered barriers [12].
- Moisture-sensitive oxides, especially $Al_2O_3$, can hydrolyze or lose their barrier performance unless protected by appropriate capping or multilayer structures [89].

Failure modes in polymer/coating systems are typically governed by interfacial quality, residual stress, moisture uptake, elastic mismatch, and cyclic deformation rather than by coating chemistry alone. Table 6 provides a qualitative screening guide; final ranking should be confirmed through device-specific testing for sterilization, soaking, bending, adhesion, and leakage.

**Table 6.** Failure modes versus materials. Qualitative synthesis of common coating/substrate failure modes in biomedical polymer and thin-film systems. Abbreviations: ABS, acrylonitrile butadiene styrene; ALD, atomic layer deposition; ORMOSIL, organically modified silicate; PA, polyamide; PC, polycarbonate; PECVD, plasma-enhanced chemical vapor deposition; PEEK, polyether ether ketone; $SiN_x$, silicon nitride; $SiO_x$, silicon oxide.

| Failure Mode | Representative System | Main Cause | Trigger | Mitigation |
|---|---|---|---|---|
| Delamination | ABS substrate with sol–gel coating [125,126] | Weak or contaminated interface [92] | Humidity or accelerated aging [127] | Silane primer or adhesion-promoting interlayer [126] |
| Buckling/wrinkling | PC or polymer/PECVD $SiN_x$ or $SiO_x$ [121] | Compressive residual stress [117] | Thermal or hygro-fatigue cycling [77] | Low-stress PECVD recipe or thinner multilayers [121] |
| Blistering | PA or hygroscopic polymer/inorganic barrier [128] | Moisture uptake and swelling [128] | Hydrothermal aging or moist heat [129] | Pre-drying plus ALD/polymer barrier stack [130] |
| Microcracking | PEEK or polymer/ceramic coating [131] | Modulus or strain mismatch [77] | Flexing or cyclic deformation [81,132] | Compliant hybrid or ORMOSIL interlayer [81,133] |
| Pinhole leakage/localized corrosion | ALD or PECVD barrier stack [90] | Particles, pinholes, or hydrolysis-prone oxide defects [89] | Soak aging or accelerated implant aging [53] | Defect-decoupling multilayer stack [90] |

This synthesis supports the use of sol–gel and ORMOSIL hybrid coatings as adhesion-promoting, stress-relieving, or corrosion-protective interlayers between stiff inorganic films and compliant polymeric substrates.

### *3.4. Sol–Gel/ORMOSIL Hybrid Coatings*

Sol–gel and organically modified silicate (ORMOSIL) coatings combine an inorganic oxide network with organic functionality, enabling tuning of the coating's modulus, chemistry, hydrophobicity, and permeability for barrier, primer, or bioactive functions [81]. In biomedical and corrosion-protection applications, sol–gel coatings can be deposited by low-temperature dip, spin, or spray processes, making them suitable for large areas and moderately complex shapes [134]. Organosilane chemistry, including methacrylate-, epoxy-, amino-, and fluorinated silanes, enables control of adhesion, flexibility, water uptake, corrosion inhibition, and surface energy [52]. Hybrid ORMOSIL systems are especially

useful where purely inorganic films would be too brittle, as organic substituents can reduce the tendency to crack and modify the elastic response [133].

Advantages:

- Low-temperature dip, spin, or spray processing enables scalable coating of large areas and moderately complex geometries [134].
- Modular silane chemistry allows tuning of hydrophobicity, corrosion inhibition, surface energy, and functional loading [52].
- ORMOSIL networks combine inorganic durability with organic flexibility, reducing brittleness compared with purely inorganic sol–gel films [133].
- Sol–gel layers can serve as protective topcoats, pore-sealing layers, or adhesion-promoting primers when properly bonded to the substrate [135].

Limitations and trade-offs:

- Drying and condensation shrinkage can cause cracking, chipping, or decohesion when coatings are too thick or poorly cured.
- Residual porosity and incomplete network formation can increase water uptake, ion transport, and the risk of corrosion [52].
- Hydrolytic or humid aging can degrade barrier performance, especially when the coating contains defects or unsealed pores [136].
- Sol aging, ambient humidity, catalyst concentration, withdrawal speed, and cure schedule can reduce reproducibility unless tightly controlled [81].

### *3.5. Plasma Polymer Films and Organic Interlayers*

Plasma polymer films are ultrathin organic, organosilicon, or fluorocarbon-like coatings deposited from plasma-fragmented precursors, enabling modification of surface chemistry and wettability without altering the bulk material [84]. They serve as adhesion-promoting interlayers because plasma treatment can increase surface energy, introduce polar functional groups, remove weak boundary layers, and improve bonding between polymers and subsequent coatings [70]. This approach is particularly relevant for inert biomedical polymers such as PEEK, where plasma treatment can enhance wettability, surface oxygen content, and cell interaction while preserving the underlying polymer [137]. Plasma–polymer interlayers can also help create graded organic–inorganic stacks that reduce the modulus mismatch between compliant polymers and stiff inorganic coatings [138]. Fluorocarbon plasma polymers may be used as hydrophobic, low-surface-energy topcoats for water repellency, contamination control, or condensation management, provided that sterilization stability and biocompatibility are verified [120].

For reproducibility, plasma activation and plasma–polymer deposition studies should report precursor identity and purity, carrier gas and flow rate, pressure, radio frequency (RF) or microwave power, pulse duty cycle, treatment/deposition time, electrode geometry, source-to-substrate distance, substrate temperature or bias, chamber history, base pressure, post-plasma storage conditions, and the time between activation and overcoating [70]. Verification should include XPS atomic percentages and peak fitting, FTIR bands, film thickness, static and advancing/receding contact angles, AFM or profilometry roughness, aging or hydrophobic recovery testing, and wet adhesion results after soaking or sterilization cycling [139].

Advantages:

- Plasma treatment can increase polymer surface energy and enhance coating adhesion [70].
- Plasma activation can functionalize inert biomedical polymers such as PEEK [137].
- Plasma–polymer interlayers can provide a graded transition between polymer substrates and inorganic coatings [138].

- Fluorocarbon plasma polymers can provide hydrophobic, low-surface-energy surfaces [120].

Limitations and trade-offs:

- Plasma-treated polymer surfaces can age or undergo hydrophobic recovery before overcoating [140,141].
- Excessive plasma exposure can cause chain scission, etching, surface damage, or weak boundary layers [70].
- Improved wettability does not always guarantee improved adhesion, so wet adhesion testing is necessary [70].
- Plasma–polymer properties are highly process- and reactor-dependent, limiting cross-study comparability without detailed recipe reporting [138].

### *3.6. Bioactive, Antimicrobial, and Anti-Fouling Functionalization*

Beyond barrier protection, biomedical coatings can be engineered to actively modulate tissue response, infection risk, and nonspecific fouling. For orthopedic and dental implants, multifunctional coatings should ideally promote osseointegration while reducing microbial colonization and the risk of periprosthetic infection [142]. Implant-associated infections are difficult to treat because bacteria can form biofilms on device surfaces, which increase resistance to host defenses and antimicrobial therapy [143]. Therefore, infection-resistant biomaterials commonly rely on antiadhesive, bactericidal, or antibiofilm surface strategies tailored to the intended clinical application [6].

Bioactive ceramic coatings, such as hydroxyapatite and β-tricalcium phosphate, promote bone bonding and osteoconduction in orthopedic and dental applications [144]. Structured $TiO_2$ nanotube surfaces increase surface area and can serve as local drug reservoirs for controlled antimicrobial or therapeutic release [145]. Micro-arc oxidation (MAO) produces porous $TiO_2$-based oxide layers on titanium that incorporate bioactive or antibacterial ions, enhancing apatite formation and antibacterial behavior [146]. Iodine-supported titanium oxide coatings are notable for iodine's broad antimicrobial activity and its clinical evaluation for infection prevention and treatment in orthopedic implants [147]. For passive anti-fouling, zwitterionic and phosphorylcholine-based polymers resist nonspecific protein adsorption and cell adhesion by forming strongly hydrated, electrically neutral surface layers [148]. Table 7 summarizes these functional coating classes, representative materials, and their primary mechanisms of action.

**Table 7.** Functional coating classes and key mechanisms. Qualitative synthesis of coating strategies used to add biological function beyond passive barrier protection. Abbreviations: DLC, diamond-like carbon; MAO, micro-arc oxidation; PC, phosphorylcholine. In this table, PC refers to phosphorylcholine, not polycarbonate.

| Coating Class | Primary Function | Material Examples | Mechanism of Action |
|---|---|---|---|
| Carbon-based films | Wear reduction and mechanical stability | Diamond-like carbon (DLC) [112] | High hardness, low friction, chemical inertness, and reduced wear-particle generation in sliding contacts [107,118] |
| Hydrophilic polymer coatings | Anti-fouling and biocompatibility | Phosphorylcholine-based polymers [148] | Strong surface hydration suppresses nonspecific protein adsorption and cell adhesion [148] |
| Non-metallic antimicrobials | Infection control | Iodine or povidone-iodine systems [147] | Broad-spectrum antimicrobial activity with lower resistance pressure than many antibiotic-release approaches [117] |

**Table 7.** *Cont.*

| Coating Class | Primary Function | Material Examples | Mechanism of Action |
| --- | --- | --- | --- |
| Smart/conductive polymers | Sensing, electrically triggered release, and wound/implant biointerfaces | Polypyrrole (PPy), polyaniline (PANI), and PEDOT-based coatings or films [149] | Conductive polymers can support biosensing and triggered therapeutic release, including pH-responsive PPy drug delivery for wound-relevant environments [150] |
| Structured oxides and bioactive ceramics | Drug delivery and osseointegration | Titania nanotubes, MAO oxides, hydroxyapatite, and tricalcium phosphate [151] | High surface area supports drug loading, while bioactive ceramic or oxide chemistry promotes tissue–implant bonding [144,145] |

The literature increasingly shows that biological activity and barrier reliability should be evaluated together. Contact-killing surfaces, release-based systems, and hydration-layer antifouling coatings can each be effective, but their translational value depends on whether the functional chemistry remains stable after wear, sterilization, corrosion, and prolonged aqueous exposure [6]. Many antimicrobial coatings fail in later development because the active species is depleted, the surface reconstructs, or the functional layer is not mechanically integrated with the underlying barrier stack [152]. Silver-based systems illustrate this trade-off: silver can provide broad antimicrobial activity, but ion release, dose, and local chemistry must be controlled to avoid cytotoxicity [153].

A common translational error is to report antimicrobial efficacy or cell response only on freshly prepared surfaces. For both contact-killing and release-based coatings, the key question is whether the active interface remains spatially uniform, mechanically attached, and toxicologically acceptable after clinically relevant conditioning [6]. Biological assays, ion release measurements, adhesion testing, post-aging surface chemistry, and barrier-performance data should therefore be planned as a single, integrated dataset rather than as separate work packages.

Advantages:

- Enables device-specific biological responses, including osseointegration, biofilm suppression, and reduced nonspecific protein adsorption [6].
- Functional topcoats can be applied over barrier stacks to separate reliability functions from biological ones [154].
- Multiple mechanisms are available, including contact killing, controlled release, and hydration-layer antifouling [148].

Limitations and trade-offs:

- Functional agents can leach, deplete, foul, or lose activity during prolonged exposure to water [152].
- Antimicrobial additives can pose cytotoxicity risks if the dose, release rate, and local chemistry are not controlled [153].
- Increased roughness or porosity can support tissue integration but may also promote bacterial adhesion, corrosion, or contaminant entrapment [21].
- Regulatory burden increases when a coating shifts from passive barrier protection to active antimicrobial or drug-like functionality [155].

### *3.7. Smart, Adaptive, and Responsive Coatings*

Smart, adaptive, and responsive coatings extend biomedical surface engineering from passive protection to active sensing, release, and feedback. In orthopedic and dental applications, these coatings can respond to local stimuli, including pH, temperature, light, enzymes, bacterial metabolites, and inflammatory microenvironments [156]. For example,

pH-responsive titanium implant coatings have been designed to switch on antibacterial activity under acidic infection conditions while maintaining osteogenic behavior under normal conditions [157]. Conductive polymers such as polypyrrole (PPy), polyaniline (PANI), and poly(3,4-ethylenedioxythiophene) (PEDOT) are attractive for biomedical interfaces because they can combine electrical conductivity, biosensing, and triggered therapeutic release [149].

A key design trade-off is that the same chemistry that improves responsiveness may also affect adhesion, flexibility, cytocompatibility, and long-term stability. In polypyrrole systems, dopant type, synthesis method, morphology, and deposition conditions strongly influence electrical, biological, and mechanical behavior [149]. Therefore, responsive coatings should be evaluated not only for initial sensing or release behavior but also for drift, repeatability, sterilization stability, wet adhesion, and failure modes after prolonged immersion. These multi-constraint requirements make smart coatings suitable candidates for design-of-experiments and AI/ML-assisted optimization workflows [158].

Advantages:

- Stimulus-responsive coatings can activate antibacterial or therapeutic functions only when local infection-related cues are present [152].
- Conductive-polymer platforms can combine pH sensing, biosensing, and on-demand drug release in biomedical wound or implant-adjacent applications [157].
- pH-responsive titanium coatings can combine infection control with osseointegration-promoting behavior [157].
- AI/ML-assisted workflows can help optimize coating formulations when mechanical, corrosion, biological, and processing objectives must be balanced [158].

Limitations and trade-offs:

- Responsive coatings are more complex to qualify because activity, stability, drift, repeatability, and degradation must all be characterized [156].
- Release-based systems can lose functionality if the active agent is depleted or released too rapidly [152].
- Conductive-polymer films can suffer from poor adhesion or limited mechanical strength unless synthesis and interfacial design are carefully controlled [149].
- Sterilization, immersion, wear, and biological fouling may alter the responsive chemistry, making post-aging testing essential [6].

### *3.8. Electronic Coatings and Encapsulation*

Electronic coatings and encapsulation layers are essential for medical and bioelectronic devices, including diagnostics, wearables, implantable sensors, and electromechanical modules. They protect circuits and interconnects from humidity, condensation, electrolytes, biological fluids, contamination, vibration, and thermal cycling while preserving electrical performance [159]. For implantable and complex medical devices, parylene C is widely used as a conformal dielectric and moisture-barrier coating for its flexibility, dielectric properties, water/gas barrier performance, and ability to coat complex geometries [11].

#### 3.8.1. Conformal Polymer Coatings and Parylene Encapsulation

Conformal polymer coatings, including acrylics, silicones, urethanes, epoxies, and parylene, protect medical electronics and mixed-material assemblies from humidity, ionic contamination, handling damage, and electrical leakage [94]. For printed-board assemblies and medical electronic modules, IPC-CC-830C provides a useful qualification framework for electrical insulating conformal coatings, with requirements covering coating integrity, moisture resistance, insulation performance, and process control [45]. Parylene C is particularly important for biomedical devices because CVD deposition yields highly conformal,

flexible, dielectric, and biocompatible coatings on complex geometries [11]. Parylene surfaces can also be modified by oxidation, grafting, and bioactive or antimicrobial functionalization when biological interactions must be controlled [119].

The main reliability risks are moisture permeation, pinhole or particle-related leakage paths, and adhesion loss during long-term wet exposure [160]. Adhesion is especially challenging at parylene–metal, parylene–polymer, and noble-metal interfaces, so plasma activation, silane primers, adhesion-promoting interlayers, and careful masking/edge design are often required [161]. For higher-risk implantable electronics, parylene is often combined with inorganic layers such as ALD $Al_2O_3$ to improve insulation stability and reduce moisture-driven failure [130].

Advantages:

- Parylene C provides conformal dielectric insulation on complex biomedical devices and implantable microstructures [11].
- Parylene can be surface engineered for biological patterning, bioactivity, or antimicrobial functionality [119].
- Polymer encapsulants provide mechanical compliance that helps accommodate flexure and mixed-material assemblies [160].
- Parylene/ALD bilayers can improve long-term encapsulation performance for implantable electronics [130].

Limitations and trade-offs:

- Conventional conformal coatings are not fully hermetic and can allow moisture ingress under cyclic humidity exposure [94].
- Parylene C can fail by moisture-assisted delamination if wet adhesion is insufficient [161].
- Particles, masking edges, vias, and defects can create localized leakage paths [160].
- Rework and local repair can be difficult for parylene-coated assemblies because removal often requires plasma etching or aggressive localized processing [119].

#### 3.8.2. Inorganic Dielectrics and Hybrid Barrier Stacks

Inorganic dielectrics such as $SiO_x$, $SiN_x$, $Al_2O_3$, and $HfO_2$ provide high electrical insulation and low permeability even at very thin thicknesses, making them attractive for miniaturized medical electronics and implantable sensors [122]. Their main weakness is brittleness: intrinsic stress, particles, pinholes, edge defects, or flexural strain can create microcracks or leakage pathways that dominate long-term reliability [77].

Hybrid barrier stacks address this limitation by combining dense inorganic layers with compliant organic layers, such as parylene, plasma polymers, or sol–gel interlayers. In these architectures, the inorganic layer provides resistance to moisture and ions, while the organic layer improves strain tolerance, adhesion, and defect decoupling [90]. ALD is particularly useful for forming conformal oxide nanolaminates on complex implantable electronics because it enables precise thickness control and high-aspect-ratio coverage [41]. Parylene and related polymer layers are commonly used to enhance mechanical durability and reduce sensitivity to local defects [119].

A representative example is the use of multilayer ALD nanolaminates for conformal, hermetic sealing of wireless implantable microelectronic chiplets. Jeong et al. showed that ALD-based multilayers can improve soak reliability under accelerated saline aging and support extrapolated long-term operation at physiological temperature [41]. For higher-risk devices, the stack design should be tied to a defined failure model: pinhole-driven ionic leakage, interfacial delamination, flexural crack growth, or dielectric breakdown. This determines whether the design emphasis should be on dense oxides, compliant polymer overcoats, adhesion-promoting interphases, or control of electrical leakage.

Primer and interphase mechanisms are summarized in Figure 2, and electrochemical evaluation methods for coating failure are summarized in Figure 3.

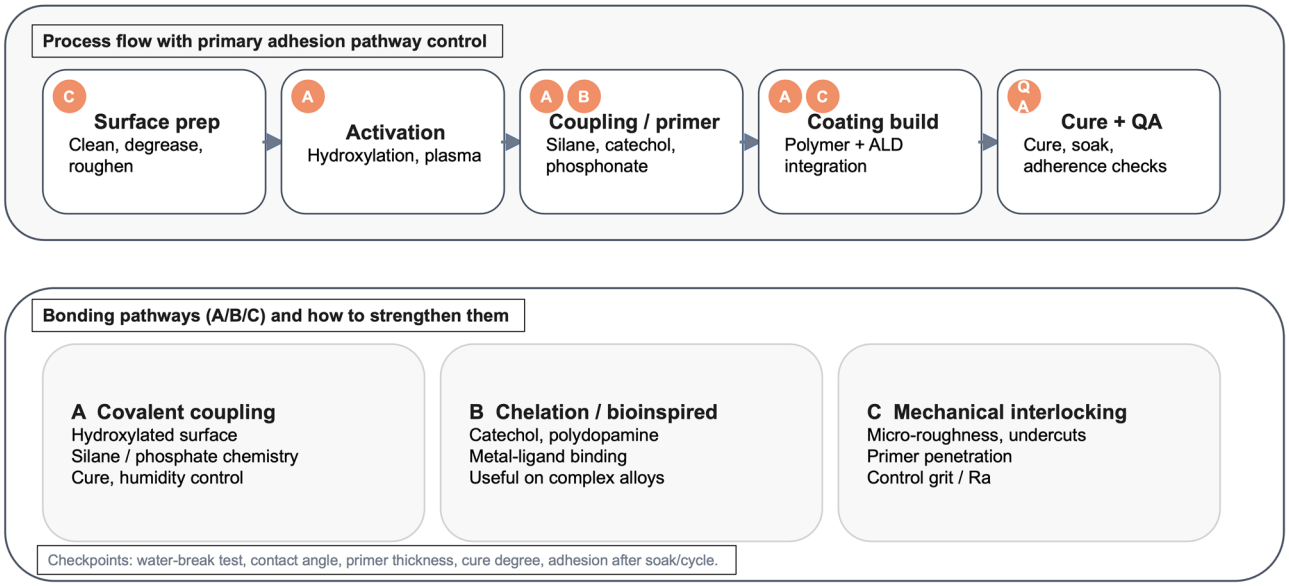



**Figure 2.** Schematic of adhesion enhancement, showing key bonding pathways and process checkpoints controlling reproducibility. QA denotes quality assurance.

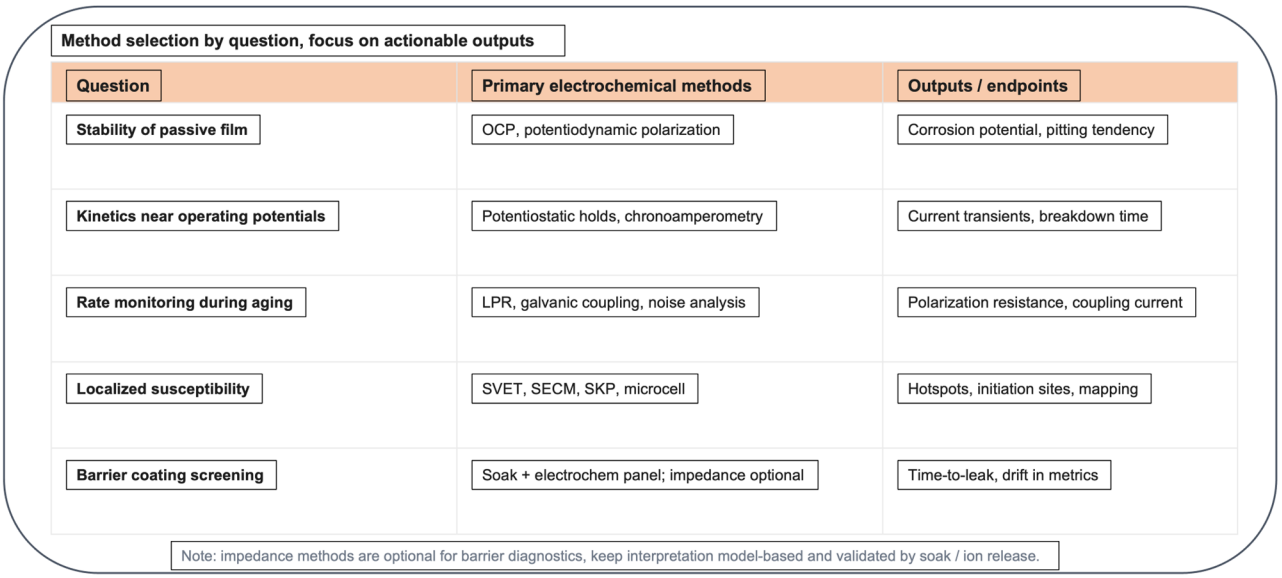



**Figure 3.** An electrochemical evaluation toolbox that links common coating-failure questions to relevant methods and outputs. Abbreviations: OCP, open circuit potential; LPR, linear polarization resistance; SVET, scanning vibrating electrode technique; SECM, scanning electrochemical microscopy; SKP, scanning Kelvin probe.

Advantages:

- Dense inorganic dielectrics provide low permeability and high dielectric strength even at minimal thickness [122].
- ALD nanolaminates enable conformal encapsulation of miniaturized implantable electronics [41].
- Hybrid inorganic/polymer stacks reduce susceptibility to pinholes, cracks, and isolated defects [90].

- Polymer layers add compliance and improve durability under flexure or during mixed-material assembly [119].

Limitations and trade-offs:

- Brittle inorganic films can crack or delaminate under flexure, vibration, or thermal cycling [77].
- Reliability may be controlled by rare pinholes or local defects rather than by average coating thickness [123].
- ALD/polymer stacks can still fail due to moisture-assisted degradation or interfacial leakage if defects reach the substrate [130].
- Process integration is complex because masking, edge coverage, adhesion, sterilization compatibility, and inspection must all be qualified [162].

Hybrid multilayers that combine ALD- or PECVD-derived inorganic barriers with flexible organic layers, such as parylene, sol–gel hybrids, or plasma polymers, are used to balance permeability, crack resistance, adhesion, and manufacturability, as shown schematically in Figure 4.

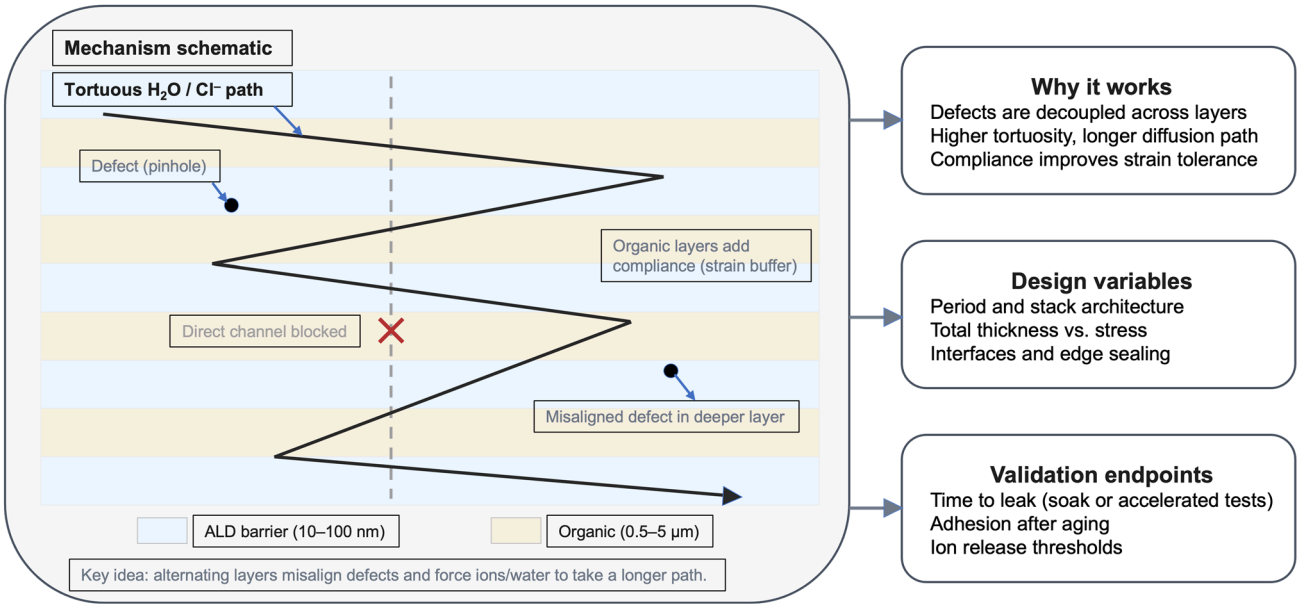



**Figure 4.** Schematic illustrating hybrid ALD-organic multilayers, emphasizing defect misalignment, longer transport paths, and strain accommodation.

### 3.8.3. Condensation Management and Electrically Driven Failure Modes

In moisture-prone medical electronics, including smart inhalers, wearables, sensors, and electromechanical modules, condensation can create thin electrolyte pathways between biased conductors, accelerating leakage-current drift, corrosion, and electrochemical migration [163]. Low-surface-energy hydrophobic or fluorinated coatings can reduce droplet adhesion and conductive bridging, but they should be treated as a complement to dielectric insulation, conformal encapsulation, and contamination control rather than as a standalone reliability solution [164]. Under humid or condensing conditions, PCB and microelectronic failures are often driven by water-film formation, ionic residues, electrochemical migration, dendritic growth, dielectric breakdown, and adhesion loss at coating edges or interfaces [163].

Qualification should therefore include dielectric testing, leakage-current monitoring, surface insulation resistance or impedance testing, environmental cycling, condensation exposure, vibration or thermal-vibration testing, and post-aging inspection of coating edges, vias, solder joints, and interfaces [94]. For electrically powered or patient-connected

medical devices, these evaluations should align with IEC 60601-1 requirements for basic safety and essential performance, particularly when leakage current, dielectric integrity, insulation stability, and moisture-assisted electrical failure are relevant [43].

Advantages:

- Hydrophobic and fluorinated coatings can reduce water adhesion and support droplet shedding in condensation-prone service [164].
- Surface-energy engineering can be paired with dielectric barrier layers to address both moisture ingress and liquid-water bridging [165].
- Condensation and humidity testing can directly reveal leakage-current drift, electrochemical migration, and dendritic growth mechanisms [163].
- Thermal-vibration testing helps capture reliability risks in electronic assemblies exposed to motion, vibration, and temperature cycling [166].

Limitations and trade-offs:

- Hydrophobic coatings may lose performance after abrasion, cleaning, sterilization, or prolonged wet exposure, so durability must be verified under realistic cycling [70,94,165].
- Low-surface-energy coatings can reduce adhesion to subsequent layers, requiring careful masking, plasma activation, primers, or stack sequencing [70,140].
- Contamination or flux residues under conformal coatings can accelerate moisture uptake, adhesion loss, leakage current, and electrochemical migration [94].
- Dielectric stacks must still be designed for breakdown strength, leakage current, and field concentration, especially in high-voltage MEMS or sensor applications [167].

## 4. Pretreatments, Adhesion, Failure Modes, and Prevention

Pretreatments, adhesion layers, and interfacial chemistry often determine whether a coating functions as an engineered multilayer stack or fails by delamination. Because many coating failures originate at the substrate–coating interface, surface preparation, activation, primer selection, and adhesion testing should be treated as design controls, rather than secondary processing steps [168].

### *4.1. Case Study: Electropolishing Versus Plasma Electrolytic Polishing (PEP) for Medical Components*

Electropolishing (EP) is a mature surface-finishing method for stainless steels and other medical alloys, but it commonly uses concentrated acidic electrolytes and requires strict residue, rinsing, and waste-control procedures [169]. Plasma electrolytic polishing (PEP) is a newer high-voltage process that can produce smooth, bright, low-roughness surfaces using dilute or more environmentally benign electrolytes [170]. For AISI 316L stainless steel, PEP has been reported to improve corrosion resistance in simulated physiological saline, supporting its relevance for medical instruments and implant-related alloys [101]. PEP has also been demonstrated clinically for patient-specific titanium orbital implants, where smooth surfaces were used to reduce tissue catching and improve handling during reconstruction [171].

The primary engineering trade-off is that PEP performance depends strongly on electrolyte composition, voltage/current response, treatment time, part geometry, and the stability of the vapor–plasma envelope [170]. Sharp edges, recesses, thin walls, and complex additively manufactured features may experience nonuniform current distribution or geometry-dependent material removal. Therefore, EP and PEP should be qualified using the same functional endpoints: roughness, edge rounding, dimensional change, passive-film chemistry, corrosion resistance, residue control, and post-polishing coating adhesion.

For downstream coatings, polishing alone is not enough. Surface activation, primer selection, and adhesion testing should be matched to the coating/substrate pair and the expected service condition. Scratch, peel, pull-off, blister, indentation, and bend-based methods are used to evaluate coating adhesion, but no single test captures all clinically relevant loading modes [168]. For thermally sprayed hydroxyapatite coatings, for example, tensile and shear adhesion strength depend on surface preparation and heat-treatment history, underscoring the need to qualify pretreatment alongside the coating process [172].

### *4.2. Surface Preparation and Activation*

Surface preparation should be treated as a controlled manufacturing step because coating failures often originate at the interface. After EP, PEP, abrasion, plasma activation, or UV–ozone treatment, roughness, cleanliness, mass loss, and corrosion response should be measured across multiple fields, parts, and batches. Nested measurements should separate batch effects from within-part variation, and comparisons should report effect sizes with confidence intervals rather than single representative traces [173,174].

Common pretreatments include solvent or aqueous cleaning, controlled abrasion or blasting, plasma activation, UV–ozone treatment, and chemical functionalization. For polymers, activation increases surface energy and introduces polar groups that enhance coating adhesion [70]. For metals, pretreatment removes weak boundary layers, controls oxide chemistry, and creates a reproducible bonding surface [168].

Electropolishing (EP) smooths conductive metals through anodic dissolution, reducing burrs, roughness, and surface defects [169]. For stents and other tight-tolerance components, EP can improve corrosion behavior but must be controlled to manage material removal, edge rounding, residues, and dimensional change [57].

Plasma electrolytic polishing (PEP) uses high-voltage electrochemical conditions to form a vapor–plasma envelope that rapidly smooths metallic surfaces in aqueous electrolytes [170]. PEP has been applied to patient-specific titanium implants and 316L stainless steel, improving roughness and corrosion resistance [101,171]. However, it requires careful control of voltage, electrolyte conductivity, temperature, treatment time, and geometry, and it can cause nonuniform polishing near sharp features [170].

Advantages:

- Surface activation improves wettability and coating adhesion [70,140].
- Dry activation methods reduce the risk of wet-chemistry residues [140].
- EP and PEP reduce roughness and surface defects before coating or passivation [169].

Limitations and trade-offs:

- Over-treatment can damage polymers or accelerate hydrophobic recovery [70].
- Activation-to-coating delay should be controlled because adhesion benefits may diminish over time [140].
- EP, PEP, abrasion, and blasting can alter dimensions or remove material nonuniformly [57].
- PEP requires high-voltage equipment and precise control of electrolyte and geometry [170].

### *4.3. Primers, Coupling Agents, and Interphase Design*

Primers and coupling agents transform a simple coating/substrate contact into an engineered interphase. They enhance wet adhesion, create chemical bonding pathways, reduce stress concentrations, and help bridge the modulus mismatch between flexible polymers and stiff coatings. Silane coupling agents are commonly used to bond oxide-rich surfaces to organic coating networks (Table 8) [135]. Plasma activation can improve adhesion on low-energy or chemically inert polymers by increasing surface energy and introducing polar functional groups [70]. Polydopamine provides a versatile biomedical

primer route for secondary functionalization [175]. Hybrid sol–gel interlayers can reduce brittleness and improve compatibility between inorganic and organic phases [81].

**Table 8.** Primer selection guide for common medical polymers. Abbreviations: ABS, acrylonitrile–butadiene–styrene; PA, polyamide; PC, polycarbonate; PI, polyimide; PEEK, polyether ether ketone; ALD, atomic layer deposition; PECVD, plasma-enhanced chemical vapor deposition; PVD, physical vapor deposition; A-174, 3-methacryloxypropyltrimethoxysilane.

| Polymer | Main Challenge | Primer/Interphase Option | Compatible Coatings | Practical Note |
|---|---|---|---|---|
| ABS | Variable oxidation and mixed-phase surface | Epoxy-silane or sol–gel hybrid | Sol–gel, PECVD, plasma–polymer films | Hybrid coatings have shown good adhesion on ABS [126]. |
| PA | Moisture uptake and swelling | Aminosilane or plasma activation after drying | Sol–gel, ALD/ polymer stacks | Pre-dry or humidity-condition before coating [128]. |
| PC | Solvent sensitivity and stress-crazing risk [51] | Low-solvent epoxy/acrylic primer or plasma activation [176] | PECVD, plasma–polymer films | Avoid aggressive solvent primers. |
| PI | Chemically stable imide surface | Oxygen plasma, amine treatment, or aminosilane | ALD, PVD, parylene, metal films | Plasma or amine treatments can improve adhesion [177]. |
| PEEK | Low surface energy and chemical inertness | Plasma activation or amine-rich plasma–polymer interlayer | ALD, PECVD, PVD, ceramic coatings | Surface modification is usually required [178]. |
| Parylene C interfaces | Wet delamination at metal/polymer interfaces | A-174, thiol primer for Au, DLC or EGDA interlayers | Parylene, ALD/parylene stacks | Wet adhesion is critical to lifetime [160]. |

Advantages:

- Silanes link oxide-rich surfaces to organic coating networks [135].
- Plasma activation improves wettability and adhesion on polymers [70].
- Polydopamine offers a broad biomedical primer route for secondary functionalization [175].
- Hybrid interlayers can reduce modulus mismatch and the risk of cracking [81].

Limitations and trade-offs:

- Silane performance depends on hydrolysis, condensation, humidity, and cure control [179].
- Plasma activation benefits can decay due to hydrophobic recovery [140].
- Primers specify process variables such as pot life, thickness, cure schedule, and contamination control [160,168].
- Wet exposure, sterilization, or cyclic loading can reveal adhesion weaknesses missed by dry tests [168].

### *4.4. Conversion Coatings and Engineered Oxide Layers*

Conversion coatings and engineered oxide layers enhance corrosion resistance, adhesion, and biological response by modifying the substrate surface. On titanium alloys, micro-arc oxidation (MAO) produces porous $TiO_2$-based layers that support osseointegration, corrosion resistance, and antibacterial functionalization [151]. On magnesium alloys, phosphate conversion coatings can slow degradation and improve bonding, wear resistance, and biocompatibility [180]. MAO layers may also be sealed with sol–gel topcoats to reduce pore-connected corrosion pathways [136].

These treatments are useful when coating stacks must withstand moisture, sterilization, corrosion, or tribological loading. However, porosity and roughness must be controlled because they can enhance mechanical anchoring but also create fluid pathways or stress concentrators.

Advantages:

- MAO produces porous, bioactive oxide layers on titanium implants [151].
- Phosphate conversion coatings enhance corrosion resistance and adhesion on magnesium alloys [136,180].
- Sol–gel topcoats can seal MAO pores and enhance corrosion resistance [136].
- Controlled roughness can enhance mechanical interlocking for subsequent coatings [172].

Limitations and trade-offs:

- Unsealed pores can permit water and ion transport [136].
- Excessive roughness may increase the risk of fretting or stress concentration [151].
- Conversion coatings require tight control of bath chemistry, temperature, pH, and time [180].
- MAO performance depends strongly on the electrolyte, voltage/current response, treatment time, and substrate geometry [151].

### *4.5. Failure Modes and Reliability Mitigation*

Common coating and interfacial failure modes include delamination, blistering, cohesive cracking, pinhole-mediated leakage, localized corrosion at defects, and dielectric breakdown under bias. In load-bearing implants, tribocorrosion can be especially important because mechanical wear and electrochemical dissolution accelerate one another [181,182]. For this reason, coating reliability should be assessed under combined mechanical, chemical, electrical, and aging conditions rather than through isolated tests alone [12,182,183].

As summarized in Table 9, failure risk is often governed by the interface, coating architecture, substrate compliance, defect population, and service environment. Practical mitigation strategies include surface cleaning or activation, compatible primers, graded or multilayer stacks, stress-balanced deposition, edge sealing, and geometry-driven design-for-coating. When wear–corrosion coupling is relevant, ASTM G119 provides a useful method for distinguishing contributions from mechanical, electrochemical, and synergistic damage [182].

**Table 9.** Representative coating and interfacial failure modes, triggers, and mitigation strategies.

| Failure Mode | Representative Systems | Typical Triggers | Mitigation Strategies |
| --- | --- | --- | --- |
| Delamination | Sol–gel, parylene, ALD, or inorganic films on polymers | Weak interface, moisture ingress, hydrothermal aging | Surface activation, silane/A-174 primer, compatible interlayer, controlled drying [52,183,184] |
| Buckling-driven delamination | PECVD/ALD oxides or nitrides on compliant polymers | Residual compressive stress, thermal cycling, modulus mismatch | Low-stress deposition, stress-balanced multilayers, compliant or graded interlayers [183,185] |
| Blistering | Polymer/inorganic barrier stacks | Moisture uptake, trapped contamination, autoclave or moist-heat exposure | Pre-drying, improved cleaning, redundant barriers, edge sealing [52,186] |
| Cohesive cracking/microcracking | Brittle ceramic, oxide, nitride, or hybrid coatings on flexible polymers | Bending, cyclic deformation, tensile stress, CTE/modulus mismatch | Hybrid coatings, ductile interlayers, reduced film thickness, bend-radius limits [77,183] |

**Table 9.** *Cont.*

| Failure Mode | Representative Systems | Typical Triggers | Mitigation Strategies |
| --- | --- | --- | --- |
| Pinhole-mediated leakage | Parylene, ALD, sol–gel, $SiO_x$, or $SiN_x$ barriers | Particulates, shadowing, incomplete coverage, aligned defects | Multilayer redundancy, clean processing, conformal deposition, inspection of edges/vias [12,52,122,186] |
| Localized corrosion at defects | Coated metallic implants, electrodes, or housings | Coating breach, crevice geometry, galvanic coupling, chloride exposure | Defect-tolerant stack, compatible substrate/coating couple, corrosion-relevant accelerated tests [52,181,182] |
| Dielectric breakdown | Encapsulation for active implants, sensors, and electronics | Moisture/ion ingress, pinholes, field concentration, bias aging | Rounded conductive features, thicker or redundant dielectric stack, biased soak testing [52,184,186] |

### *4.6. Design Rules for Qualification and Reliability*

Reliability-focused design should treat the coating, substrate, geometry, process window, and qualification plan as a single system. The recommended sequence is to define the clinically or functionally relevant failure event, identify applicable standards and acceptance criteria, select sentinel measurements that detect the same failure pathway early, and only then optimize the coating stack or process conditions. This approach avoids over-optimizing convenient but weak proxy metrics, such as initial contact angle, single-point corrosion potential, or as-deposited adhesion.

For regulated medical device development, ISO 13485 and ISO 14971 require traceability among user needs, design inputs, risk controls, verification, validation, and residual-risk evaluation [14,42,187]. Therefore, critical process parameters and inspection rules should be justified by the hazards they control. Models and data-driven reliability tools are useful only when they preserve the chain from hazard to endpoint, to measurable sentinel, to validated model output.

## 5. Analysis and Characterization Methods

Coating qualification requires a coordinated characterization approach that links chemistry and microstructure to mechanical integrity, barrier performance, and functional behavior. Because many degradation pathways originate at defects or interfaces, depth- and time-resolved methods are particularly valuable (Table 10).

**Table 10.** Surface and interface characterization techniques for biomedical coatings. Abbreviations: XPS, X-ray photoelectron spectroscopy; FTIR, Fourier transform infrared spectroscopy; ATR-FTIR, attenuated total reflectance FTIR; QCM-D, quartz crystal microbalance with dissipation monitoring; EIS, electrochemical impedance spectroscopy.

| Technique | Surface or Interface Property Measured | Information Provided | Value in Biomedical-Coating Evaluation |
| --- | --- | --- | --- |
| XPS [188] | Elemental composition and chemical state | Surface chemistry, oxidation state, contamination, and shallow depth-profile information | Confirms coating deposition, passive-film chemistry, surface cleanliness, and interfacial composition |
| FTIR/ATR-FTIR [188] | Chemical bonding and molecular structure | Functional groups, organic/inorganic bonding, polymer modification, and primer or silane chemistry | Verifies chemical functionalization, coating conversion, and interlayer bonding |

**Table 10.** *Cont.*

| Technique | Surface or Interface Property Measured | Information Provided | Value in Biomedical-Coating Evaluation |
|---|---|---|---|
| Adhesion testing [189] | Coating attachment and mechanical integrity | Qualitative or quantitative adhesion, cohesive failure, and interfacial weakness | Screens risk of delamination during handling, sterilization, implantation, or service loading |
| QCM-D [190] | Mass uptake, adsorption/desorption kinetics, and viscoelastic response | Real-time protein adsorption, fouling behavior, hydration-layer stability, or release kinetics | Links surface chemistry to early biofluid interactions, antifouling performance, and drug-release behavior |
| Contact angle [191] | Wettability and apparent surface energy | Hydrophilic/hydrophobic character and surface-energy changes after treatment | Rapidly screens surface modification and likely early protein/cell interaction trends |
| Electrochemical testing [31] | Corrosion response and barrier integrity | Open circuit potential, polarization behavior, EIS response, breakdown potential, and passivation stability | Evaluates corrosion resistance of coated metallic implants and identifies coating defects or breakdown susceptibility |
| Localized electrochemical mapping [192] | Spatially resolved corrosion or electrochemical activity | Local anodic/cathodic sites, defect activity, under-film corrosion, and heterogeneous coating response | Identifies coating defects and local failure pathways that may be missed by bulk electrochemical tests |
| 3D imaging/ tomography [193] | Subsurface morphology and defect architecture | Pits, pores, cracks, coating thickness variation, and internal defect networks | Supports failure analysis by connecting surface damage to subsurface corrosion or crack propagation |

### *5.1. Mechanical and Adhesion Testing*

Mechanical and adhesion tests confirm that biomedical coatings remain attached and functional throughout manufacturing, sterilization, implantation, and clinical use. For calcium-phosphate and metallic implant coatings, tensile testing measures adhesion strength [194]. Shear and bending fatigue tests are useful when coatings are subjected to interfacial shear or repeated loading during gait, mastication, or instrument reuse [195]. Tape testing can provide a rapid qualitative screen, but it should not replace quantitative testing for safety-critical coatings [189].

Test selection should align with the expected clinical failure mode. Load-bearing implants may fail due to debonding, fretting, wear, fatigue, or tribocorrosion [196]. Implantable electronics and biosensors may fail due to cracking, moisture ingress, leakage current, or dielectric breakdown [182]. Fracture-surface analysis should distinguish adhesive failure from cohesive cracking or substrate damage, as each failure pathway has distinct biological and regulatory implications [196,197].

Because biomedical coating data are often scattered, full distributions and confidence intervals are more informative than means alone. Weibull analysis is useful for assessing lower-tail reliability [197]. Kaplan–Meier analysis is appropriate for censored fatigue or time-to-failure data [198]. Regression-based implant-survival analyses can relate failure time to covariates and risk factors [199].

Advantages:

- Provides clinically relevant metrics such as adhesion strength, fatigue resistance, hardness, modulus, wear resistance, and coating integrity [194].
- Supports comparison of substrate preparation, coating parameters, sterilization exposure, hydration state, and interlayer design [195].
- Can be combined with simulated body fluids, cyclic loading, fretting, wear, or tribocorrosion for more service-relevant evaluation [182].
- Helps distinguish minor coating damage from clinically significant risks, such as delamination, particle release, corrosion acceleration, or electrical leakage [196].

Limitations and trade-offs:

- Results depend on specimen geometry, coating thickness, porosity, substrate modulus, fixture alignment, and loading mode [194].
- Tensile, shear, tape, bend, fatigue, and wear tests may rank the same coating differently because they subject it to different stress states [195].
- In vitro tests may not fully replicate tissue loading, inflammation, protein adsorption, sterilization, corrosion, and long-term aging [182].
- High scatter in porous, ceramic, polymeric, and multilayer coatings requires an adequate sample size and distribution-based analysis [197].

### *5.2. Microstructural Characterization*

Microstructural characterization employs scanning electron microscopy (SEM), transmission electron microscopy (TEM), atomic force microscopy (AFM) [200], and, for crystalline substrates, electron backscatter diffraction (EBSD) to quantify thickness, porosity, grain structure, defects, and interfacial morphology [193]. For bioactive and porous architectures, three-dimensional techniques such as tomography, FIB-SEM, micro-computed tomography, or synchrotron-based imaging can link structure to tissue integration, crack development, pit propagation, and pit-to-crack transitions [201]. Synchrotron-based methods are particularly useful when passive-film chemistry, localized corrosion, or in situ degradation processes must be resolved at high spatial or temporal resolution [202].

Advantages:

- Microstructural characterization reveals thickness, defects, cracking, and interfacial morphology, all of which often dominate barrier and adhesion performance [193].
- High-resolution tools such as SEM, TEM, and AFM enable root-cause analysis of failures, including pinholes, voids, and delamination pathways [193].
- Three-dimensional methods such as FIB-SEM and micro-computed tomography can visualize complex structures and internal porosity in conversion coatings and hybrid materials [201].

Limitations and trade-offs:

- Many methods are destructive and/or require vacuum and sample preparation that can alter soft polymers or hydrated coatings [193].
- Local imaging can overlook rare but critical defects [35]; combining imaging with statistical sampling is essential to support reliability claims [203].
- Quantitative interpretation of porosity fraction, crack density, defect size, and interface roughness requires calibrated image-analysis workflows and uncertainty reporting [204].
- Three-dimensional and synchrotron methods provide powerful structural information, but access, cost, field of view, reconstruction artifacts, and dose or preparation effects can limit routine qualification use [202].

### 5.3. Chemical and Interfacial Analysis

Chemical and interfacial analyses often employ X-ray photoelectron spectroscopy (XPS) to determine elemental composition and valence states, including depth profiling to confirm multilayer integrity and interphase chemistry [193]. Fourier-transform infrared spectroscopy (FTIR), attenuated total reflectance FTIR (ATR-FTIR), Raman spectroscopy, and time-of-flight secondary ion mass spectrometry (ToF-SIMS) provide complementary insights into bonding, functional groups, and molecular fragments, helping verify coupling reactions and identify contamination [193,205]. For metallic biomedical implants, these methods are especially useful when surface chemistry, oxide composition, and passive-film stability influence corrosion resistance and biocompatibility [188,205]. Silane-related analyses can verify primer coupling, hydrolysis/condensation chemistry, and adhesion-promoting interphases at polymer, oxide, or metal interfaces [73,96,135]. Synchrotron-based X-ray methods provide additional in situ or microscopic information on passive films and localized corrosion processes [202].

Advantages:

- Chemical analysis identifies surface chemistry, bonding states, oxide composition, and contaminants that influence adhesion, bioactivity, and corrosion performance [193].
- Depth profiling and interface-sensitive techniques can confirm primer coupling, interlayer diffusion, multilayer integrity, and oxide composition [95].
- Spectroscopic fingerprints provide mechanistic insight into hydrolysis, oxidation, and polymer degradation after sterilization or accelerated aging [49].
- Sterilization-specific analysis is useful because ethylene oxide, radiation, moist heat, and low-temperature alternatives can affect polymers, coatings, residues, and interfacial chemistry in different ways [8,9,44,50].

Limitations and trade-offs:

- Surface sensitivity and charging effects can complicate quantification, particularly for polymers, insulating oxides, hydrated coatings, and mixed organic–inorganic stacks [193,202].
- Depth profiling can introduce artifacts such as preferential sputtering, ion-beam reduction, interface mixing, and beam damage, so depth-resolved chemistry must be interpreted carefully [188,193].
- Correlating chemical signatures with mechanical performance often requires paired adhesion, corrosion, aging, or biological testing rather than relying solely on spectroscopy [205].
- Chemical maps and spectra are local measurements; therefore, sampling design and statistical treatment are needed when rare contamination, batch drift, or heterogeneous interphases may affect reliability [206].

### 5.4. Wettability, Fouling, and Kinetic Measurements

Surface wetting and biofouling-related properties are evaluated using contact angle measurements and surface energy analysis, as wettability strongly influences biomolecule adhesion and early biological interactions with material surfaces [191]. Quartz crystal microbalance with dissipation monitoring (QCM-D) can provide real-time data on protein-fouling adsorption and desorption kinetics or quantitative release profiles for drug-delivery coatings, making it valuable for validating antifouling and responsive systems [190]. Hydration layers and charge-neutral coatings are commonly evaluated in this context because stable surface hydration is a key mechanism in low-fouling and nonfouling biomaterials [15,207]. For antimicrobial or therapeutic coatings, release-based assays help distinguish passive antifouling behavior from active elution or stimuli-responsive antimi-

crobial delivery [207]. QCM-based approaches can also monitor cell–substrate adhesion and related cellular responses in real time [208].

Advantages:

- Contact-angle measurements rapidly assess changes in surface energy, while QCM-D provides real-time adsorption kinetics for antifouling performance [15,190,191].
- These measurements support mechanism-based design of hydration-layer and charge-neutral coatings [15,191].
- QCM and related kinetic assays enable real-time monitoring of release, adsorption, and desorption under controlled conditions [190,208].
- Cell-based QCM measurements can noninvasively monitor cell–substrate adhesion, morphology, mechanics, motility, and signaling responses relevant to biomedical surfaces [191,208].

Limitations and trade-offs:

- Single-point wettability metrics can be misleading if hysteresis, surface heterogeneity, protein adsorption, and aging are not accounted for, since many surfaces change over time [191].
- Biological assays show variability across batches, donors, and media; converting in vitro results to in vivo performance requires caution [190].
- QCM and related assays often rely on idealized model surfaces, so device-level translation may require additional validation [190].
- Acoustic cell-sensing outputs can be difficult to interpret because QCM signals may reflect coupled changes in adhesion, cell morphology, viscoelasticity, and cell–surface contact geometry [208].

### *5.5. Environmental Aging, Sterilization Cycling, and Dielectric Testing*

Environmental aging and sterilization cycles are essential for linking short-term material testing to real-world device lifetimes. Sterilization methods impose distinct stressors: thermal and moisture loads for steam (ISO 17665), oxidative and radical reactions for radiation (ISO 11137), and gas-phase chemistry with temperature and humidity changes for ethylene oxide (EtO) processes (ISO 11135) [8,9,44]. These stressors can alter polymer chain structure, residual stress, adhesion, and dielectric strength [30,49]. Accelerated aging procedures such as ASTM F1980 [209] support time-temperature equivalence studies, but they must be paired with appropriate failure indicators (such as adhesion loss, increased permeability, corrosion onset, or dielectric leakage) to avoid misinterpreting mechanical-property retention [49,210].

For coated electronics and assemblies, sterilization cycling should be evaluated alongside bias-driven stress tests because many clinically significant failures arise from the combination of moisture ingress and electric fields [130]. In practice, qualification plans benefit from a matrixed approach that covers sterilant type, cycle count, and post-sterilization dwell times (to monitor desorption or recovery), with pre-set acceptance criteria aligned with risk controls (ISO 14971) and materials biocompatibility standards (ISO 10993-1) [13,14,187].

Advantages:

- Environmental aging directly examines the stressors that cause field failures, including humidity, thermal cycling, sterilization, and chemical cleaning [30,211].
- Dielectric tests, including leakage current and breakdown strength, are sensitive indicators of barrier degradation in electronic protection [30,212].
- Accelerated protocols facilitate comparisons across architectures and help identify primary degradation pathways [49,210].

Limitations and trade-offs:

- Acceleration factors are not universal; poorly designed tests can alter failure modes and mislead lifetime extrapolations [210,211].
- Coupled exposures, such as humidity plus bias plus temperature or wear plus corrosion, are often necessary but more difficult to reproduce consistently [213–217].
- Device-level boundary conditions, including crevices, edges, and interfaces, can strongly influence results and should be represented in test coupons [205,218].

### *5.6. Electrochemical Characterization Toolbox*

Electrochemical endpoints, including $i_{corr}$, $E_{pit}$, $R_p$, passive current density, and impedance-derived parameters, are protocol-sensitive and often variable. Defensible interpretation therefore requires replicate measurements, prespecified endpoints, robust summaries such as medians with confidence intervals, and sufficient procedural detail to distinguish true material effects from test-condition effects [210,219,220]. In practice, electrochemical data are most persuasive when embedded in a broader failure argument that also includes the exposed-area definition, seal geometry, electrolyte composition, post-test imaging, ion release, and the physical location of failure initiation [205,219].

Electrochemical testing is commonly used to evaluate passivation, breakdown risk, corrosion kinetics, galvanic interactions, and coating-barrier integrity in metallic implants, alloys, and coated devices [205]. Because uniform corrosion, localized pitting or crevice corrosion, fretting or tribocorrosion, coating-pore development, and galvanic coupling occur across different time and length scales, a toolbox approach is preferable to any single canonical test. The most informative test set is usually small and deliberately complementary: one method tracks spontaneous evolution, another perturbs the system to probe susceptibility, and a third localizes damage or links it to transport through a coating defect [218,219,221].

Method selection should follow the failure question rather than routine habit. For intact barrier or encapsulation systems, long-duration open-circuit potential (OCP), linear polarization resistance (LPR), and electrochemical impedance spectroscopy (EIS) protocols are often more informative than aggressive polarization because they preserve the coating and reveal time-dependent barrier loss [220,221]. For passive metallic implants, cyclic polarization and controlled potentiostatic holds are more appropriate for probing breakdown, repassivation, and susceptibility to localized corrosion [31]. For multi-material assemblies or coated devices with deliberate defects, galvanic measurements and localized probes are often more informative than a single apparent corrosion-rate estimate [192]. In all cases, the following should be reported: exposed area, seal geometry, electrolyte composition, temperature, protein or peroxide content, stabilization time, scan rate, perturbation amplitude, and replicate structure, because these variables can alter both material ranking and inferred mechanism [218]. A recurring analytical problem is overinterpreting standardized polarization metrics, including ASTM F2129-style pitting data, as direct surrogates for lifetime. These metrics are valuable for comparative susceptibility, but they should be interpreted alongside coupon geometry, crevice control, surface finish, and post-test damage localization, especially when the intended claim concerns long-term implanted performance rather than short-duration breakdown ranking [31,205].

#### 5.6.1. Open Circuit Potential (OCP) and Immersion Monitoring

Open-circuit potential (OCP, $E_{corr}$) tracking during immersion provides a minimally invasive view of passive-film development, repassivation, and surface-chemistry changes, including protein adsorption, dissolved-oxygen variation, and crevice formation [218]. OCP trends are most valuable when paired with mass-loss or ion release measurements, for example, by inductively coupled plasma mass spectrometry (ICP-MS), and with surface

analysis to distinguish noble shifts caused by film thickening from those caused by reduced cathodic kinetics [205].

Advantages:

- Simple, non-destructive, and suitable for long-term monitoring in physiologically relevant media [218].
- Useful for tracking passive-film evolution, surface conditioning, and recovery after mechanical or chemical disturbance [205].

Limitations and trade-offs:

- OCP alone does not determine corrosion rate and should not be interpreted as a direct lifetime metric [219].
- Results can be affected by reference-electrode stability, solution buffering, oxygen content, protein adsorption, and changes in exposed area during immersion [218].

#### 5.6.2. Potentiodynamic and Cyclic Polarization (Including Pitting Metrics)

Potentiodynamic polarization yields corrosion potential and kinetic information, such as Tafel slopes and apparent $i_{corr}$, during controlled potential sweeps [219]. Cyclic polarization, including standardized implant protocols such as ASTM F2129, can determine breakdown and repassivation potentials and assess susceptibility to metastable or stable pitting in small metallic implant devices [31]. These tests are useful for evaluating how alloy chemistry, heat treatment, surface finishing, coatings, or primers affect passive-film durability [205].

Advantages:

- Rapid comparative screening of passive-film stability and localized corrosion susceptibility [31].
- Provides quantitative breakdown and repassivation metrics that are often sensitive to surface processing and coating defects [205].

Limitations and trade-offs:

- Results are accelerated and scan-rate dependent, so they may not reproduce long-term in vivo kinetics [31,219].
- Test artifacts can arise from crevices at seals, oxygen depletion, local heating, surface damage, or unrealistic polarization limits [31].
- Breakdown metrics should be interpreted as susceptibility indicators rather than direct service-life predictions [210].

#### 5.6.3. Polarization Resistance ($R_p$)/Linear Polarization Resistance (LPR), Galvanic Coupling, and Electrochemical Noise

Linear polarization resistance near $E_{corr}$ enables calculation of $R_p$ and supports time-series monitoring of corrosion progress during immersion [222]. Galvanic current and mixed-potential measurements, including zero-resistance ammetry in coupled assemblies, help quantify dissimilar-metal interactions and the effects of coatings at interfaces [219]. Electrochemical noise analysis can detect stochastic transients associated with metastable pitting, film rupture, or coating-defect activation when interpreted alongside complementary methods [223].

Advantages:

- Relatively low disturbance and suitable for repeated monitoring when perturbation amplitudes are controlled [222].
- Supports ranking of processing variables, surface treatments, and coating defects during immersion [219].
- Galvanic testing is directly applicable to multi-material implant assemblies and to coated electronic packages [205].

Limitations and trade-offs:

- Converting $R_p$ to corrosion rate requires assumptions about the Stern–Geary coefficient and the active reaction mechanisms [222].
- Localized corrosion, evolving passive films, and coating defects can violate the linearity assumptions underlying simple $R_p$ interpretation [224].
- Electrochemical noise is sensitive to instrumentation, filtering, sampling frequency, and reference electrode stability [223].

#### 5.6.4. Chrono-Methods and Controlled Pit/Crevice Propagation (Potentiostatic/Galvanostatic Holds)

Potential-step or constant-potential chronoamperometric protocols can assess passive-film stability, pit nucleation statistics, and pit or crevice propagation under controlled driving forces [205,219]. Constant-current methods are useful for studying propagation under transport limitations and for producing reproducible damage morphologies suitable for post-test microscopy. For coatings, chrono-methods can accelerate electrolyte ingress and enable correlation of current transients with pore formation, under-film corrosion, and interfacial failure [29].

Advantages:

- Directly probes initiation and propagation behavior under controlled electrochemical driving force [205].
- Enables mechanistic linkage between current transients, microscopy, surface chemistry, and localized damage [225].

Limitations and trade-offs:

- Requires precise control of exposed area, seal geometry, and crevice geometry [219].
- May drive conditions beyond service-relevant potentials if the imposed potential or current is not clinically justified [218].

#### 5.6.5. Localized and Scanning Electrochemical Methods (Micro-/Nano-Probes)

Localized techniques map spatial heterogeneity in electrochemical activity and help link corrosion behavior to microstructure, coating defects, and coating holidays [156]. The scanning vibrating electrode technique (SVET) and related scanning reference-electrode approaches provide solution-field or current-density maps above active sites [156]. Scanning electrochemical microscopy (SECM) probes local reactivity with microelectrodes, while scanning electrochemical cell microscopy (SECCM) and related droplet-cell methods can target individual grains, second phases, weld regions, or interfacial regions for localized polarization and transport measurements [192,225,226]. Frequency-domain mapping and scanning Kelvin probe approaches can also help distinguish coating degradation and under-film delamination fronts when combined with complementary surface imaging [156].

Advantages:

- Provides spatially resolved insight into grain-boundary effects, defects, galvanic micro-couples, and coating holidays [192].
- Enables correlative mapping with EBSD, SEM, XPS, Raman, or localized damage imaging [226].

Limitations and trade-offs:

- Higher experimental complexity and lower throughput than global electrochemical methods [192,226,227].
- Sensitive to topography, probe positioning, electrolyte geometry, and mass-transport conditions [157].
- Quantitative interpretation often requires field geometry and transport modeling [158].

#### 5.6.6. Impedance and Frequency-Domain Methods

Electrochemical impedance spectroscopy (EIS) and related frequency-domain methods can distinguish coating-barrier response, interfacial charge transfer, and transport time constants, especially in coated systems and thin-film encapsulation stacks [221,224]. Because equivalent-circuit fits can be non-unique, EIS should be treated primarily as a model-discrimination and trend-tracking tool rather than as a source of automatically identifiable physical constants [224]. Interpretation is strengthened when candidate circuits are constrained by the known coating architecture, frequency-domain artifacts are reported, and fitted trends are cross-checked against polarization behavior, ion release, microscopy, or localized electrochemical probes [220,221].

Advantages:

- Sensitive to early-stage barrier degradation and to water or ion ingress in coatings [221,224].
- Supports in situ monitoring over time and can be less destructive than DC polarization methods [37].
- Compatible with coated systems where DC tests may be dominated by isolated defects [221].
- Machine-learning tools may help classify or interpret EIS spectra, but they require careful design and validation of the training set [228].

Limitations and trade-offs:

- Equivalent-circuit non-uniqueness and parameter correlation can make fitted constants appear more physically certain than they actually are [220,224].
- Results depend on perturbation amplitude, stationarity, frequency range, and instrument verification [192,220].
- Spatial averaging can obscure localized attacks unless EIS is paired with microscopy or localized electrochemical methods [192,227].
- Machine-learning interpretation of EIS data is constrained by training-set representativeness, dataset size, and the realism of simulated spectra [228].

### *5.7. Synchrotron-Based Characterization and Operando Corrosion Analytics*

For synchrotron tomography and correlative mapping, especially X-ray fluorescence (XRF) and X-ray absorption near-edge structure (XANES) workflows, segmentation and registration uncertainties should be quantified, and pit or defect metrics should be reported as distributions across multiple regions of interest (ROIs) and specimens [201,229]. Time-alignment of operando imaging with electrochemical signals is equally important for model calibration and for avoiding cherry-picked single volumes [201].

Synchrotron facilities produce high-brightness, energy-tunable X-rays that enable in situ/operando analysis of passive films, corrosion byproducts, and under-film chemistry with spatial resolutions from micro- to nano-scale and time resolutions that are difficult to match with laboratory tools [202]. For implant alloys and protective coatings, synchrotron methods are especially useful for directly assessing oxidation states and local coordination, mapping compositional variations across microstructures and defects, and monitoring the growth of pits, cracks, and corrosion byproducts in real time [202,205].

#### 5.7.1. Synchrotron XPS Family: Ambient-Pressure XPS (AP-XPS), Hard X-Ray Photoelectron Spectroscopy (HAXPES), and Photoemission Electron Microscopy (PEEM)

Synchrotron-based XPS enhances traditional surface chemistry analysis by delivering higher photon flux and tunable excitation energy [202]. Near-ambient/ambient-pressure XPS (AP-XPS) enables the study of solid–vapor, solid–liquid, or humid interfaces under more realistic environmental conditions [230,231]. Hard X-ray photoelectron spectroscopy (HAXPES) increases information depth, enabling examination of buried oxide-metal inter-

faces, subsurface alloy enrichment, and multilayer stacks beyond the shallow sampling depth of conventional XPS [232]. Photoelectron emission microscopy, including PEEM and XPEEM, provides laterally resolved chemical and electronic imaging that can reveal microstructural heterogeneity in passive films and corrosion products [233].

#### 5.7.2. X-Ray Absorption Spectroscopy (XAS): X-Ray Absorption Near-Edge Structure (XANES), Extended X-Ray Absorption Fine Structure (EXAFS), and Micro-XAS

X-ray absorption spectroscopy (XAS) provides element-specific information on electronic structure and local coordination in corrosion products, passive films, and protective surface layers [201]. XANES is sensitive to oxidation state and bonding environment, whereas extended X-ray absorption fine structure (EXAFS) provides short-range structural information, including coordination numbers and bond-distance trends. Micro-XAS and related nano-probe approaches enable spatially resolved speciation across heterogeneous microstructures and at localized corrosion sites.

#### 5.7.3. Grazing-Incidence X-Ray Diffraction (GI-XRD) and X-Ray Reflectivity (XRR)

Grazing-incidence X-ray diffraction (GI-XRD/GIXD) can detect crystalline phases in ultrathin surface films and corrosion products with enhanced surface sensitivity [234]. X-ray reflectivity (XRR) provides complementary information on film thickness, density, and roughness in layered stacks [235]. Together, GI-XRD and XRR can validate growth models for conversion coatings, passive films, and ALD-based multilayers and help distinguish densification from chemical transformation during aging or electrochemical exposure.

#### 5.7.4. X-Ray Fluorescence (XRF) Mapping and Correlative Microanalysis

Synchrotron XRF imaging maps elemental distributions with high sensitivity and can detect redistribution of alloying elements, inhibitor uptake, and localized enrichment or depletion around pits, cracks, and interfaces [236]. When combined with SEM, EBSD, TEM, and localized electrochemical mapping, XRF can help attribute localized breakdown to specific microstructural or compositional features.

#### 5.7.5. Radiography and Tomography for Real-Time Pit and Crack Evolution

Synchrotron radiography and micro-tomography enable direct observation of pit nucleation, pit growth morphology, lacy-cover evolution, and transport-limited propagation under electrochemical control [201]. In situ synchrotron X-ray radiography has also been used to determine pit propagation parameters for stainless steels during pitting in chloride environments, linking growth kinetics to diffusion control and solution conductivity [237]. Pit-to-crack studies further link localized corrosion morphology to environmentally assisted cracking and fatigue-relevant damage evolution [225].

#### 5.7.6. Practical Considerations and Integration with Modeling

Key practical considerations include customizing electrochemical cells to match the beamline geometry, mitigating beam-induced heating or chemical changes, and managing large multimodal datasets. Synchrotron datasets are well suited to hybrid analysis pipelines that combine physics-based models with machine learning for tomogram segmentation, spectral deconvolution, uncertainty quantification, and automated detection of breakdown precursors [229]. When synchrotron and electrochemical measurements are planned together, they can reduce parameter uncertainty, improve model calibration, and shorten the iterate-and-test cycle for coating and alloy development.

## 6. Data-Driven Design, Statistics, and Artificial Intelligence-Enabled Service-Life Prediction

This section links mechanistic degradation modeling with statistical inference, reliability analysis, and artificial intelligence-assisted workflows to translate laboratory, accelerated-aging, and in vivo evidence into defensible service-life statements. The central premise is that data-driven methods are most useful when they preserve the problem's causal structure: endpoints should be prespecified, features should remain traceable to chemistry, mechanics, or transport, and validation should mirror how decisions will be made during development or qualification [238,239].

### *6.1. Multiphysics Modeling and Simulation of Degradation, Interfaces, and In Vivo Environments*

Multiphysics models aim to capture the coupled fields that drive failure, including electrochemical kinetics and transport (ions, oxygen, water) [205], polymer or oxide barrier transport, electro-chemo-mechanical damage (stress, plasticity, cracking) [34], and tribocorrosion under load and motion [181]. For coated metallic implants and device housings, the most informative models typically combine (i) Poisson-Nernst-Planck or dilute-solution transport [205], (ii) Butler-Volmer or Tafel kinetics with film-growth or film-breakdown terms [33], (iii) cohesive-zone or fracture-delamination mechanics for interfaces [240], and (iv) microstructure-aware pit or crevice growth using phase-field or moving-boundary descriptions [34].

A practical modeling approach is to start with a calibrated minimum viable physics model that matches available measurements (for example, OCP, polarization, or LPR-derived kinetics [222], localized current mapping [192], thickness, porosity, or defect metrology), then add couplings only when they explain a verified failure mode. Model credibility depends on parameter identifiability, sensitivity analysis, and uncertainty quantification because many corrosion and transport parameters are strongly correlated and can otherwise yield non-unique fits that appear numerically precise but are physically weak [241]. In this context, a smaller model with traceable assumptions is often more useful for qualification than a larger model whose parameters cannot be independently identified [242].

Representative case study: phase-field modeling of pitting and mechanically assisted corrosion in biodegradable Mg alloys shows that localized electrochemical dissolution can interact with stress concentrations to accelerate pit growth and damage progression, explaining why purely electrochemical models often underestimate degradation under load [34].

### *6.2. Time-to-Event (Time-to-Failure) and Service-Life Prediction for Complex Systems*

The logic of censoring-aware durability comparison, including right-censored observations, Kaplan–Meier-style survival curves, and B10 life markers, is summarized schematically in Figure 5. Many reliability questions are naturally expressed as time-to-event outcomes: time to coating failure, time to threshold ion release, time to hermeticity loss, or time to performance drift beyond specification. Such datasets commonly include right-censoring (items that have not failed by the study end), interval censoring (failures detected only between inspections), and competing failure modes. Survival and reliability analysis methods, including reliability statistics [243]; Kaplan–Meier analysis [244]; DeepSurv [245], transparent prediction-model reporting guidance [246], and the Cox model [247], are therefore more appropriate than simple mean-time summaries because they preserve incomplete information and allow materials, process conditions, and environments to be compared on a common durability scale.

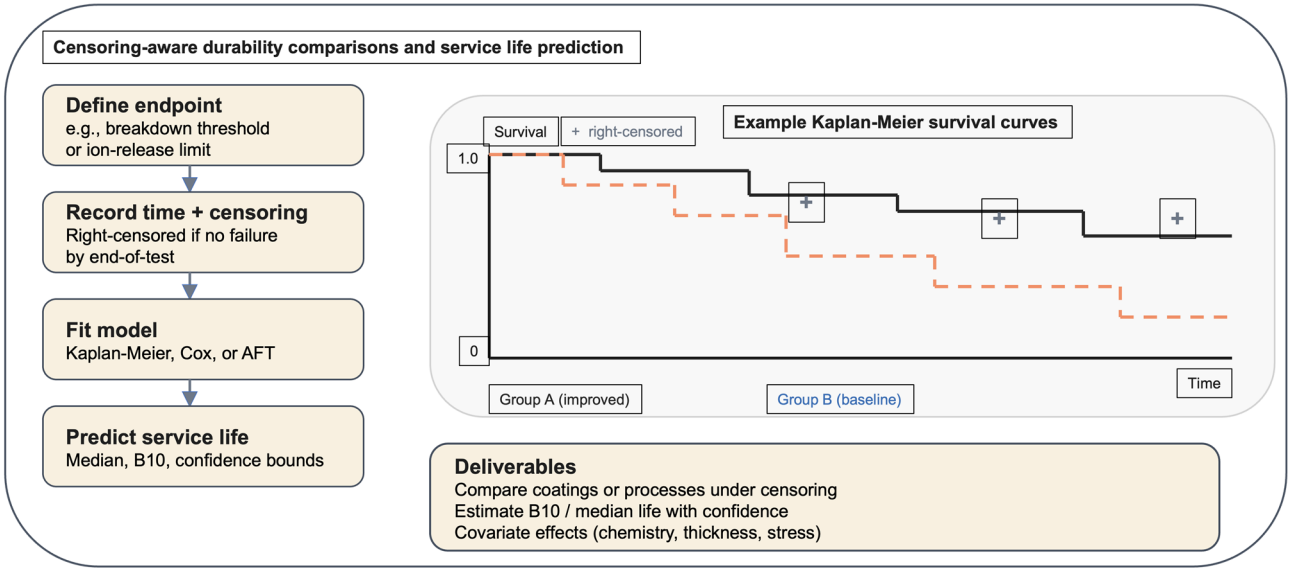



**Figure 5.** Illustrative schematic of censoring-aware time-to-event durability modeling and service-life comparison, including right-censored observations, Kaplan–Meier-style survival curves, and B10 life markers (the time by which 10% of units have failed under the defined endpoint). The curves are illustrative only and intended to clarify the analysis logic rather than to report measured data. Abbreviations: AFT, accelerated failure time.

Common tools include Kaplan–Meier curves with confidence bands for nonparametric survival estimation, Cox proportional hazards models for assessing covariate effects, and accelerated-failure-time (AFT) models with Weibull or lognormal distributions to relate accelerated aging conditions to usage environments [247]. For devices with multiple competing degradation mechanisms, such as pitting, fretting-corrosion, or delamination, competing-risk models can assess how process changes affect the occurrence of each mode rather than collapsing all failures into a single undifferentiated endpoint [248]. The key discipline is to define the event before fitting the model, retain censored units in the dataset, and report diagnostics to assess whether proportional-hazards or acceleration assumptions are plausible for the observed mechanism.

### Worked Example: Combining Accelerated Fatigue Testing and Clinical Survival Modeling in Dental Implant Systems

A published biomedical example of time-to-event reliability analysis is the study by Bergamo et al., which evaluated anterior crowns supported by narrow dental implant systems using step-stress accelerated life testing (SSALT) in water [249]. The authors first used single-load-to-failure testing to define accelerated fatigue profiles, then loaded the implant-supported crown assemblies off-axis until fracture or suspension. Survival was analyzed using Weibull curves for use-level probabilities, mission reliability estimates, Weibull shape parameters, and failure-mode analysis, providing a laboratory framework for translating accelerated fatigue data into implant-system reliability statements [249]. The article describes SSALT as a method in biomaterials science for evaluating the failure behavior of implant-supported rehabilitations under clinically relevant mechanical loading scenarios.

This type of experimental dataset can be structured at the device level, with each implant-supported assembly assigned to a design group, fatigue profile, event or suspension status, cycle count or equivalent service time, and observed failure mode. In this framing, fractured specimens are treated as events, while specimens that survive the test profile are treated as censored or suspended observations. Weibull-based reliability esti-

mates then provide more decision-relevant information than mean lifetime alone because they describe the lower-tail failure probability and mission survival under a defined loading condition [249].

A complementary clinical example is the multi-task survival modeling study by Nooraldaim et al., which modeled dental implant failure and subsequent reimplantation as dependent, sequential clinical events. The study introduced a multi-task survival framework with conditional masking, attention-based feature interactions, monotonicity regularization, and dependency alignment to jointly predict implant failure and subsequent reimplantation [250]. This approach is useful for complex biomedical systems because traditional single-event survival models may not capture conditional dependencies between linked clinical outcomes, such as implant failure followed by reimplantation at the same site.

Together, these two cases illustrate a defensible workflow for biomedical service-life prediction. SSALT and Weibull analyses can estimate laboratory reliability under controlled mechanical or environmental stress, while clinical survival models can evaluate how patient-, site-, procedure-, and device-level factors affect real-world failure trajectories. For coated or surface-engineered implants, the same framework can be extended by defining coating delamination, threshold ion release, excessive wear, loss of osseointegration, or implant removal as prespecified events. The key requirement is that the event definition, censoring rule, failure mode, and model assumptions be specified before fitting the survival or reliability model.

### *6.3. Artificial Intelligence (AI)-Assisted Modeling, Inverse Analysis, and Multimodal Data Fusion*

Artificial intelligence can enhance both physics-based and statistical reliability models by (i) building fast surrogates for expensive multiphysics simulations, (ii) supporting inverse analysis or parameter inference from limited measurements, and (iii) integrating diverse data streams, including electrochemical metrics, microscopy or computed tomography, spectroscopy, and in situ sensor logs. Physics-informed machine learning is particularly valuable when experimental data are scarce, but governing equations, bounds, or conservation constraints are known [250].

For durability prediction, modern survival machine-learning techniques, such as random survival forests, deep Cox models, and gradient-boosted survival methods, can accommodate nonlinear covariate effects, interactions, and high-dimensional features from images or spectra while still providing time-dependent risk estimates [251]. Their main weakness in surface-engineering datasets is not algorithmic capacity but data fragility: small $n$, lot effects, partially observed failure modes, and hidden correlations among specimens from the same deposition run can inflate apparent performance. Model governance should therefore focus on leakage-free validation, preferably by manufacturing lot or test campaign rather than by individual specimen; calibration of predicted failure probabilities; and uncertainty statements that are decision-relevant for qualification rather than merely impressive on internal cross-validation.

A recommended workflow is hybrid: use multiphysics simulation or mechanistic metrology to generate physically meaningful features, such as local chloride activity, interfacial stress intensity, defect density, or predicted water-uptake gradients, and then apply statistical or machine-learning survival models, including the Cox model and random survival forests [247,252], to link those features to time-to-event outcomes under real-world variability and censoring [244]. This approach keeps the model interpretable enough to support process decisions while preserving flexibility for multimodal data integration.

### 6.4. How AI Can Accelerate R&D of Surface Engineering Methods and Techniques

Beyond prediction, AI can accelerate the design-build-test cycle by guiding experiments and process development. Active learning and Bayesian optimization [253] can adaptively select the next experiments (chemistry, surface-prep settings, coating thickness/stack) that are most informative for the target goal, thereby reducing the number of runs required to achieve a qualified design window [253]. A useful literature review is available in [254].

In manufacturing and metrology, computer vision can detect defects such as pits, pores, and delamination fronts and generate standardized descriptors for subsequent modeling. Meanwhile, natural-language processing can systematically extract evidence from the literature and internal reports. When combined with calibrated multiphysics models, these techniques enable digital twin-style decision support by updating risk assessments and remaining useful life estimates as new inspection or sensor data become available [250,255].

AI-integrated workflows that combine experiments, simulations, and historical qualification data can accelerate screening, broaden process windows, and reduce time-to-qualification while preserving interpretability (Figure 6) [255]. The methods covered include cross-validation [256], model calibration [257], SHAP (SHapley Additive exPlanations) [258], bias-aware cross-validation assessment [259], proper scoring rules [260], and the Brier score [261]. Feature-contribution tools can further translate durability-model outputs into global design drivers and local sample-level explanations, as illustrated schematically in Figure 7.

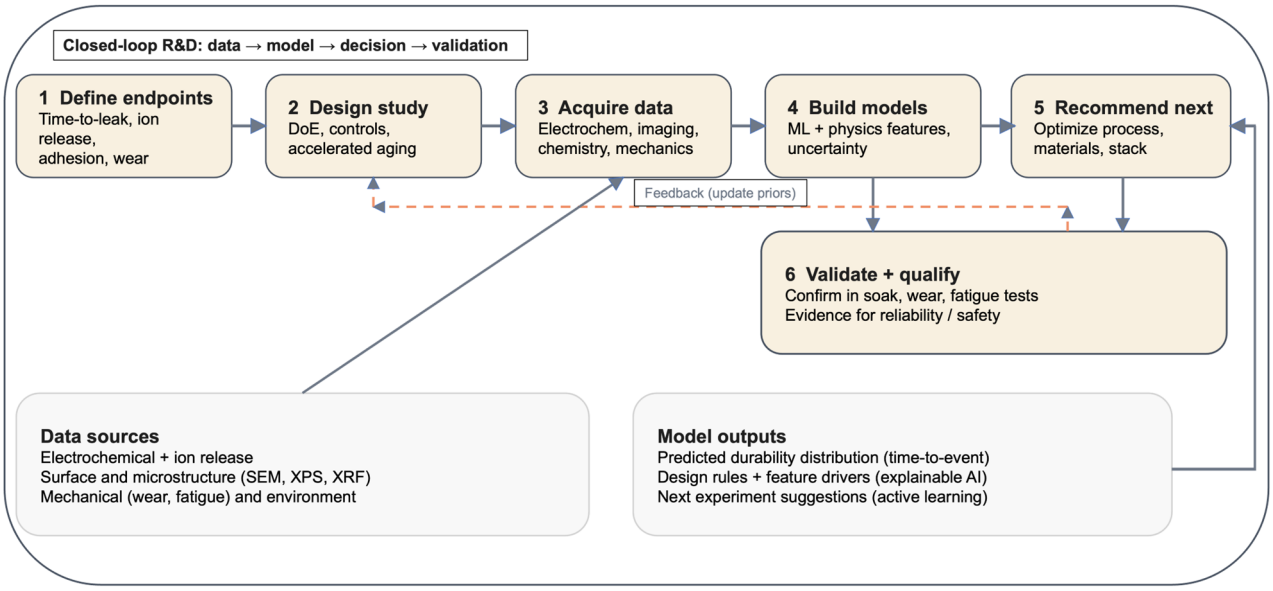



**Figure 6.** An illustrative schematic of an artificial intelligence-assisted workflow linking endpoint definition, controlled experimentation, modeling, and qualification evidence. The figure is conceptual rather than quantitative and intended to show the workflow's dependency structure. Abbreviations in the schematic include DoE (design of experiments); ML (machine learning); SEM (scanning electron microscopy); XPS (X-ray photoelectron spectroscopy); and XRF (X-ray fluorescence).

Key factors for dependable AI in medical-device surface engineering:

- High-quality metadata (surface-prep timing, plasma recipe, humidity history, sterilization cycles) helps avoid hidden confounders.
- Standardized endpoints (adhesion after conditioning, including tape adhesion [189] and thermal-spray adhesion [262], leakage current thresholds, and barrier resistance and capacitance metrics, including impedance-derived parameters when used) to support cross-study comparability [193].

- Include 'negative' and failure data to prevent overly optimistic models and to train classifiers on realistic defect distributions [263,264]. See reviews on implant corrosion [205] and MAO implants [83].
- Human-in-the-loop review and mechanistic sanity checks to ensure predictions remain physically plausible and clinically relevant.

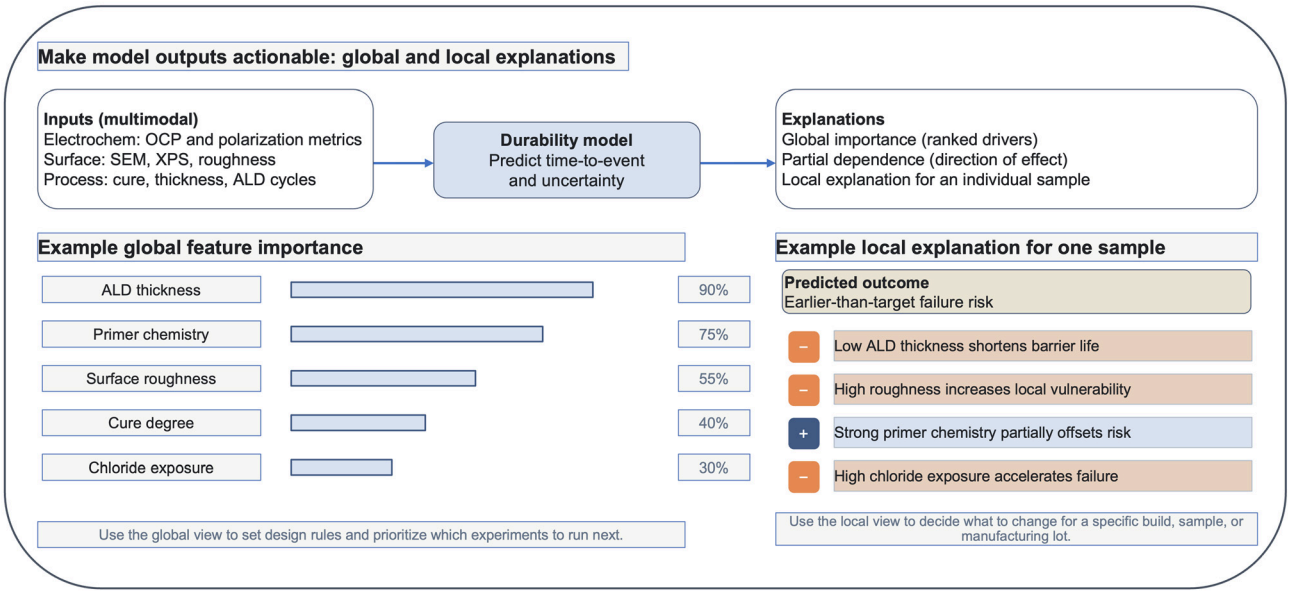



**Figure 7.** An illustrative schematic of durability analytics and feature-contribution interpretation for explainable, decision-oriented coating models. The importance rankings and local contributions shown in the figure are hypothetical examples intended to illustrate interpretation rather than represent measured results. Abbreviations in the schematic include OCP (open circuit potential); SEM (scanning electron microscopy); XPS (X-ray photoelectron spectroscopy); and ALD (atomic layer deposition).

### *6.5. Statistical Design, Inference, and Reporting for Surface/Coating Studies*

To make performance claims defensible, studies should report uncertainty and variability rather than relying on a single best-case curve. Recommended practices include (i) a priori power or precision planning, (ii) replicate measurements across days or batches, (iii) effect sizes with confidence intervals, and (iv) proper control for multiple comparisons when screening many factors [265].

Because surface engineering outcomes are often batch- and geometry-dependent, mixed-effects models (random intercepts and slopes) can distinguish within-batch noise from between-batch drift (e.g., electrolyte age, tool wear, chamber history). For time-series electrochemical transients, signal-processing techniques (change-point detection, event counting of metastable breakdowns) can yield robust summary metrics that are more reproducible than raw traces [229]. When repeated inspections produce binary pass/fail sequences, the observation process should be modeled explicitly rather than reduced to a single uncensored outcome [266].

For publication-quality comparisons, report: sample size (n), replicate structure (within- or between-batch), summary statistics (mean/median and spread), confidence intervals, and a clear definition of the endpoint (e.g., time-to-breakdown defined by a current threshold or an ion release criterion) [206].

#### 6.5.1. Minimum Statistical Reporting Checklist for Durability and Interface Studies

Table 11 presents a minimum reporting checklist that enhances comparability across studies and reduces over-claiming in underpowered, multi-endpoint experiments. The

checklist highlights clear endpoint definitions, uncertainty quantification, and model validation, using established methods in experimental design, survival and reliability analysis, and modern model calibration and interpretability [206].

**Table 11.** Minimum statistical reporting checklist for durability, adhesion, and barrier performance studies. Abbreviations: ALT, accelerated life testing; LOD, limit of detection; FDR, false discovery rate.

| Category | Minimum Items to Report | Why it Matters |
| --- | --- | --- |
| Study design and data provenance | Design type (factorial, response surface, split plot), randomization, blocking, and replication plan [267].<br>Unit of analysis and independence assumptions (device, site, batch), and how batches/animals were handled (fixed vs. random effects) [229].<br>Missing data handling and data inclusion/exclusion rules, pre-registered if possible [246]; CV assessment [259]. | Enables valid inference and reduces confounding, especially when lot, animal, or operator effects dominate variance [229,267]. |
| Endpoints and censoring | Primary endpoint(s) with operational definition, measurement resolution, and censoring rules (right, interval, left) [210].<br>Inspection schedule and how detection limits are treated (below LOD, saturated sensors). | Prevents biased time-to-failure or rate estimates and supports reproducible time-to-event comparisons across labs [210,244]. |
| Model choice and assumptions | Justification for distributional form (Weibull, lognormal) or semi-parametric model, and assumption checks (proportional hazards, goodness-of-fit) [197].<br>Acceleration model choice and stress variables (Arrhenius, Eyring, inverse power) with sensitivity analysis [210]. | Model mismatch can shift predicted service life by orders of magnitude, especially when extrapolating from ALT to use conditions [210]. |
| Uncertainty and multiple endpoints | Confidence intervals for key metrics (median survival, hazard ratio, acceleration factor), and uncertainty propagation to service-life predictions [210,247].<br>Multiple comparisons control when screening many chemistries, sites, or imaging channels (false discovery rate, FDR or family-wise approaches) [268]. | Quantifies decision risk and avoids false discoveries when many coatings or metrics are evaluated in parallel [268]. |
| Validation, calibration, interpretability | Out-of-sample evaluation plan (nested cross-validation or time-split), and appropriate scoring rules for probabilistic predictions [259,260].<br>Calibration checks for probabilistic durability forecasts (reliability diagrams, expected calibration error) [257].<br>Interpretability method for feature drivers, with caveats (e.g., Shapley-based attributions) [258]. | Separates models that fit historical data from models that generalize, and supports defensible engineering decisions under uncertainty [257,258,260]. |

#### 6.5.2. Endpoint-to-Model Mapping and Recommended Analytics

Table 12 provides a practical mapping of common coating and interface endpoints to recommended statistical models and reporting targets. The goal is to align the analysis

with the data-generating process, such as censored time-to-leak data versus repeated ion release measurements, and to make assumptions transparent to reviewers and regulators.

**Table 12.** Recommended statistical models by endpoint and data structure. Abbreviations: AFT, accelerated failure time; PH, proportional hazards; CI, confidence interval; CV, cross-validation; ANOVA, analysis of variance; AUC/PR, area under the precision-recall curve; LOD, limit of detection.

| Endpoint (Typical Data) | Recommended Model(s) | Key Outputs to Report | Notes and Pitfalls |
|---|---|---|---|
| Time-to-leak, time-to-failure, revision-free survival (right or interval censored) | Kaplan–Meier curves, log rank test, Cox PH with covariates, parametric Weibull or lognormal AFT [197,244,247]. | Median or quantiles with CI, hazard ratio or acceleration factor, survival at clinically relevant times [244,247]. | State censoring and inspection intervals explicitly [247]; check PH assumptions [269]; consider competing risks when multiple failure modes exist. |
| ALT at elevated temperature, voltage, load, and humidity | Arrhenius, Eyring, inverse power, or generalized Eyring models with uncertainty propagation [210,270]. | Model form, fitted acceleration parameters, prediction interval at use condition, model sensitivity [14]. | Do not extrapolate from a single stress level, validate stress relevance, and report model diagnostics [49,210]. |
| Ion release or drug release vs. time (repeated measures, often log-normal) | Mixed effects regression or nonlinear mixed effects, with batch and subject random effects [229]. | Release rate constants or area under the curve with CI, between batch variance, and residual variance [229,271]. | Account for limit of detection (LOD) censoring, correlation across time, and lot-to-lot effects that can dominate mean trends [229]. |
| Adhesion strength, scratch critical load, pull off force (continuous, sometimes skewed) | ANOVA or regression with DoE factors, robust or generalized linear models if non-normal, hierarchical models for batches [229,267]. | Effect sizes with CI, variance components, interaction effects, and model residual checks [267,268]. | Avoid pseudoreplication, report specimen count vs. device count, and correct for multiple endpoints if screening many primers [268]. |
| Wear rate, friction coefficient, impedance and electrochemical metrics, corrosion current (continuous, repeated, or time series) | Mixed effects, generalized estimating equations, or state-space models for drift, plus change-point detection for regime shifts [229,272]. | Slope or steady state value with CI, within-device variability, time of transition [273,274]. | Time correlation matters; random effects are needed when multiple tracks or sites per device are measured [229]. |
| Defect counts, pitting events, crack density (counts, overdispersed) | Poisson or negative binomial regression, zero-inflated models when many zeros, spatial point process models if location matters [274,275]. | Event rate ratio with CI, dispersion parameters, spatial clustering metrics [274–276]. | Report area or volume normalization, imaging thresholding, and uncertainty from segmentation [277,278]. |
| Image-based classification or segmentation (ML outputs, probabilities) | Train/validation split with nested CV, calibration, uncertainty, and interpretable feature attribution [246,257–259]. | AUC/PR, calibration error, confusion matrix at chosen threshold, explanation summary [257,258]. | Report data leakage controls, class imbalance handling, and calibration because uncalibrated probabilities mislead reliability decisions [257]. |

### *6.6. Service-Life Prediction: Acceleration Models and System-Level Reliability*

Accelerated life testing (ALT) relates increased stress conditions to usage conditions via an acceleration model, such as temperature, chloride activity, applied potential, or cyclic

strain. Widely used methods include Arrhenius-type thermal acceleration, Eyring models that combine temperature with an additional stress factor, and inverse power relationships for mechanical or electrical stress. These methods, such as the Arrhenius model [49] and the Eyring model [270], help extrapolate time-to-failure distributions, assuming the stress is mechanically relevant and that multiple stress levels are tested [210].

Complex implantable systems rarely fail from a single cause. A practical approach is to model each main component or interface as a subsystem with its own failure distribution, then combine them using system reliability logic (series, parallel, common cause), while monitoring how manufacturing lot effects and use environments alter the parameters [210,229]. This breakdown also supports targeted design improvements by clarifying whether the main hazard stems from barrier breakdown, adhesion loss, wear-generated debris, or electrochemical instability [219].

Model validation should avoid leakage by splitting training and validation data by manufacturing lot, test campaign, or subject cohort rather than by individual specimens. For probabilistic durability forecasts, calibration should be verified, for example, via CV assessment [259] by checking whether a predicted 20% failure rate at a given time matches the observed 20% failure rate on held-out data [257]. When models are used for decision-making (such as screening candidates or recommending next experiments), proper scoring rules (e.g., Brier score [261]) and uncertainty-aware evaluation help reduce the risk of optimizing for miscalibrated or overconfident predictors [260].

### *6.7. Concrete Biomedical and Coatings-Relevant AI Examples*

Concrete examples of journal articles are now emerging, and their value lies less in the mere use of machine learning than in whether the model addresses a decision-relevant materials question. In antifouling surface design, Le et al. used machine learning to relate molecular descriptors and surface chemistry to protein adsorption, producing quantitative design rules for protein-resistant coatings and enabling more efficient prioritization of candidate surfaces [279]. In electrochemical analysis, Klemm and Frömling developed a machine-learning-assisted pipeline to detect equivalent-circuit diagrams in scientific publications and convert them into machine-readable circuit descriptions, supporting meta-analysis of equivalent-circuit usage across electrochemical impedance spectroscopy (EIS) studies [280]. More directly relevant to biomedical metallic systems, Kurtz et al. used unsupervised clustering of EIS-derived features to correlate oxide degradation with selective dissolution in additively manufactured Ti-6Al-4V, using Ti-29Nb-21Zr as a comparison alloy [27]. Outside coatings per se but still relevant to implant design, Chen et al. combined finite-element simulations with an artificial neural network and particle swarm optimization to enable rapid design optimization of complete-arch implant-supported prostheses [28].

These examples are promising, yet they also show why adoption in biomedical coatings remains limited. Many datasets remain small, protocol-specific, and weakly annotated with process metadata, defect statistics, censoring structure, lot effects, or true failure outcomes. Many studies also stop at classification accuracy rather than addressing calibration, uncertainty, and qualification relevance. For polymeric biomaterials, McDonald et al. emphasize that machine-learning progress depends on better, medically relevant datasets and standardized characterization [281]. For antimicrobial surfaces, Chen et al. show that literature-derived datasets can support machine-learning prediction of bactericidal efficiency for nanostructured surfaces [282]. For sensor-interfacing or cell-contacting biomaterials, real-time QCM measurements can provide cell–substrate adhesion and response data that could feed future multimodal models [59,208]. For biodegradable metallic biomaterials, Zn-based additive-manufacturing studies illustrate the need to link processing,

degradation behavior, mechanical properties, antibacterial activity, and biocompatibility in unified datasets [59]. In that setting, artificial intelligence can shorten iteration cycles and improve experimental prioritization, but only if features remain traceable to failure physics, validation splits reflect how new lots or chemistries will appear in practice, and final outputs are expressed in terms that matter for qualification.

A practical open-source software workflow for EIS analysis, censored time-to-failure modeling, materials descriptors, uncertainty analysis, and experiment planning is provided in Appendix A.

### *6.8. Integrative Case Study: TiN-Coated Orthopedic Implant*

To make the proposed integration concrete, consider a titanium nitride (TiN)-coated Ti6Al4V orthopedic component, where the primary risks are localized corrosion at coating defects, tribocorrosion under micromotion, and delamination driven by residual stress and cyclic contact loading [196]. A risk-managed qualification path begins by translating hazards such as ion release, wear debris, third-body particle generation, and loss of function into prespecified endpoints per ISO 14971 [14]. Cyclic potentiodynamic polarization of representative metallic components or coupons can assess breakdown and repassivation metrics per ASTM F2129 [31]. Wear-corrosion synergy analysis can be applied when mechanical wear and electrochemical dissolution act together [182]. Adhesion or critical-load screening should be paired with post-test fractography to distinguish interfacial delamination from cohesive coating damage [196]. Biocompatibility planning under ISO 10993-1 is appropriate when coating chemistry, degradation products, or debris profile changes [13].

The resulting qualification dataset is naturally multimodal because it integrates imaging, mechanical, electrochemical, tribological, and chemical evidence. Defect metrics, roughness, thickness, residual stress, adhesion results, polarization or impedance outputs, wear-corrosion responses, ion release data, and post-test microscopy can be incorporated into a minimal multiphysics model that links defect-mediated transport to interfacial mechanics.

## 7. Outlook and Future Directions

Several priorities recur in the next phase of surface and interface engineering for medical and biomedical devices. Together, they signal a shift away from single-property optimization toward qualification strategies that account for coupled chemical, mechanical, biological, and environmental failure pathways.

### *7.1. Sterilization-Resistant Coating Chemistry and Architecture*

Low-stress coatings, primers, and multilayer stacks designed for repeated steam, radiation, ethylene oxide, or plasma-based sterilization remain a major need. Sterilization can alter residual stress, interfacial water uptake, adhesion, or brittle-film cracking before conventional room-temperature barrier metrics visibly deteriorate (Table 2) [186]. This challenge is especially important for thin-film encapsulation and chip-scale biomedical devices, where small defects can become dominant reliability risks [130].

### *7.2. Durable Bioactive and Anti-Infective Interfaces*

A second priority is developing bioactive and anti-infective interfaces that preserve biological function and structural durability. Structured oxides, ceramic phases, and Ti implant coatings are promising only if their chemistry and adhesion remain stable after clinically relevant conditioning (Table 8) [105]. Hydration-layer-based antifouling polymers are attractive because they reduce nonspecific biomolecule adsorption, but their long-term value depends on interphase stability during aqueous exposure [15]. Active antimicrobial

systems, including release-based strategies, require control of release kinetics, antimicrobial efficacy, and coating retention over time [15]. Silver-based systems must balance antimicrobial activity with dose-dependent cytotoxicity and tissue compatibility [283]. Antimicrobial peptides and other biologically inspired approaches offer additional opportunities, but they require durability testing under realistic sterilization and biofluid exposure conditions [284].

### *7.3. Continuing Efforts in the Development of Smart, Adaptive, and Responsive Coatings*

Smart coatings with sensing, controlled-release, or environment-responsive behavior are attractive because they can respond to local pH, redox state, infection cues, or interfacial damage. Their adoption will require dynamic characterization rather than static before-and-after testing, because responsiveness can introduce new trade-offs in mechanical integrity, reproducibility, and failure predictability [285]. Multi-objective optimization will be needed to balance antifouling, antimicrobial, mechanical, and degradation requirements within the same coating system [191].

### *7.4. Long-Term Stability of Grafted Polymers and Interphases*

A fourth priority is improving the durability of grafted functional polymers, silane layers, and hybrid interphases. Degradation processes such as degrafting, hydrolysis, oxidation, and interfacial reconstruction can undermine antifouling or bioactive surfaces, even when initial biological performance is strong. This issue is central to translation because many coating concepts fail due to interphase degradation rather than the intended biological mechanism.

### *7.5. In Situ and Time-Resolved Characterization*

Broader adoption of in situ and time-resolved characterization is needed to validate structure–function relationships under realistic cycling conditions. Quartz crystal microbalance methods can track adsorption, desorption, and cell–surface interactions in real time (Table 9) [208]. Operando synchrotron tomography and radiography can capture pit growth, defect evolution, and corrosion propagation that would be missed by post-mortem imaging alone [286]. Electrochemical impedance and time-lapse electrochemical monitoring can reveal early barrier degradation and interfacial transport before macroscopic failure [221].

### *7.6. Manufacturing Translation and Process Control*

Multilayer systems will be adopted only if scale-up, purity control, and contamination prevention are managed with the same rigor as the nominal coating chemistry. Buried particles, lot drift, activation-to-coating delay, chamber history, and interfacial contamination can dominate failure in interface-sensitive stacks. Reliability statistics and distribution-based reporting are therefore essential for distinguishing robust process improvements from isolated best-case results [210]. Weibull-type analyses are particularly useful when lower-tail performance, rather than average performance, determines qualification risk [197].

### *7.7. Benchmark Datasets and Protocol-Aware Metadata*

Shared benchmark datasets and protocol-aware metadata standards are needed to advance physics-informed and interpretable AI models beyond isolated proof-of-concept demonstrations. Machine-learning studies of antifouling coatings demonstrate the value of linking surface chemistry and molecular descriptors to biological performance [279]. EIS-based machine-learning studies show that data-driven tools can help organize complex electrochemical evidence, but only when metadata and validation are handled carefully [280]. For biomedical alloys, lot-aware and protocol-aware datasets are especially important because model performance can be inflated when specimens from the same processing route or test campaign are split across training and validation sets [27].

### *7.8. Biodegradable and Additively Manufactured Biomaterials*

The expansion of zinc-based biodegradable and additively manufactured biomaterial platforms will require tighter integration of corrosion control, surface finishing, coating design, and in vivo validation. In these systems, the acceptable degradation trajectory is a design target rather than merely a failure mode to be delayed [59]. Machine-learning-guided biomaterials design may help accelerate this process, but only when datasets jointly capture composition, processing, interfacial chemistry, electrochemical response, mechanical integrity, and biological outcome [200,281].

Overall, the field is shifting from single-layer protection to engineered stacks designed around coupled failure pathways. The strongest opportunities lie where mechanistic characterization, standards-aware qualification, and statistically sound durability modeling are planned from the start rather than added sequentially at the end of development. In this framework, electrochemical models, corrosion simulations, antifouling design rules, and reliability statistics become complementary components of a unified qualification argument rather than separate validation exercises [224].

## 8. Conclusions

This review integrated coating technologies, surface pretreatments, interfacial science, standards-based qualification, electrochemical diagnostics, and data-driven reliability methods into a practical framework for medical and biomedical devices. Across these areas, the literature supports a central conclusion: the decisive property is often interfacial rather than purely bulk. Durable systems are achieved when coating architecture, substrate class, device geometry, process history, and test methods are matched to the dominant failure pathway, whether that pathway involves tribocorrosion, loss of wet adhesion, dielectric leakage, sterilization damage, localized corrosion, or depletion of functional surface chemistry.

Accordingly, claims of corrosion resistance, adhesion, sterilization stability, antifouling performance, antimicrobial function, or electronic protection should not be considered in isolation. Electrochemical, mechanical, chemical, biological, and microstructural results are most useful when evaluated together and, where possible, translated into censoring-aware durability, accelerated-aging, or service-life analyses. The most reliable path forward is therefore not a universal coating recipe but an application-specific stack-design strategy supported by explicit process control, mechanistic characterization, clinically relevant conditioning, and statistically defensible qualification data.

**Author Contributions:** Conceptualization, Data curation, Formal analysis, Investigation, Methodology, Project administration, Resources, Supervision, Validation, Visualization, Writing—original draft, Writing—review & editing, M.S.Y.; Conceptualization, Data curation, Formal analysis, Investigation, Methodology, Project administration, Resources, Supervision, Validation, Visualization, Writing—original draft, Writing—review & editing C.X. All authors have read and agreed to the published version of the manuscript.

**Funding:** This research received no external funding.

**Data Availability Statement:** No new data were created or analyzed in this study.

**Acknowledgments:** During the preparation of this manuscript, the authors used ChatGPT (OpenAI, GPT-5) for language editing, grammar correction, and improving the clarity and readability of the text. The authors have reviewed and edited the output and take full responsibility for the content of this publication.

**Conflicts of Interest:** The authors declare no conflicts of interest.

## Appendix A. Open-Source Software Resources and Literature-Derived Workflow for AI/Statistics in Biomedical Surface Reliability

This appendix presents a reproducible, literature-derived workflow for AI- and statistical analyses of biomedical-device surface reliability. The workflow supports electrochemical impedance fitting, source provenance tracking, censored time-to-failure analysis, accelerated life modeling, materials descriptor generation, uncertainty and sensitivity analysis, image-derived failure feature extraction, and next experiment planning.

The workflow should begin with source-labeled rows extracted from published papers, internal reports, or new experiments. At a minimum, each row should include the source identifier, DOI or report identifier, device or material system, substrate, coating stack, process variables, exposure environment, endpoint definition, measured value or failure time, censoring indicator, inspection schedule, and evidence of independent validation. Relevant validation evidence may include microscopy, XPS/ToF-SIMS, ion release, leakage current, impedance, post-aging adhesion, or post-test fractography. Values should not be pooled when endpoint definitions, exposure protocols, inspection intervals, or failure thresholds are incompatible.

A practical workflow is as follows. First, define the unit of analysis, endpoint, censoring rule, and failure mode before fitting any model. Second, extract physically meaningful descriptors, such as coating thickness, roughness, defect density, EIS parameters, ion release rate, sterilization history, or processing lot. Third, analyze time-to-event outcomes using methods that preserve censored observations rather than summarizing them as a mean lifetime. Fourth, use accelerated-life models only when the acceleration mechanism is justified and tested across multiple stress levels. Fifth, validate predictive models using leakage-free splits by source study, manufacturing lot, test campaign, or subject cohort. Finally, report calibration, uncertainty, and failure-mode interpretation alongside any accuracy metric.

**Table A1.** Open-source software resources for reproducible AI/statistical workflows in biomedical surface reliability. Repository names are listed as GitHub identifiers where available. Entries with peer-reviewed software or methods papers are cited accordingly; entries primarily supported by repository, documentation, PyPI, CRAN, or Zenodo records should be treated as practical open-code resources rather than biomedical coating validation studies.

| Task in this Review | Open-Source Software/Repository | What the Code Contributes | Reader-Useful Output | Critical Caution |
|---|---|---|---|---|
| EIS/barrier-parameter extraction | ECSHackWeek/ impedance.py [287] | Reads EIS data, preprocesses spectra, fits equivalent-circuit models, and plots Nyquist/Bode outputs. | Coating resistance, capacitance/CPE terms, diffusion-related terms, residuals, and fitted spectra that can be joined to aging or failure rows. | Equivalent circuits must be physically justified and checked against soak tests, ion release, microscopy, and failure location. |
| Automated EIS model screening | AutoEIS [288] | Uses automated model-generation and Bayesian/model-selection logic to propose statistically plausible equivalent circuits. | Candidate ECMs, parameter uncertainty indicators, and reduced user bias in high-throughput EIS triage. | Automated circuit selection does not prove mechanism; implausible circuits should be rejected using electrochemical and physical evidence. |

**Table A1.** *Cont.*

| Task in this Review | Open-Source Software/Repository | What the Code Contributes | Reader-Useful Output | Critical Caution |
|---|---|---|---|---|
| EIS validation, DRT, and GUI/API workflows | DearEIS [289] | Provides Kramers–Kronig/Z-HIT validation, DRT estimation, circuit fitting, simulation, visualization, and GUI/API access. | Validated spectra, DRT features, fit checks, and transparent project files for readers who cannot rely on proprietary EIS software. | Consistency tests detect spectral problems; they do not identify a coating failure mode without linked physical evidence. |
| Right-censored durability comparison | lifelines [290] | Implements Kaplan–Meier curves, log-rank tests, Cox models, and related survival tools for right-censored observations. | Survival curves, median/B10 life, hazard ratios, confidence intervals, and group comparisons for coating designs or process lots. | Weekly inspections create interval-censored data unless detection-week times are explicitly treated as an approximation. |
| Machine-learning survival models | scikit-survival [291] | Provides random survival forests, penalized Cox models, survival SVMs, and validation metrics for censored data. | Nonlinear risk scores, survival functions, time-dependent validation, and grouped cross-validation by lot or source study. | Requires enough independent specimens or lots; report calibration and uncertainty, not accuracy alone. |
| Deep and counterfactual survival modeling | pycox [292]; auton-survival [293] | Implements neural Cox/time-to-event models, counterfactual survival, phenotyping, and flexible survival prediction workflows. | Nonlinear survival predictions from EIS features, images, process logs, and metadata when datasets are sufficiently large. | Avoid for small-n coating studies unless external validation, calibration, and leakage-free grouping are possible. |
| Parametric/AFT survival and interval censoring | flexsurv [294] | Fits Weibull, lognormal, and flexible parametric survival models; supports interval-censored survival objects and publication-ready plots. | AFT ratios, life quantiles, extrapolated survival curves, interval-aware analyses, and censoring plots. | Distributional assumptions, inspection windows, and proportional-hazards/AFT assumptions should be reported and sensitivity-tested. |
| Materials and process descriptors | matminer [295] | Generates composition and structure descriptors from materials-science datasets. | Numerical descriptors for alloys, oxides, ceramics, or additives that can be combined with coating thickness, roughness, and process variables. | Composition descriptors alone are insufficient for coatings; add stack architecture, interface chemistry, environment, and sterilization variables. |
| Structure, phase, and Pourbaix-style analysis | pymatgen [296] | Represents structures/compositions and supports phase, electrochemical, and Materials Project-linked analyses. | Standardized chemistry/structure fields and mechanistically meaningful descriptors for alloy/oxide/coating datasets. | Database-derived descriptors must be reconciled with actual surface state, oxide chemistry, and manufacturing history. |

**Table A1.** *Cont.*

| Task in this Review | Open-Source Software/Repository | What the Code Contributes | Reader-Useful Output | Critical Caution |
|---|---|---|---|---|
| Closed-loop process optimization | botorch [297] | Implements Bayesian optimization tools for expensive experiments and simulations. | Next-experiment suggestions for ALD thickness, plasma dose, cure temperature, multilayer period, or roughness constraints. | Use only after objectives, constraints, feasible ranges, and stopping rules are defined; confirm suggestions experimentally. |
| Global sensitivity analysis | SALib [298] | Provides Sobol, Morris, FAST, and related sensitivity-analysis methods. | Ranking of assumptions or variables that most affect predicted service life, such as activation energy, Weibull shape, roughness, or chloride level. | Sensitivity analysis depends on credible parameter ranges; do not hide unsupported assumptions behind numerical rankings. |
| Uncertainty propagation and probabilistic reliability | openturns [299] | Supports probabilistic modeling, uncertainty propagation, metamodeling, and reliability analysis. | Prediction intervals, probability-of-failure estimates, and uncertainty budgets for ALT-to-use-condition extrapolation. | Propagate model uncertainty together with measurement uncertainty and parameter uncertainty. |
| Explainable ML for durability models | shap [258] | Computes feature-contribution explanations for trained ML models. | Global and local drivers of predicted coating failure risk, such as thickness, primer chemistry, roughness, and chloride exposure. | Explanations are model explanations, not causal proof; confirm with experiments and mechanistic evidence. |
| Defect, pit, crack, and delamination image features | scikit-image [300] | Provides image-processing tools for segmentation, morphology, texture, filtering, and feature extraction. | Pore/pit density, crack length, delamination area, roughness surrogates, and defect maps from optical, SEM, or CT images. | Image thresholds and segmentation parameters must be reported and validated against representative manual labels. |
| Cell, biofilm, fluorescence, and biological-response images | CellProfiler [301] | Provides reproducible biological image-analysis pipelines for object segmentation and measurement. | Cell coverage, morphology, fluorescence intensity, biofilm area, and phenotype descriptors linked to surface chemistry or coating aging. | Biological image features require assay controls and should not be interpreted as durability metrics without matched surface/failure evidence. |
| Open physics/ PDE examples | fipy [302] | Provides finite-volume PDE tools for diffusion, reaction-transport, and phase-field-style examples. | Transparent toy models for water/ion ingress, diffusion barriers, or coupled transport assumptions in coating stacks. | Do not extrapolate PDE outputs without calibrated parameters, boundary conditions, sensitivity checks, and experimental validation. |

## References

1. Yang, X.; Yu, X.; Qiu, S. Advances and Applications in Medical Coating Materials: A Comprehensive Review. *Front. Chem.* **2026**, *14*, 1760661. [CrossRef]
2. Tipnis, N.P.; Burgess, D.J. Sterilization of Implantable Polymer-Based Medical Devices: A Review. *Int. J. Pharm.* **2018**, *544*, 455–460. [CrossRef] [PubMed]

3. Costa, T.N.Q.; Dotta, T.C.; Galo, R.; Soares, M.E.d.C.; Pedrazzi, V. Effect of Tribocorrosion on Surface-Treated Titanium Alloy Implants: A Systematic Review with Meta-Analysis. *J. Mech. Behav. Biomed. Mater.* **2023**, *145*, 106008. [CrossRef]
4. Donlan, R.M. Biofilms and Device-Associated Infections. *Emerg. Infect. Dis.* **2001**, *7*, 277–281. [CrossRef] [PubMed]
5. Caldara, M.; Belgiovine, C.; Secchi, E.; Rusconi, R. Environmental, Microbiological, and Immunological Features of Bacterial Biofilms Associated with Implanted Medical Devices. *Clin. Microbiol. Rev.* **2022**, *35*, e0022120. [CrossRef]
6. Campoccia, D.; Montanaro, L.; Arciola, C.R. A Review of the Biomaterials Technologies for Infection-Resistant Surfaces. *Biomaterials* **2013**, *34*, 8533–8554. [CrossRef]
7. Gittens, R.A.; Olivares-Navarrete, R.; Schwartz, Z.; Boyan, B.D. Implant Osseointegration and the Role of Microroughness and Nanostructures: Lessons for Spine Implants. *Acta Biomater.* **2014**, *10*, 3363–3371. [CrossRef]
8. *ISO 11137-1:2025*; Sterilization of Health Care Products—Radiation—Part 1: Requirements for the Development, Validation and Routine Control of a Sterilization Process for Medical Devices. ISO: Geneva, Switzerland, 2025.
9. *ISO 17665:2024*; Sterilization of Health Care Products—Moist Heat—Requirements for the Development, Validation and Routine Control of a Sterilization Process for Medical Devices. ISO: Geneva, Switzerland, 2024.
10. Malisz, K.; Świeczko-Żurek, B.; Sionkowska, A. Preparation and Characterization of Diamond-like Carbon Coatings for Biomedical Applications—A Review. *Materials* **2023**, *16*, 3420. [CrossRef]
11. Golda-Cepa, M.; Engvall, K.; Hakkarainen, M.; Kotarba, A. Recent Progress on Parylene C Polymer for Biomedical Applications: A Review. *Prog. Org. Coat.* **2020**, *140*, 105493. [CrossRef]
12. George, S.M. Atomic Layer Deposition: An Overview. *Chem. Rev.* **2010**, *110*, 111–131. [CrossRef]
13. *ISO 10993-1:2025*; Biological Evaluation of Medical Devices—Part 1: Requirements and General Principles for the Evaluation of Biological Safety within a Risk Management Process. ISO: Geneva, Switzerland, 2025.
14. *ISO 14971:2019*; Medical Devices—Application of Risk Management to Medical Devices. ISO: Geneva, Switzerland, 2019.
15. Chen, S.; Li, L.; Zhao, C.; Zheng, J. Surface Hydration: Principles and Applications toward Low-Fouling/Nonfouling Biomaterials. *Polymer* **2010**, *51*, 5283–5293. [CrossRef]
16. Castner, D.G.; Ratner, B.D. Biomedical Surface Science: Foundations to Frontiers. *Surf. Sci.* **2002**, *500*, 28–60. [CrossRef]
17. Hetrick, E.M.; Schoenfisch, M.H. Reducing Implant-Related Infections: Active Release Strategies. *Chem. Soc. Rev.* **2006**, *35*, 780–789. [CrossRef] [PubMed]
18. AshaRani, P.V.; Mun, G.L.K.; Hande, M.P.; Valiyaveettil, S. Cytotoxicity and Genotoxicity of Silver Nanoparticles in Human Cells. *ACS Nano* **2009**, *3*, 279–290. [CrossRef]
19. Kazemzadeh-Narbat, M.; Cheng, H.; Chabok, R.; Alvarez, M.M.; de la Fuente-Nunez, C.; Phillips, K.S.; Khademhosseini, A. Strategies for Antimicrobial Peptide Coatings on Medical Devices: A Review and Regulatory Science Perspective. *Crit. Rev. Biotechnol.* **2021**, *41*, 94–120. [CrossRef]
20. Zhang, R.; Lin, H.; Wang, Z.; Cheng, S.; Li, C.; Wang, Y. Research Progress on Antimicrobial Biomaterials. *Macromol. Biosci.* **2025**, *25*, e00239. [CrossRef]
21. Yoda, I.; Koseki, H.; Tomita, M.; Shida, T.; Horiuchi, H.; Sakoda, H.; Osaki, M. Effect of Surface Roughness of Biomaterials on Staphylococcus Epidermidis Adhesion. *BMC Microbiol.* **2014**, *14*, 234. [CrossRef]
22. Lu, X.; Wu, Z.; Xu, K.; Wang, X.; Wang, S.; Qiu, H.; Li, X.; Chen, J. Multifunctional Coatings of Titanium Implants Toward Promoting Osseointegration and Preventing Infection: Recent Developments. *Front. Bioeng. Biotechnol.* **2021**, *9*, 783816. [CrossRef]
23. Skjöldebrand, C.; Tipper, J.L.; Hatto, P.; Bryant, M.; Hall, R.M.; Persson, C. Current Status and Future Potential of Wear-Resistant Coatings and Articulating Surfaces for Hip and Knee Implants. *Mater. Today Bio* **2022**, *15*, 100270. [CrossRef] [PubMed]
24. Chen, Q.; Thouas, G.A. Metallic Implant Biomaterials. *Mater. Sci. Eng. R Rep.* **2015**, *87*, 1–57. [CrossRef]
25. Shabalovskaya, S.; Anderegg, J.; Van Humbeeck, J. Critical Overview of Nitinol Surfaces and Their Modifications for Medical Applications. *Acta Biomater.* **2008**, *4*, 447–467. [CrossRef]
26. Tang, Y.; Wei, J.; Liu, Y.; Chang, Y.; Zheng, J. Machine Learning Aided Design and Optimization of Antifouling Surfaces. *Langmuir* **2024**, *40*, 22504–22515. [CrossRef] [PubMed]
27. Kurtz, M.A.; Alaniz, K.; Kurtz, P.W.; Wessinger, A.C.; Moreno-Reyes, A.; Gilbert, J.L. Oxide Degradation Precedes Additively Manufactured Ti-6Al-4V Selective Dissolution: An Unsupervised Machine Learning Correlation of Impedance and Dissolution Compared to Ti-29Nb-21Zr. *J. Biomed. Mater. Res. A* **2024**, *112*, 1250–1264. [CrossRef] [PubMed]
28. Chen, Y.C.; Lin, J.W.; Wang, K.H.; Lin, C.L. Real-Time Optimization of Prosthetic Design for Complete Arch Implant-Supported Treatments Using Finite Element-Based Machine Learning. *J. Prosthet. Dent.* **2025**, *134*, 1920–1928. [CrossRef] [PubMed]
29. Rupp, F.; Liang, L.; Geis-Gerstorfer, J.; Scheideler, L.; Hüttig, F. Surface Characteristics of Dental Implants: A Review. *Dent. Mater.* **2018**, *34*, 40–57. [CrossRef]
30. Xie, X.; Rieth, L.; Williams, L.; Negi, S.; Bhandari, R.; Caldwell, R.; Sharma, R.; Tathireddy, P.; Solzbacher, F. Long-Term Reliability of $Al_2O_3$ and Parylene C Bilayer Encapsulated Utah Electrode Array Based Neural Interfaces for Chronic Implantation. *J. Neural Eng.* **2014**, *11*, 026016. [CrossRef]

31. *ASTM F2129-25*; Test Method for Conducting Cyclic Potentiodynamic Polarization Measurements to Determine the Corrosion Susceptibility of Small Implant Devices. ASTM International: West Conshohocken, PA, USA, 2025.
32. Pound, B.G. The Use of Electrochemical Techniques to Evaluate the Corrosion Performance of Metallic Biomedical Materials and Devices. *J. Biomed. Mater. Res. B Appl. Biomater.* **2019**, *107*, 1189–1198. [CrossRef]
33. Bao, Y.; Muñoz, A.I.; Jolles, B.M.; Mischler, S. Assessment of In-Vivo Corrosion of Ti and CoCrMo Joint Implants by Electrochemical Measurements in Human Synovial Liquids. *Electrochim. Acta* **2024**, *476*, 143708. [CrossRef]
34. Kovacevic, S.; Ali, W.; Martínez-Pañeda, E.; LLorca, J. Phase-Field Modeling of Pitting and Mechanically-Assisted Corrosion of Mg Alloys for Biomedical Applications. *Acta Biomater.* **2023**, *164*, 641–658. [CrossRef]
35. Page, M.J.; McKenzie, J.E.; Bossuyt, P.M.; Boutron, I.; Hoffmann, T.C.; Mulrow, C.D.; Shamseer, L.; Tetzlaff, J.M.; Akl, E.A.; Brennan, S.E.; et al. The PRISMA 2020 Statement: An Updated Guideline for Reporting Systematic Reviews. *BMJ* **2021**, *372*, n71. [CrossRef]
36. McDonnell, G.; Burke, P. Disinfection: Is It Time to Reconsider Spaulding? *J. Hosp. Infect.* **2011**, *78*, 163–170. [CrossRef] [PubMed]
37. Rutala, W.A.; Weber, D.J. Disinfection and Sterilization in Health Care Facilities: What Clinicians Need to Know. *Clin. Infect. Dis.* **2004**, *39*, 702–709. [CrossRef] [PubMed]
38. Liu, Y.; Pharr, M.; Salvatore, G.A. Lab-on-Skin: A Review of Flexible and Stretchable Electronics for Wearable Health Monitoring. *ACS Nano* **2017**, *11*, 9614–9635. [CrossRef] [PubMed]
39. Kim, J.; Campbell, A.S.; de Ávila, B.E.F.; Wang, J. Wearable Biosensors for Healthcare Monitoring. *Nat. Biotechnol.* **2019**, *37*, 389–406. [CrossRef]
40. Ahn, S.H.; Jeong, J.; Kim, S.J. Emerging Encapsulation Technologies for Long-Term Reliability of Microfabricated Implantable Devices. *Micromachines* **2019**, *10*, 508. [CrossRef]
41. Jeong, J.; Laiwalla, F.; Lee, J.; Ritasalo, R.; Pudas, M.; Larson, L.; Leung, V.; Nurmikko, A. Conformal Hermetic Sealing of Wireless Microelectronic Implantable Chiplets by Multilayered Atomic Layer Deposition (ALD). *Adv. Funct. Mater.* **2019**, *29*, 1806440. [CrossRef]
42. *ISO 13485:2016*; Medical Devices—Quality Management Systems—Requirements for Regulatory Purposes. ISO: Geneva, Switzerland, 2016.
43. *IEC 60601-1:2005+AMD1:2012+AMD2:2020*; Medical Electrical Equipment—Part 1: General Requirements for Basic Safety and Essential Performance. International Electrotechnical Commission: Geneva, Switzerland, 2020.
44. *ISO 11135:2014*; Sterilization of Health-Care Products—Ethylene Oxide—Requirements for the Development, Validation and Routine Control of a Sterilization Process for Medical Devices. ISO: Geneva, Switzerland, 2014.
45. *IPC-CC-830C*; Qualification and Performance of Electrical Insulating Compound for Printed Wiring Assemblies. IPC: Bannockburn, IL, USA, 2018.
46. Das, P.P.; Vadlamudi, V.; Raihan, R. Dielectric State Variables as Qualitative Indicators of Moisture Absorption-Caused Mechanical Property Degradation in GFRP Composite Structures. *Compos. Part C Open Access* **2022**, *9*, 100295. [CrossRef]
47. Rubeck, S.; Cartailler, V.; Coutellier, V.; Imbert, G.; Gallois-Garreignot, S.; Meille, S.; Steyer, P.; Chevalier, J. Effect of Accelerated Hydrothermal Aging on the Durability of Si-Based Dielectric Thin Films. *Microelectron. Eng.* **2022**, *264*, 111858. [CrossRef]
48. Tran, D.P.; Lin, C.K.; To, B.D. Effects of Cyclic Deformation on a Barrier Thin Film for Flexible Organic Optoelectronic Devices. *Thin Solid Films* **2018**, *650*, 20–31. [CrossRef]
49. Janting, J.; Theander, J.G.; Egesborg, H. On Thermal Acceleration of Medical Device Polymer Aging. *IEEE Trans. Device Mater. Reliab.* **2019**, *19*, 313–321. [CrossRef]
50. McEvoy, B.; Rowan, N.J. Terminal Sterilization of Medical Devices Using Vaporized Hydrogen Peroxide: A Review of Current Methods and Emerging Opportunities. *J. Appl. Microbiol.* **2019**, *127*, 1403–1420. [CrossRef]
51. Al-Saidi, L.F.; Mortensen, K.; Almdal, K. Environmental Stress Cracking Resistance. Behaviour of Polycarbonate in Different Chemicals by Determination of the Time-Dependence of Stress at Constant Strains. *Polym. Degrad. Stab.* **2003**, *82*, 451–461. [CrossRef]
52. Figueira, R.B. Hybrid Sol-Gel Coatings for Corrosion Mitigation: A Critical Review. *Polymers* **2020**, *12*, 689. [CrossRef]
53. Li, C.; Cauwe, M.; Yang, Y.; Schaubroeck, D.; Mader, L.; de Beeck, M.O. Ultra-Long-Term Reliable Encapsulation Using an Atomic Layer Deposited $HfO_2/Al_2O_3/HfO_2$ Triple-Interlayer for Biomedical Implants. *Coatings* **2019**, *9*, 579. [CrossRef]
54. Jambagi, S.C.; Malik, V.R. A Review on Surface Engineering Perspective of Metallic Implants for Orthopaedic Applications. *JOM* **2021**, *73*, 4349–4364. [CrossRef]
55. Kaliaraj, G.S.; Siva, T.; Ramadoss, A. Surface Functionalized Bioceramics Coated on Metallic Implants for Biomedical and Anticorrosion Performance—A Review. *J. Mater. Chem. B* **2021**, *9*, 9433–9460. [CrossRef]
56. Xu, Y.; Li, Y.; Chen, T.; Dong, C.; Zhang, K.; Bao, X. A Short Review of Medical-Grade Stainless Steel: Corrosion Resistance and Novel Techniques. *J. Mater. Res. Technol.* **2024**, *29*, 2788–2798. [CrossRef]
57. Zhao, H.; Van Humbeeck, J.; È Rgen Sohier, J.; Scheerder, I. DE Electrochemical Polishing of 316L Stainless Steel Slotted Tube Coronary Stents. *J. Mater. Sci. Mater. Med.* **2002**, *13*, 911–916. [CrossRef] [PubMed]

58. Wang, Y.; Chen, M.; Zhao, Y. Preparation and Corrosion Resistance of Microarc Oxidation-Coated Biomedical Mg-Zn-Ca Alloy in the Silicon-Phosphorus-Mixed Electrolyte. *ACS Omega* **2019**, *4*, 20937–20947. [CrossRef]
59. Yuan, K.-S.; Deng, C.-C.; Wang, X.-X.; Li, Y.-C.; Zhou, C.; Zhao, C.-R.; Dai, X.-Z.; Khan, A.-R.; Zhang, Z.; Guidoin, R.; et al. Research Advances and Future Perspectives of Zinc-Based Biomaterials for Additive Manufacturing. *Rare Met.* **2025**, *44*, 4376–4410. [CrossRef]
60. Hanawa, T. Metal Ion Release from Metal Implants. *Mater. Sci. Eng. C* **2004**, *24*, 745–752. [CrossRef]
61. Lo, K.H.; Shek, C.H.; Lai, J.K.L. Recent Developments in Stainless Steels. *Mater. Sci. Eng. R Rep.* **2009**, *65*, 39–104. [CrossRef]
62. Saad, K.S.K.; Saba, T.; Bin Rashid, A. Application of PVD Coatings in Medical Implantology for Enhanced Performance, Biocompatibility, and Quality of Life. *Heliyon* **2024**, *10*, e35541. [CrossRef]
63. Sun, B.; Liu, Z.; He, Y.; Cao, F.; Li, X. A New Study for Healing Pitting Defects of 316L Stainless Steel Based on Microarc Technology. *Corros. Sci.* **2021**, *187*, 109505. [CrossRef]
64. Kirkland, N.T.; Birbilis, N.; Staiger, M.P. Assessing the Corrosion of Biodegradable Magnesium Implants: A Critical Review of Current Methodologies and Their Limitations. *Acta Biomater.* **2012**, *8*, 925–936. [CrossRef]
65. Witte, F. The History of Biodegradable Magnesium Implants: A Review. *Acta Biomater.* **2010**, *6*, 1680–1692. [CrossRef]
66. Li, Y.; Deng, C.; Xiao, D.; Bai, C.; Chang, L.; Feng, H.; Zhang, H.; Wang, G. Degradation Behavior and Biological Properties of a Novel Biodegradable Zinc Alloy Biliary Stent. *Bioact. Mater.* **2026**, *59*, 492–511. [CrossRef]
67. Shaik, Y.P.; Naidu, N.K.; Yadavalli, V.R.; Muthyala, M.R. The Comparison of the Mechanical Characteristics of ABS Using Three Different Plastic Production Techniques. *OAlib* **2023**, *10*, e10097. [CrossRef]
68. Savvides, N.; Bell, T.J. Hardness and Elastic Modulus of Diamond and Diamond-like Carbon Films. *Thin Solid Films* **1993**, *228*, 289–292. [CrossRef]
69. Yu, H.-H.; Hutchinson, J.W. Influence of Substrate Compliance on Buckling Delamination of Thin Films. *Int. J. Fract.* **2002**, *113*, 39–55. [CrossRef]
70. Primc, G.; Mozetič, M. Surface Modification of Polymers by Plasma Treatment for Appropriate Adhesion of Coatings. *Materials* **2024**, *17*, 1494. [CrossRef]
71. Sridhara, P.K.; Masso, F.; Olsén, P.; Vilaseca, F. Strong Polyamide-6 Nanocomposites with Cellulose Nanofibers Mediated by Green Solvent Mixtures. *Nanomaterials* **2021**, *11*, 2127. [CrossRef] [PubMed]
72. Tripp, M.K.; Stampfer, C.; Miller, D.C.; Helbling, T.; Herrmann, C.F.; Hierold, C.; Gall, K.; George, S.M.; Bright, V.M. The Mechanical Properties of Atomic Layer Deposited Alumina for Use in Micro- and Nano-Electromechanical Systems. *Sens. Actuators A Phys.* **2006**, *130–131*, 419–429. [CrossRef]
73. Aziz, T.; Ullah, A.; Fan, H.; Jamil, M.I.; Khan, F.U.; Ullah, R.; Iqbal, M.; Ali, A.; Ullah, B. Recent Progress in Silane Coupling Agent with Its Emerging Applications. *J. Polym. Environ.* **2021**, *29*, 3427–3443. [CrossRef]
74. Fasano, A.; Woyessa, G.; Stajanca, P.; Markos, C.; Stefani, A.; Nielsen, K.; Rasmussen, H.K.; Krebber, K.; Bang, O. Fabrication and Characterization of Polycarbonate Microstructured Polymer Optical Fibers for High-Temperature-Resistant Fiber Bragg Grating Strain Sensors. *Opt. Mater. Express* **2016**, *6*, 649–659. [CrossRef]
75. Framil, D.; Van Gompel, M.; Bourgeois, F.; Furno, I.; Leterrier, Y. The Influence of Microstructure on Nanomechanical and Diffusion Barrier Properties of Thin PECVD $SiO_x$ Films Deposited on Parylene C Substrates. *Front. Mater.* **2019**, *6*, 319. [CrossRef]
76. Howells, D.G.; Henry, B.M.; Leterrier, Y.; Månson, J.A.E.; Madocks, J.; Assender, H.E. Mechanical Properties of $SiO_x$ Gas Barrier Coatings on Polyester Films. *Surf. Coat. Technol.* **2008**, *202*, 3529–3537. [CrossRef]
77. Leterrier, Y.; Mottet, A.; Bouquet, N.; Gilliéron, D.; Dumont, P.; Pinyol, A.; Lalande, L.; Waller, J.H.; Månson, J.A.E. Mechanical Integrity of Thin Inorganic Coatings on Polymer Substrates under Quasi-Static, Thermal and Fatigue Loadings. *Thin Solid Films* **2010**, *519*, 1729–1737. [CrossRef]
78. Najeeb, S.; Zafar, M.S.; Khurshid, Z.; Siddiqui, F. Applications of Polyetheretherketone (PEEK) in Oral Implantology and Prosthodontics. *J. Prosthodont. Res.* **2016**, *60*, 12–19. [CrossRef]
79. Poilane, C.; Delobelle, P.; Bornier, L.; Mounaix, P.; Melique, X.; Lippens, D. Determination of the Mechanical Properties of Thin Polyimide Films Deposited on a GaAs Substrate by Bulging and Nanoindentation Tests. *Mater. Sci. Eng. A* **1999**, *262*, 101–106. [CrossRef]
80. Hu, L.; Zhang, X.; Sun, Y.I.; Williams, R.J.J. Hardness and Elastic Modulus Profiles of Hybrid Coatings. *J. Sol-Gel Sci. Technol.* **2005**, *34*, 41–46. [CrossRef]
81. Barrino, F. Hybrid Organic–Inorganic Materials Prepared by Sol–Gel and Sol–Gel-Coating Method for Biomedical Use: Study and Synthetic Review of Synthesis and Properties. *Coatings* **2024**, *14*, 425. [CrossRef]
82. Smith, J.R.; Lamprou, D.A. Polymer Coatings for Biomedical Applications: A Review. *Trans. Inst. Met. Finish.* **2014**, *92*, 9–19. [CrossRef]
83. Wen, X.; Liu, Y.; Xi, F.; Zhang, X.; Kang, Y. Micro-Arc Oxidation (MAO) and Its Potential for Improving the Performance of Titanium Implants in Biomedical Applications. *Front. Bioeng. Biotechnol.* **2023**, *11*, 1282590. [CrossRef]

84. Coad, B.R.; Favia, P.; Vasilev, K.; Griesser, H.J. Plasma Polymerization for Biomedical Applications: A Review. *Plasma Process. Polym.* **2022**, *19*, 2200121. [CrossRef]
85. Volinsky, A.A.; Moody, N.R.; Gerberich, W.W. Interfacial Toughness Measurements for Thin Films on Substrates. *Acta Mater.* **2002**, *50*, 441–466. [CrossRef]
86. Böke, F.; Giner, I.; Keller, A.; Grundmeier, G.; Fischer, H. Plasma-Enhanced Chemical Vapor Deposition (PE-CVD) Yields Better Hydrolytical Stability of Biocompatible $SiO_x$ Thin Films on Implant Alumina Ceramics Compared to Rapid Thermal Evaporation Physical Vapor Deposition (PVD). *ACS Appl. Mater. Interfaces* **2016**, *8*, 17805–17816. [CrossRef] [PubMed]
87. Kim, K.; Luo, H.; Zhu, T.; Pierron, O.N.; Graham, S. Influence of Polymer Substrate Damage on the Time Dependent Cracking of $SiN_x$ Barrier Films. *Sci. Rep.* **2018**, *8*, 4560. [CrossRef] [PubMed]
88. Jarvis, K.L.; Evans, P.J. Growth of Thin Barrier Films on Flexible Polymer Substrates by Atomic Layer Deposition. *Thin Solid Films* **2017**, *624*, 111–135. [CrossRef]
89. Willis, S.A.; McGuinness, E.K.; Li, Y.; Losego, M.D. Re-Examination of the Aqueous Stability of Atomic Layer Deposited (ALD) Amorphous Alumina ($Al_2O_3$) Thin Films and the Use of a Postdeposition Air Plasma Anneal to Enhance Stability. *Langmuir* **2021**, *37*, 14509–14519. [CrossRef]
90. Wu, J.; Fei, F.; Wei, C.; Chen, X.; Nie, S.; Zhang, D.; Su, W.; Cui, Z. Efficient Multi-Barrier Thin Film Encapsulation of OLED Using Alternating $Al_2O_3$ and Polymer Layers. *RSC Adv.* **2018**, *8*, 5721–5727. [CrossRef] [PubMed]
91. Deb, A.; Vihervaara, A.; Popov, G.; Chundak, M.; Abdelaal, A.O.; Santos, H.L.S.; Heikkilä, M.J.; Kemell, M.; Camargo, P.H.C.; Ritala, M.; et al. Atomic Layer Deposition of $Ti_xFe_2$-$XO_3$ Photoanodes and Photocurrent Response Optimization Using the Response Surface Methodology. *ACS Omega* **2025**, *10*, 14522–14535. [CrossRef] [PubMed]
92. Mercier, D.; Nicolay, A.; Boudiba, A.; Vanden Eynde, X.; Libralesso, L.; Daniel, A.; Olivier, M. Mechanical Properties and Decohesion of Sol–Gel Coatings on Metallic and Glass Substrates. *J. Solgel Sci. Technol.* **2020**, *93*, 229–243. [CrossRef]
93. Hegemann, D.; Brunner, H.; Oehr, C. Plasma Treatment of Polymers for Surface and Adhesion Improvement. *Nucl. Instrum. Methods Phys. Res. Sect. B Beam Interact. Mater. At.* **2003**, *208*, 281–286. [CrossRef]
94. Li, F.; Verdingovas, V.; Mantis, I.; Jellesen, M.S.; Ambat, R. Compatibility Study of No-Clean Flux Residue and Conformal Coatings Using Two Electrode Electrochemical Impedance Method. *Microelectron. Reliab.* **2024**, *159*, 115452. [CrossRef]
95. Ahangaran, F.; Navarchian, A.H. Recent Advances in Chemical Surface Modification of Metal Oxide Nanoparticles with Silane Coupling Agents: A Review. *Adv. Colloid Interface Sci.* **2020**, *286*, 102298. [CrossRef]
96. Perrin, F.; Grard, A.; Belec, L. Silane Primers as Adhesion Promotors for Coatings. *Proceedings* **2019**, *29*, 73. [CrossRef]
97. Zaki, S.; Zhang, N.; Gilchrist, M.D. Electropolishing and Shaping of Micro-Scale Metallic Features. *Micromachines* **2022**, *13*, 468. [CrossRef]
98. Beamud-González, E.M.; Núñez-López, P.J.; García-Plaza, E. Electropolishing Stainless Steel Optimization Using Surface Quality, Dimensional Accuracy, and Electrical Consumption Criteria. *Materials* **2023**, *16*, 1770. [CrossRef]
99. ur Rahman, Z.; Deen, K.M.; Cano, L.; Haider, W. The Effects of Parametric Changes in Electropolishing Process on Surface Properties of 316L Stainless Steel. *Appl. Surf. Sci.* **2017**, *410*, 432–444. [CrossRef]
100. Yan, T.; Wang, S.; He, W.; Jin, R.; Zhao, J.; Zou, Y.; Ouyang, J.; Wang, Y.; Zhou, Y. Precision Machining of Different Metals by Plasma Electrolytic Polishing: A Review for Improving Surface Smoothness and Properties. *Lubricants* **2025**, *13*, 412. [CrossRef]
101. Zatkalíková, V.; Podhorský, Š.; Štrbák, M.; Liptáková, T.; Markovičová, L.; Kuchariková, L. Plasma Electrolytic Polishing—An Ecological Way for Increased Corrosion Resistance in Austenitic Stainless Steels. *Materials* **2022**, *15*, 4223. [CrossRef]
102. Yang, D.; Sun, H.; Ji, G.; Xiang, Y.; Wang, J. Effect of Electrolytic Plasma Polishing on Surface Properties of Titanium Alloy. *Coatings* **2024**, *14*, 615. [CrossRef]
103. Nestler, K.; Böttger-Hiller, F.; Adamitzki, W.; Glowa, G.; Zeidler, H.; Schubert, A. Plasma Electrolytic Polishing—An Overview of Applied Technologies and Current Challenges to Extend the Polishable Material Range. *Procedia CIRP* **2016**, *42*, 503–507. [CrossRef]
104. Liu, D.; Zong, X.; Xue, P.; Gao, Z.; Wu, W.; Song, Z.; Ye, F.; Pang, Y.; Zhang, Y.; Zhou, H.; et al. Effects of Plasma Electrolytic Polishing Treatment on the Surface Morphology, Microstructure and Corrosion Resistance of Additively Manufactured TC4 Titanium Alloy. *J. Mater. Res. Technol.* **2025**, *35*, 7008–7017. [CrossRef]
105. AbuAlia, M.; Fullam, S.; Cinotti, F.; Manninen, N.; Wimmer, M.A. Titanium Nitride Coatings on CoCrMo and Ti6Al4V Alloys: Effects on Wear and Ion Release. *Lubricants* **2024**, *12*, 96. [CrossRef]
106. Bolton, J.; Hu, X. In Vitro Corrosion Testing of PVD Coatings Applied to a Surgical Grade Co–Cr–Mo Alloy. *J. Mater. Sci. Mater. Med.* **2002**, *13*, 567–574. [CrossRef]
107. Thorwarth, K.; Thorwarth, G.; Figi, R.; Weisse, B.; Stiefel, M.; Hauert, R. On Interlayer Stability and High-Cycle Simulator Performance of Diamond-like Carbon Layers for Articulating Joint Replacements. *Int. J. Mol. Sci.* **2014**, *15*, 10527–10540. [CrossRef]

108. Noori, M.; Atapour, M.; Ashrafizadeh, F.; Elmkhah, H.; di Confiengo, G.G.; Ferraris, S.; Perero, S.; Cardu, M.; Spriano, S. Nanostructured Multilayer CAE-PVD Coatings Based on Transition Metal Nitrides on Ti6Al4V Alloy for Biomedical Applications. *Ceram. Int.* **2023**, *49*, 23367–23382. [CrossRef]
109. Van Huy, W.; Rodionov, N.B.; Karpov, V.A.; Binh, N.T.; Khoa, N.D.; Vi, V.T.L. Topography, Mechanical Performance, and Corrosion Resistance of Multilayer Ti/CrN/TiN Coatings Prepared by Cathodic Arc Deposition under Varying Substrate Bias. *Prot. Met. Phys. Chem. Surf.* **2025**, *61*, 661–672. [CrossRef]
110. Mazzonello, A.; Buhagiar, J.; Chetcuti, R.; Dearnley, P.A.; Valsesia, A.; Colpo, P.; Mallia, B. A Tribocorrosion Appraisal of a Dual Layer PVD Coated CoCrMo Alloy Tribopair. *Surf. Coat. Technol.* **2022**, *442*, 128341. [CrossRef]
111. Spagnuolo, G.; Ametrano, G.; D'Antò, V.; Rengo, C.; Simeone, M.; Riccitiello, F.; Amato, M. Effect of Autoclaving on the Surfaces of TiN -Coated and Conventional Nickel-Titanium Rotary Instruments. *Int. Endod. J.* **2012**, *45*, 1148–1155. [CrossRef]
112. Peng, Y.; Peng, J.; Wang, Z.; Xiao, Y.; Qiu, X. Diamond-like Carbon Coatings in the Biomedical Field: Properties, Applications and Future Development. *Coatings* **2022**, *12*, 1088. [CrossRef]
113. Lan, G.; Deng, Y.; Chen, W.; Wang, C. Development and Application of Physical Vapor Deposited Coatings for Medical Devices: A Review. *Procedia CIRP* **2019**, *89*, 250–262. [CrossRef]
114. Stuart, B.W.; Stan, G.E. Physical Vapour Deposited Biomedical Coatings. *Coatings* **2021**, *11*, 619. [CrossRef]
115. Baptista, A.; Silva, F.; Porteiro, J.; Míguez, J.; Pinto, G. Sputtering Physical Vapour Deposition (PVD) Coatings: A Critical Review on Process Improvement Andmarket Trend Demands. *Coatings* **2018**, *8*, 402. [CrossRef]
116. Panjan, P.; Drnovšek, A.; Gselman, P.; Čekada, M.; Panjan, M. Review of Growth Defects in Thin Films Prepared by PVD Techniques. *Coatings* **2020**, *10*, 447. [CrossRef]
117. Abadias, G.; Chason, E.; Keckes, J.; Sebastiani, M.; Thompson, G.B.; Barthel, E.; Doll, G.L.; Murray, C.E.; Stoessel, C.H.; Martinu, L. Review Article: Stress in Thin Films and Coatings: Current Status, Challenges, and Prospects. *J. Vac. Sci. Technol. A Vac. Surf. Films* **2018**, *36*, 020801. [CrossRef]
118. Kashyap, V.; Ramkumar, P. DLC Coating over Pre-Oxidized and Textured Ti6Al4V for Superior Adhesion and Tribo-Performance of Hip Implant. *Surf. Coat. Technol.* **2022**, *440*, 128492. [CrossRef]
119. Tan, C.P.; Craighead, H.G. Surface Engineering and Patterning Using Parylene for Biological Applications. *Materials* **2010**, *3*, 1803–1832. [CrossRef]
120. Yim, J.H.; Rodriguez-Santiago, V.; Williams, A.A.; Gougousi, T.; Pappas, D.D.; Hirvonen, J.K. Atmospheric Pressure Plasma Enhanced Chemical Vapor Deposition of Hydrophobic Coatings Using Fluorine-Based Liquid Precursors. *Surf. Coat. Technol.* **2013**, *234*, 21–32. [CrossRef]
121. Dong, Y.; Yin, X.; Liu, W.; Shaikh, F.A.; Zhang, Z.; Wang, X. Suppression of Crack Formation in Wafer-Scale Amorphous $SiN_x$ Films by Residual Hydrogen-Ligands Manipulation. *Nano Trends* **2024**, *7*, 100044. [CrossRef]
122. Cremers, V.; Puurunen, R.L.; Dendooven, J. Conformality in Atomic Layer Deposition: Current Status Overview of Analysis and Modelling. *Appl. Phys. Rev.* **2019**, *6*, 021302. [CrossRef]
123. Yersak, A.S.; Lee, Y.-C. Probabilistic Distributions of Pinhole Defects in Atomic Layer Deposited Films on Polymeric Substrates. *J. Vac. Sci. Technol. A Vac. Surf. Films* **2016**, *34*, 4938496. [CrossRef]
124. Nam, T.; Lee, H.; Seo, S.; Cho, S.M.; Shong, B.; Lee, H.B.R.; Kim, H. Moisture Barrier Properties of Low-Temperature Atomic Layer Deposited $Al_2O_3$ Using Various Oxidants. *Ceram. Int.* **2019**, *45*, 19105–19112. [CrossRef]
125. Aslan, M.; Cava, K.; İpek, H.; Kumaran, S.T.; Kalusuraman, G.; Uthayakumar, M.; Prakash, C. Surface and Mechanical Properties of 3D-Printed Biocompatible ABS Polymers. *J. Mater. Eng. Perform.* **2024**, *33*, 6398–6407. [CrossRef]
126. Kacar, E.; Erdem, A.; Sanli, M.M.; Kayan, A.; Candan, L.; Yildiz, U.; Demir, A. Functionalized Hybrid Coatings on ABS Surfaces by PLD and Dip Coatings. *J. Inorg. Organomet. Polym. Mater.* **2016**, *26*, 895–906. [CrossRef]
127. Frigione, M.; Rodríguez-Prieto, A. Can Accelerated Aging Procedures Predict the Long Term Behavior of Polymers Exposed to Different Environments? *Polymers* **2021**, *13*, 2688. [CrossRef]
128. Wetzel, P.; Sambale, A.K.; Uhlig, K.; Stommel, M.; Schneider, B.; Kaiser, J.M. Hygromechanical Behavior of Polyamide 6.6: Experiments and Modeling. *Polymers* **2023**, *15*, 3387. [CrossRef]
129. Fang, M.; Zhang, N.; Huang, M.; Lu, B.; Lamnawar, K.; Liu, C.; Shen, C. Effects of Hydrothermal Aging of Carbon Fiber Reinforced Polycarbonate Composites on Mechanical Performance and Sand Erosion Resistance. *Polymers* **2020**, *12*, 2453. [CrossRef] [PubMed]
130. Xie, X.; Rieth, L.; Merugu, S.; Tathireddy, P.; Solzbacher, F. Plasma-Assisted Atomic Layer Deposition of $Al_2O_3$ and Parylene C Bi-Layer Encapsulation for Chronic Implantable Electronics. *Appl. Phys. Lett.* **2012**, *101*, 093702. [CrossRef]
131. Kurtz, S.M.; Devine, J.N. PEEK Biomaterials in Trauma, Orthopedic, and Spinal Implants. *Biomaterials* **2007**, *28*, 4845–4869. [CrossRef]
132. Ben Cheikh, I.; Parry, G.; Dalmas, D.; Estevez, R.; Marthelot, J. Analysis of the Multi-Cracking Mechanism of Brittle Thin Films on Elastic-Plastic Substrates. *Int. J. Solids Struct.* **2019**, *180–181*, 176–188. [CrossRef]

133. Atanacio, A.J.; Latella, B.A.; Barbé, C.J.; Swain, M.V. Mechanical Properties and Adhesion Characteristics of Hybrid Sol-Gel Thin Films. *Surf. Coat. Technol.* **2005**, *192*, 354–364. [CrossRef]
134. Montazerian, M.; Hosseinzadeh, F.; Migneco, C.; Fook, M.V.L.; Baino, F. Bioceramic Coatings on Metallic Implants: An Overview. *Ceram. Int.* **2022**, *48*, 8987–9005. [CrossRef]
135. Plueddemann, E.P. Silane Adhesion Promoters in Coatings. *Prog. Org. Coat.* **1983**, *11*, 297–308. [CrossRef]
136. Zhang, N.; Yu, S.; Xing, Q.; Chen, X.; Zhang, M.; Shen, D. Corrosion Performance of Composite MAO/$TiO_2$ Sol–Gel Coatings on Magnesium Alloy AZ91D. *J. Mater. Eng. Perform.* **2018**, *27*, 6080–6086. [CrossRef]
137. Novotna, Z.; Reznickova, A.; Rimpelova, S.; Vesely, M.; Kolska, Z.; Svorcik, V. Tailoring of PEEK Bioactivity for Improved Cell Interaction: Plasma Treatment in Action. *RSC Adv.* **2015**, *5*, 41428–41436. [CrossRef]
138. Carneiro de Oliveira, J.; Airoudj, A.; Kunemann, P.; Bally-Le Gall, F.; Roucoules, V. Mechanical Properties of Plasma Polymer Films: A Review. *SN Appl. Sci.* **2021**, *3*, 656. [CrossRef]
139. Ghobeira, R.; Esbah Tabaei, P.S.; Morent, R.; De Geyter, N. Chemical Characterization of Plasma-Activated Polymeric Surfaces via XPS Analyses: A Review. *Surf. Interfaces* **2022**, *31*, 102087. [CrossRef]
140. Sundriyal, P.; Pandey, M.; Bhattacharya, S. Plasma-Assisted Surface Alteration of Industrial Polymers for Improved Adhesive Bonding. *Int. J. Adhes. Adhes.* **2020**, *101*, 102626. [CrossRef]
141. Ma, X.; Li, T.; Yu, L.; Liu, P.; Yang, W.Y.; Li, W. From Hydrophobic to Hydrophilic: Enhancing Surface Properties of Parylene F Coatings through Oxygen Plasma Modification. *Colloids Surf. B Biointerfaces* **2026**, *258*, 115248. [CrossRef]
142. Raphel, J.; Holodniy, M.; Goodman, S.B.; Heilshorn, S.C. Multifunctional Coatings to Simultaneously Promote Osseointegration and Prevent Infection of Orthopaedic Implants. *Biomaterials* **2016**, *84*, 301–314. [CrossRef]
143. Khatoon, Z.; McTiernan, C.D.; Suuronen, E.J.; Mah, T.-F.; Alarcon, E.I.; Alarcon Bacterial, E.I. Bacterial Biofilm Formation on Implantable Devices and Approaches to Its Treatment and Prevention. *Heliyon* **2018**, *4*, e01067. [CrossRef] [PubMed]
144. Makishi, S.; Watanabe, T.; Saito, K.; Ohshima, H. Effect of Hydroxyapatite/β-Tricalcium Phosphate on Osseointegration after Implantation into Mouse Maxilla. *Int. J. Mol. Sci.* **2023**, *24*, 3124. [CrossRef]
145. Wang, Q.; Huang, J.Y.; Li, H.Q.; Chen, Z.; Zhao, A.Z.J.; Wang, Y.; Zhang, K.Q.; Sun, H.T.; Al-Deyab, S.S.; Lai, Y.K. $TiO_2$ Nanotube Platforms for Smart Drug Delivery: A Review. *Int. J. Nanomed.* **2016**, *11*, 4819–4834. [CrossRef] [PubMed]
146. Du, Q.; Wei, D.; Wang, Y.; Cheng, S.; Liu, S.; Zhou, Y.; Jia, D. The Effect of Applied Voltages on the Structure, Apatite-Inducing Ability and Antibacterial Ability of Micro Arc Oxidation Coating Formed on Titanium Surface. *Bioact. Mater.* **2018**, *3*, 426–433. [CrossRef] [PubMed]
147. Tsuchiya, H.; Shirai, T.; Nishida, H.; Murakami, H.; Kabata, T.; Yamamoto, N.; Watanabe, K.; Nakase, J. Innovative Antimicrobial Coating of Titanium Implants with Iodine. *J. Orthop. Sci.* **2012**, *17*, 595–604. [CrossRef]
148. Goda, T.; Ishihara, K.; Miyahara, Y. Critical Update on 2-Methacryloyloxyethyl Phosphorylcholine (MPC) Polymer Science. *J. Appl. Polym. Sci.* **2015**, *132*, 41766. [CrossRef]
149. Borges, M.H.R.; Nagay, B.E.; Costa, R.C.; Souza, J.G.S.; Mathew, M.T.; Barão, V.A.R. Recent Advances of Polypyrrole Conducting Polymer Film for Biomedical Application: Toward a Viable Platform for Cell-Microbial Interactions. *Adv. Colloid Interface Sci.* **2023**, *314*, 102860. [CrossRef]
150. Liubchak, I.; Lawrence, M.T.; Holness, F.B.; Price, A.D. Soft Template Electropolymerization of Polypyrrole for Improved Ph-Induced Drug Delivery. *Int. J. Mol. Sci.* **2020**, *21*, 8114. [CrossRef]
151. Yang, G.; Meng, Y.; Qian, C.; Chen, X.; Liu, P.; Zhou, H.; Kang, B.; Tang, X.; Diao, L.; Zhou, F. Review of Microarc Oxidation of Titanium Implant. *J. Vac. Sci. Technol. B* **2023**, *41*, 060801. [CrossRef]
152. Ul Haq, I.; Krukiewicz, K. Antimicrobial Approaches for Medical Implants Coating to Prevent Implants Associated Infections: Insights to Develop Durable Antimicrobial Implants. *Appl. Surf. Sci. Adv.* **2023**, *18*, 100532. [CrossRef]
153. Jamuna-Thevi, K.; Bakar, S.A.; Ibrahim, S.; Shahab, N.; Toff, M.R.M. Quantification of Silver Ion Release, in Vitro Cytotoxicity and Antibacterial Properties of Nanostuctured Ag Doped TiO2 Coatings on Stainless Steel Deposited by RF Magnetron Sputtering. *Vacuum* **2011**, *86*, 235–241. [CrossRef]
154. Singh, J.; Chatha, S.S.; Singh, H. Microstructural and In-Vitro Characteristics of Functional Calcium Silicate Topcoat on Hydroxyapatite Coating for Bio-Implant Applications. *Prog. Biomater.* **2022**, *11*, 95–108. [CrossRef] [PubMed]
155. Drexelius, M.G.; Neundorf, I. Application of Antimicrobial Peptides on Biomedical Implants: Three Ways to Pursue Peptide Coatings. *Int. J. Mol. Sci.* **2021**, *22*, 13212. [CrossRef] [PubMed]
156. Joshi, M.U.; Kulkarni, S.P.; Choppadandi, M.; Keerthana, M.; Kapusetti, G. Current State of Art Smart Coatings for Orthopedic Implants: A Comprehensive Review. *Smart Mater. Med.* **2023**, *4*, 661–679. [CrossRef]
157. Zhang, F.; Hu, Q.; Wei, Y.; Meng, W.; Wang, R.; Liu, J.; Nie, Y.; Luo, R.; Wang, Y.; Shen, B. Surface Modification of Titanium Implants by PH-Responsive Coating Designed for Self-Adaptive Antibacterial and Promoted Osseointegration. *Chem. Eng. J.* **2022**, *435*, 134802. [CrossRef]
158. Verma, J.; Khanna, A.S. Digital Advancements in Smart Materials Design and Multifunctional Coating Manufacturing. *Phys. Open* **2023**, *14*, 100133. [CrossRef]

159. Song, E.; Li, J.; Rogers, J.A. Barrier Materials for Flexible Bioelectronic Implants with Chronic Stability—Current Approaches and Future Directions. *APL Mater.* **2019**, *7*, 050902. [CrossRef]
160. Ortigoza-DIaz, J.; Scholten, K.; Meng, E. Characterization and Modification of Adhesion in Dry and Wet Environments in Thin-Film Parylene Systems. *J. Microelectromech. Syst.* **2018**, *27*, 874–885. [CrossRef]
161. Pawlik, J.T.; Barrera, N.D.; Yoon, E.J.; Booth, J.C.; Long, C.J.; Orloff, N.D.; Meng, E.; Stelson, A.C. The Influence of Intrinsic Water and Ion Permeation on the Dielectric Properties of Parylene C Films. *IEEE J. Electromagn. RF Microw. Med. Biol.* **2023**, *7*, 328–335. [CrossRef]
162. Iqbal, Z.; Moses, W.; Kim, S.; Kim, E.J.; Fissell, W.H.; Roy, S. Sterilization Effects on Ultrathin Film Polymer Coatings for Silicon-Based Implantable Medical Devices. *J. Biomed. Mater. Res. B Appl. Biomater.* **2018**, *106*, 2327–2336. [CrossRef] [PubMed]
163. Lakkaraju, A.R.; Rao, J.M.; Gupta, K.K.; Ambat, R. Mechanistic Insight into Water Film Formation and Subsequent Corrosion-Linked Dendritic Growth on PCBs. *Corros. Sci.* **2025**, *246*, 112741. [CrossRef]
164. Hubert, J.; Mertens, J.; Dufour, T.; Vandencasteele, N.; Reniers, F.; Viville, P.; Lazzaroni, R.; Raes, M.; Terryn, H. Synthesis and Texturization Processes of (Super)-Hydrophobic Fluorinated Surfaces by Atmospheric Plasma. *J. Mater. Res.* **2015**, *30*, 3177–3191. [CrossRef]
165. Hoque, M.J.; Li, L.; Ma, J.; Cha, H.; Sett, S.; Yan, X.; Rabbi, K.F.; Ho, J.Y.; Khodakarami, S.; Suwala, J.; et al. Ultra-Resilient Multi-Layer Fluorinated Diamond like Carbon Hydrophobic Surfaces. *Nat. Commun.* **2023**, *14*, 4902. [CrossRef] [PubMed]
166. Liu, F.; Gong, R.; Duan, Z.; Wang, Z.; Zhou, J. Research on Vibration Reliability of Solder Joint Based on Modal Experiment of PCBA. *J. Mater. Sci. Mater. Electron.* **2025**, *36*, 43. [CrossRef]
167. Getz, M.N.; Ellingsen, A.; Dahl-Hansen, R.; Escobedo-Cousin, E.; Vereshchagina, E. Dielectric Breakdown and Reliability of Thin Film Insulators for High-Voltage Microelectromechanical Systems Applications. *Thin Solid Films* **2026**, *836*, 140876. [CrossRef]
168. Lei, W.S.; Mittal, K.; Yu, Z. Adhesion Measurement of Coatings on Biodevices/Implants: A Critical Review. *Rev. Adhes. Adhes.* **2016**, *4*, 367–396. [CrossRef]
169. Han, W.; Fang, F. Fundamental Aspects and Recent Developments in Electropolishing. *Int. J. Mach. Tools Manuf.* **2019**, *139*, 1–23. [CrossRef]
170. Huang, Y.; Wang, C.; Ding, F.; Yang, Y.; Zhang, T.; He, X.; Zheng, L.; Li, N. Principle, Process, and Application of Metal Plasma Electrolytic Polishing: A Review. *Int. J. Adv. Manuf. Technol.* **2021**, *114*, 1893–1912. [CrossRef]
171. Schorn, L.; Wilkat, M.; Lommen, J.; Borelli, M.; Muhammad, S.; Rana, M. Plasma Electrolytic Polished Patient-Specific Orbital Implants in Clinical Use—A Technical Note. *J. Pers. Med.* **2023**, *13*, 148. [CrossRef]
172. Ohki, M.; Takahashi, S.; Jinnai, R.; Hoshina, T. Interfacial Strength of Plasma-Sprayed Hydroxyapatite Coatings. *J. Therm. Spray Technol.* **2020**, *29*, 1119–1133. [CrossRef]
173. Nakagawa, S.; Cuthill, I.C. Effect Size, Confidence Interval and Statistical Significance: A Practical Guide for Biologists. *Biol. Rev.* **2007**, *82*, 591–605. [CrossRef]
174. Yu, Z.; Guindani, M.; Grieco, S.F.; Chen, L.; Holmes, T.C.; Xu, X. Beyond t Test and ANOVA: Applications of Mixed-Effects Models for More Rigorous Statistical Analysis in Neuroscience Research. *Neuron* **2022**, *110*, 21–35. [CrossRef]
175. Ding, Y.H.; Floren, M.; Tan, W. Mussel-Inspired Polydopamine for Bio-Surface Functionalization. *Biosurf. Biotribol.* **2016**, *2*, 121–136. [CrossRef]
176. Hofrichter, A.; Bulkin, P.; Drévillon, B. Plasma Treatment of Polycarbonate for Improved Adhesion. *J. Vac. Sci. Technol. A Vac. Surf. Films* **2002**, *20*, 245–250. [CrossRef]
177. Cen-Puc, M.; Schander, A.; Vargas-leason, M.G.; Lang, W. An Assessment of Surface Treatments for Adhesion of Polyimide Thin Films. *Polymers* **2021**, *13*, 1955. [CrossRef]
178. Münstedt, H.; Grossmann, J. Surface Modifications of Polyetheretherketone (PEEK): Results from the Literature and Special Studies of Copper-Coated Films. *Polymers* **2022**, *14*, 4797. [CrossRef]
179. Dimitriadi, M.; Panagiotopoulou, A.; Pelecanou, M.; Yannakopoulou, K.; Eliades, G. Stability and Reactivity of γ-MPTMS Silane in Some Commercial Primer and Adhesive Formulations. *Dent. Mater.* **2018**, *34*, 1089–1101. [CrossRef]
180. Hafeez, M.A.; Farooq, A.; Zang, A.; Saleem, A.; Deen, K.M. Phosphate Chemical Conversion Coatings for Magnesium Alloys: A Review. *J. Coat. Technol. Res.* **2020**, *17*, 827–849. [CrossRef]
181. Dini, C.; Costa, R.C.; Sukotjo, C.; Takoudis, C.G.; Mathew, M.T.; Barão, V.A.R. Progression of Bio-Tribocorrosion in Implant Dentistry. *Front. Mech. Eng.* **2020**, *6*, 1. [CrossRef]
182. *ASTM G119-09 (2021)*; Standard Guide for Determining Synergism Between Wear and Corrosion. ASTM International: West Conshohocken, PA, USA, 2021.
183. Thouless, M.D.; Hutchinson, J.W.; Liniger, E.G. Plane-Strain, Buckling-Driven Delamination of Thin Films: Model Experiments and Mode-II Fracture. *Acta Metall. Mater.* **1992**, *40*, 2639–2649. [CrossRef]
184. Lin, C.Y.; Lou, W.S.; Chen, J.C.; Weng, K.Y.; Shih, M.C.; Hung, Y.W.; Chen, Z.Y.; Wang, M.C. Bio-Compatibility and Bio-Insulation of Implantable Electrode Prosthesis Ameliorated by A-174 Silane Primed Parylene-C Deposited Embedment. *Micromachines* **2020**, *11*, 1064. [CrossRef]

185. Huff, M. Review Paper: Residual Stresses in Deposited Thin-Film Material Layers for Micro- and Nano-Systems Manufacturing. *Micromachines* **2022**, *13*, 2084. [CrossRef]
186. Li, C.; Cauwe, M.; Mader, L.; Schaubroeck, D.; de Beeck, M.O. Accelerated Hermeticity Testing of Biocompatible Moisture Barriers Used for the Encapsulation of Implantable Medical Devices. *Coatings* **2020**, *10*, 19. [CrossRef]
187. *ISO/TR 24971:2020*; Medical Devices—Guidance on the Application of ISO 14971. ISO: Geneva, Switzerland, 2020.
188. Baio, J.E.; Graham, D.J.; Castner, D.G. Surface Analysis Tools for Characterizing Biological Materials. *Chem. Soc. Rev.* **2020**, *49*, 3278–3296. [CrossRef]
189. *ASTM D3359-23*; Test Methods for Rating Adhesion by Tape Test. ASTM International: West Conshohocken, PA, USA, 2023.
190. Tonda-Turo, C.; Carmagnola, I.; Ciardelli, G. Quartz Crystal Microbalance with Dissipation Monitoring: A Powerful Method to Predict the in Vivo Behavior of Bioengineered Surfaces. *Front. Bioeng. Biotechnol.* **2018**, *6*, 158. [CrossRef]
191. Fan, H.; Guo, Z. Bioinspired Surfaces with Wettability: Biomolecule Adhesion Behaviors. *Biomater. Sci.* **2020**, *8*, 1502–1535. [CrossRef]
192. Jadhav, N.; Gelling, V.J. Review—The Use of Localized Electrochemical Techniques for Corrosion Studies. *J. Electrochem. Soc.* **2019**, *166*, C3461–C3476. [CrossRef]
193. Kravanja, K.A.; Finšgar, M. Analytical Techniques for the Characterization of Bioactive Coatings for Orthopaedic Implants. *Biomedicines* **2021**, *9*, 1936. [CrossRef]
194. *ASTM F1147-24*; Test Method for Tension Testing of Calcium Phosphate and Metallic Coatings. ASTM International: West Conshohocken, PA, USA, 2024.
195. *ASTM F1160-25*; Test Method for Shear and Bending Fatigue Testing of Calcium Phosphate and Metallic Medical and Composite Calcium Phosphate/Metallic Coatings. ASTM International: West Conshohocken, PA, USA, 2025.
196. Bull, S.J. Failure Modes in Scratch Adhesion Testing. *Surf. Coat. Technol.* **1991**, *50*, 25–32. [CrossRef]
197. Weibull, W. A Statistical Distribution Function of Wide Applicability. *J. Appl. Mech.* **1951**, *18*, 293–297. [CrossRef]
198. Chuangl, S.K.; Tian, L.; Wei, L.J.; Dodson, T.B. Kaplan-Meier Analysis of Dental Implant Survival: A Strategy for Estimating Survival with Clustered Observations. *J. Dent. Res.* **2001**, *80*, 2016–2020. [CrossRef] [PubMed]
199. Park, J.H.; Kim, Y.S.; Ryu, J.J.; Shin, S.W.; Lee, J.Y. Cumulative Survival Rate and Associated Risk Factors of Implantium Implants: A 10-Year Retrospective Clinical Study. *J. Adv. Prosthodont.* **2017**, *9*, 195–199. [CrossRef]
200. Liu, X.; Yu, L.; Xiao, A.; Sun, W.; Wang, H.; Wang, X.; Zhou, Y.; Li, C.; Li, J.; Wang, Y.; et al. Analytical Methods in Studying Cell Force Sensing: Principles, Current Technologies and Perspectives. *Regen. Biomater.* **2025**, *12*, rbaf007. [CrossRef]
201. Ghahari, S.M.; Davenport, A.J.; Rayment, T.; Suter, T.; Tinnes, J.P.; Padovani, C.; Hammons, J.A.; Stampanoni, M.; Marone, F.; Mokso, R. In Situ Synchrotron X-Ray Micro-Tomography Study of Pitting Corrosion in Stainless Steel. *Corros. Sci.* **2011**, *53*, 2684–2687. [CrossRef]
202. Pan, J. Synchrotron X-Ray Techniques for In Situ or Microscopic Study of Passive Films on Industrial Alloys: A Mini Review. *Corros. Mater. Degrad.* **2025**, *6*, 56. [CrossRef]
203. Decost, B.L.; Holm, E.A. A Computer Vision Approach for Automated Analysis and Classification of Microstructural Image Data. *Comput. Mater. Sci.* **2015**, *110*, 126–133. [CrossRef]
204. Anderson, M.J.; Basoalto, H.C. Automated Stereology and Uncertainty Quantification Considering Spherical Non-Penetrating Dispersions. *Crystals* **2023**, *13*, 464. [CrossRef]
205. Eliaz, N. Corrosion of Metallic Biomaterials: A Review. *Materials* **2019**, *12*, 407. [CrossRef] [PubMed]
206. Pszczółkowski, B.; Nowak, K.W.; Rejmer, W.; Bramowicz, M.; Dzadz, Ł.; Gałęcki, R. A Comparative Analysis of Selected Methods for Determining Young's Modulus in Polylactic Acid Samples Manufactured with the FDM Method. *Materials* **2022**, *15*, 149. [CrossRef] [PubMed]
207. Cyphert, E.L.; von Recum, H.A. Emerging Technologies for Long-Term Antimicrobial Device Coatings: Advantages and Limitations. *Exp. Biol. Med.* **2017**, *242*, 788–798. [CrossRef]
208. Chen, J.Y.; Penn, L.S.; Xi, J. Quartz Crystal Microbalance: Sensing Cell-Substrate Adhesion and Beyond. *Biosens. Bioelectron.* **2018**, *99*, 593–602. [CrossRef]
209. *ASTM F1980-21*; Standard Guide for Accelerated Aging of Sterile Barrier Systems and Medical Devices. ASTM International: West Conshohocken, PA, USA, 2021.
210. Escobar, L.A.; Meeker, W.Q. A Review of Accelerated Test Models. *Stat. Sci.* **2006**, *21*, 552–577. [CrossRef]
211. Lee, D.H.; Kim, C.H.; Youn, J.; Jeong, J. Evaluation Methods for Long-Term Reliability of Polymer-Based Implantable Biomedical Devices. *Biomed. Eng. Lett.* **2021**, *11*, 97–105. [CrossRef]
212. Padovani, A.; La Torraca, P.; Strand, J.; Larcher, L.; Shluger, A.L. Dielectric Breakdown of Oxide Films in Electronic Devices. *Nat. Rev. Mater.* **2024**, *9*, 607–627. [CrossRef]
213. Ható, Z.; Horváth, B.; Guba, S.; Tóth, Z.; Kocsis, E.; Boda, D.; Szalai, I. Electrochemical Migration and Dendrite Growth between Two Electrodes: Experiments and Brownian Dynamics Simulations. *Int. J. Heat Mass Transf.* **2024**, *234*, 126108. [CrossRef]

214. Lakkaraju, A.R.; Conseil-Gudla, H.; Bixenman, M.; Ambat, R. Reflow Solder Flux Residue and Humidity Interaction: Investigation Using Real PCBA Component Designs. *Sci. Rep.* **2025**, *15*, 22496. [CrossRef]
215. Selbmann, F.; Scherf, C.; Langenickel, J.; Roscher, F.; Wiemer, M.; Kuhn, H.; Joseph, Y. Impact of Non-Accelerated Aging on the Properties of Parylene C. *Polymers* **2022**, *14*, 5246. [CrossRef]
216. Boonpok, S.; Koonrungsrisomboon, K.; Suttiat, K.; Yavirach, P.; Boonyawan, D. Dissolution Behavior of Hydrothermally Treated Hydroxyapatite–Titanium Nitride Films Coated on PEEK: In Vitro Study. *J. Funct. Biomater.* **2022**, *13*, 99. [CrossRef] [PubMed]
217. Kohler, A.; Blendinger, F.; Müller, S.; Mescheder, U.; Bucher, V. Feasibility of Parylene C for Encapsulating Piezoelectric Actuators in Active Medical Implants. *Front. Med. Technol.* **2023**, *5*, 1211423. [CrossRef] [PubMed]
218. Bao, Y.; Muñoz, A.I.; Olsson, C.O.A.; Jolles, B.M.; Mischler, S. The Electrochemical Behavior of Ti in Human Synovial Fluids. *Materials* **2022**, *15*, 1726. [CrossRef]
219. *ASTM G3-14(2024)*; Practice for Conventions Applicable to Electrochemical Measurements in Corrosion Testing. ASTM International: West Conshohocken, PA, USA, 2024.
220. *ASTM G106-89(2023)*; Practice for Verification of Algorithm and Equipment for Electrochemical Impedance Measurements. ASTM International: West Conshohocken, PA, USA, 2023.
221. *ISO 16773-1:2016*; Electrochemical Impedance Spectroscopy (EIS) on Coated and Uncoated Metallic Specimens Part 1: Terms and Definitions. ISO: Geneva, Switzerland, 2016.
222. *ASTM G59-23*; Test Method for Conducting Potentiodynamic Polarization Resistance Measurements. ASTM International: West Conshohocken, PA, USA, 2023.
223. Bihade, M.S.; Patil, A.P.; Khobragade, N.K. Analysis of Electrochemical Current Noise from Metastable Pitting of SS304L in NaCl Solutions. *Trans. Indian Inst. Met.* **2013**, *66*, 155–161. [CrossRef]
224. Hallemans, N.; Howey, D.; Battistel, A.; Saniee, N.F.; Scarpioni, F.; Wouters, B.; La Mantia, F.; Hubin, A.; Widanage, W.D.; Lataire, J. Electrochemical Impedance Spectroscopy beyond Linearity and Stationarity—A Critical Review. *Electrochim. Acta* **2023**, *466*, 142939. [CrossRef]
225. Turnbull, A. Corrosion Pitting and Environmentally Assisted Small Crack Growth. *Proc. R. Soc. A Math. Phys. Eng. Sci.* **2014**, *470*, 20140254. [CrossRef]
226. Gaudin, L.F.; Wright, I.R.; Harris-Lee, T.R.; Jayamaha, G.; Kang, M.; Bentley, C.L. Five Years of Scanning Electrochemical Cell Microscopy (SECCM): New Insights and Innovations. *Nanoscale* **2024**, *16*, 12345–12367. [CrossRef]
227. Polcari, D.; Dauphin-Ducharme, P.; Mauzeroll, J. Scanning Electrochemical Microscopy: A Comprehensive Review of Experimental Parameters from 1989 to 2015. *Chem. Rev.* **2016**, *116*, 13234–13278. [CrossRef]
228. Bongiorno, V.; Gibbon, S.; Michailidou, E.; Curioni, M. Exploring the Use of Machine Learning for Interpreting Electrochemical Impedance Spectroscopy Data: Evaluation of the Training Dataset Size. *Corros. Sci.* **2022**, *198*, 110119. [CrossRef]
229. Laird, N.M.; Ware, J.H. Random-Effects Models for Longitudinal Data. *Biometrics* **1982**, *38*, 963–974. [CrossRef]
230. Starr, D.E.; Liu, Z.; Hävecker, M.; Knop-Gericke, A.; Bluhm, H. Investigation of Solid/Vapor Interfaces Using Ambient Pressure X-Ray Photoelectron Spectroscopy. *Chem. Soc. Rev.* **2013**, *42*, 5833–5857. [CrossRef] [PubMed]
231. Schnadt, J.; Knudsen, J.; Johansson, N. Present and New Frontiers in Materials Research by Ambient Pressure X-Ray Photoelectron Spectroscopy. *J. Phys. Condens. Matter* **2020**, *32*, 413003. [CrossRef] [PubMed]
232. Matsuda, H.; Matsui, F. 90°-Deflection Imaging Electron Analyzer for Measuring Wide 2D Angular Distribution and Perpendicular Spin Texture. *J. Electron Spectros. Relat. Phenom.* **2020**, *245*, 147001. [CrossRef]
233. Menteş, T.O.; Locatelli, A. Angle-Resolved X-Ray Photoemission Electron Microscopy. *J. Electron Spectros. Relat. Phenom.* **2012**, *185*, 323–329. [CrossRef]
234. Colombi, P.; Agnihotri, D.K.; Asadchikov, V.E.; Bontempi, E.; Bowen, D.K.; Chang, C.H.; Depero, L.E.; Farnworth, M.; Fujimoto, T.; Gibaud, A.; et al. Reproducibility in X-Ray Reflectometry: Results from the First World-Wide Round-Robin Experiment. *J. Appl. Crystallogr.* **2008**, *41*, 143–152. [CrossRef]
235. Chang, S.-L. Thin-Film Characterization by Grazing Incidence X-Ray Diffraction and Multiple Beam Interference. *J. Phys. Chem. Solids* **2021**, *62*, 1766–1775. [CrossRef]
236. Paunesku, T.; Vogt, S.; Maser, J.; Lai, B.; Woloschak, G. X-Ray Fluorescence Microprobe Imaging in Biology and Medicine. *J. Cell. Biochem.* **2006**, *99*, 1489–1502. [CrossRef]
237. Ghahari, M.; Krouse, D.; Laycock, N.; Rayment, T.; Padovani, C.; Stampanoni, M.; Marone, F.; Mokso, R.; Davenport, A.J. Synchrotron X-Ray Radiography Studies of Pitting Corrosion of Stainless Steel: Extraction of Pit Propagation Parameters. *Corros. Sci.* **2015**, *100*, 23–35. [CrossRef]
238. Harrell, F.E.; Lee, K.L.; Mark, D.B. Multivariable Prognostic Models: Issues in Developing Models, Evaluating Assumptions and Adequacy, and Measuring and Reducing Errors. *Stat. Med.* **1996**, *15*, 361–387. [CrossRef]
239. Joshi, S.; Urteaga, I.; Van Amsterdam, W.A.C.; Hripcsak, G.; Elias, P.; Recht, B.; Elhadad, N.; Fackler, J.; Sendak, M.P.; Wiens, J.; et al. AI as an Intervention: Improving Clinical Outcomes Relies on a Causal Approach to AI Development and Validation. *J. Am. Med. Inform. Assoc.* **2025**, *32*, 589–594. [CrossRef]

240. Jain, S.; Liechti, K.M.; Bonnecaze, R.T. Cohesive Zone Models to Understand the Interface Mechanics of Thin Film Transfer Printing. *J. Appl. Phys.* **2019**, *125*, 075301. [CrossRef]
241. Preston, S.P.; Wilkinson, R.D.; Clayton, R.H.; Chappell, M.J.; Mirams, G.R. Think before You Fit: Parameter Identifiability, Sensitivity and Uncertainty in Systems Biology Models. *Curr. Opin. Syst. Biol.* **2025**, *42*, 100563. [CrossRef]
242. Aldieri, A.; Curreli, C.; Szyszko, J.A.; La Mattina, A.A.; Viceconti, M. Credibility Assessment of Computational Models According to ASME V&V40: Application to the Bologna Biomechanical Computed Tomography Solution. *Comput. Methods Programs Biomed.* **2023**, *240*, 107727. [CrossRef]
243. Kann, L.; Sobotta, B.; Göb, R. Failure Prediction with Reporting Delay. *Qual. Reliab. Eng. Int.* **2018**, *34*, 1329–1338. [CrossRef]
244. Kaplan, E.L.; Meier, P. Nonparametric Estimation from Incomplete Observations. *J. Am. Stat. Assoc.* **1958**, *53*, 457–481. [CrossRef]
245. Katzman, J.L.; Shaham, U.; Cloninger, A.; Bates, J.; Jiang, T.; Kluger, Y. DeepSurv: Personalized Treatment Recommender System Using a Cox Proportional Hazards Deep Neural Network. *BMC Med. Res. Methodol.* **2018**, *18*, 24. [CrossRef]
246. Collins, G.S.; Reitsma, J.B.; Altman, D.G.; Moons, K.G.M. Transparent Reporting of a Multivariable Prediction Model for Individual Prognosis or Diagnosis (TRIPOD): The TRIPOD Statement. *J. Br. Surg.* **2015**, *102*, 148–158. [CrossRef] [PubMed]
247. Cox, D.R. Regression Models and Life-Tables. *J. R. Stat. Soc. Ser. B Methodol.* **1972**, *34*, 187–202. [CrossRef]
248. Fine, J.P.; Gray, R.J. A Proportional Hazards Model for the Subdistribution of a Competing Risk. *J. Am. Stat. Assoc.* **1999**, *94*, 496–509. [CrossRef]
249. Bergamo, E.T.P.; De Araújo-Júnior, E.N.S.; Lopes, A.C.O.; Coelho, P.G.; Zahoui, A.; Benalcázar Jalkh, E.B.; Bonfante, E.A.; Lerner, H. Failure Modes and Survival of Anterior Crowns Supported by Narrow Implant Systems. *BioMed Res. Int.* **2020**, *2020*, 1057846. [CrossRef]
250. Karniadakis, G.E.; Kevrekidis, I.G.; Lu, L.; Perdikaris, P.; Wang, S.; Yang, L. Physics-Informed Machine Learning. *Nat. Rev. Phys.* **2021**, *3*, 422–440. [CrossRef]
251. Wang, P.; Li, Y.; Reddy, C.K. Machine Learning for Survival Analysis: A Survey. *ACM Comput. Surv.* **2019**, *51*, 110. [CrossRef]
252. Ishwaran, H.; Kogalur, U.B.; Blackstone, E.H.; Lauer, M.S. Random Survival Forests. *Ann. Appl. Stat.* **2008**, *2*, 841–860. [CrossRef]
253. Kusne, A.G.; Yu, H.; Wu, C.; Zhang, H.; Hattrick-Simpers, J.; DeCost, B.; Sarker, S.; Oses, C.; Toher, C.; Curtarolo, S.; et al. On-the-Fly Closed-Loop Materials Discovery via Bayesian Active Learning. *Nat. Commun.* **2020**, *11*, 5966. [CrossRef]
254. Jones, D.R.; Schonlau, M.; Welch, W.J. Efficient Global Optimization of Expensive Black-Box Functions. *J. Glob. Optim.* **1998**, *13*, 455–492. [CrossRef]
255. Ritto, T.G.; Rochinha, F.A. Digital Twin, Physics-Based Model, and Machine Learning Applied to Damage Detection in Structures. *Mech. Syst. Signal Process.* **2021**, *155*, 107614. [CrossRef]
256. Stone, M. Cross-Validatory Choice and Assessment of Statistical Predictions. *J. R. Stat. Soc. Ser. B Methodol.* **1973**, *36*, 111–133. [CrossRef]
257. Van Calster, B.; McLernon, D.J.; Van Smeden, M.; Wynants, L.; Steyerberg, E.W.; Bossuyt, P.; Collins, G.S.; MacAskill, P.; Moons, K.G.M.; Vickers, A.J. Calibration: The Achilles Heel of Predictive Analytics. *BMC Med.* **2019**, *17*, 230. [CrossRef]
258. Lundberg, S.M.; Allen, P.G.; Lee, S.-I. A Unified Approach to Interpreting Model Predictions. In Proceedings of the 31st Conference on Neural Information Processing Systems (NIPS 2017), Long Beach, CA, USA, 4–9 December 2017; pp. 1–10.
259. Varma, S.; Simon, R. Bias in Error Estimation When Using Cross-Validation for Model Selection. *BMC Bioinform.* **2006**, *7*, 91. [CrossRef]
260. Gneiting, T.; Raftery, A.E. Strictly Proper Scoring Rules, Prediction, and Estimation. *J. Am. Stat. Assoc.* **2007**, *102*, 359–378. [CrossRef]
261. Gerds, T.A.; Schumacher, M. Consistent Estimation of the Expected Brier Score in General Survival Models with Right-Censored Event Times. *Biom. J.* **2006**, *48*, 1029–1040. [CrossRef]
262. *ASTM C633-24*; Test Method for Adhesion or Cohesion Strength of Thermal Spray Coatings. ASTM International: West Conshohocken, PA, USA, 2024.
263. Xu, P.; Ji, X.; Li, M.; Lu, W. Small Data Machine Learning in Materials Science. *npj Comput. Mater.* **2023**, *9*, 42. [CrossRef]
264. Taniike, T.; Takahashi, K. The Value of Negative Results in Data-Driven Catalysis Research. *Nat. Catal.* **2023**, *6*, 108–111. [CrossRef]
265. Hale, C. Basic Statistical Reporting for Articles Published in Biomedical Journals: Classic Methods Paper. *Int. J. Nurs. Stud.* **2015**, *52*, 4. [CrossRef]
266. Burzykowski, T. Survival Analysis: Methods for Analyzing Data with Censored Observations. *Semin. Orthod.* **2024**, *30*, 29–36. [CrossRef]
267. Box, G.E.P.; Wilson, K.B. On the Experimental Attainment of Optimum Conditions. In *Breakthroughs in Statistics*; Springer: New York, NY, USA, 1951. [CrossRef]
268. Benjaminit, Y.; Hochberg, Y. Controlling the False Discovery Rate: A Practical and Powerful Approach to Multiple Testing. *J. R. Stat. Soc. Ser. B Methodol.* **1995**, *57*, 289–300. [CrossRef]
269. Patricia Grambsch, B.M.; Therneau, T.M. Proportional Hazards Tests and Diagnostics Based on Weighted Residuals. *Biometrika* **1994**, *81*, 515–526. [CrossRef]

270. Smit, N.; Raubenheimer, L.; Mazzuchi, T.; Soyer, R. A Bayesian Generalized Eyring-Weibull Accelerated Life Testing Model. *Qual. Reliab. Eng. Int.* **2024**, *40*, 1110–1125. [CrossRef]
271. Bergstrand, M.; Söderlind, E.; Eriksson, U.G.; Weitschies, W.; Karlsson, M.O. A Semi-Mechanistic Modeling Strategy to Link in Vitro and in Vivo Drug Release for Modified Release Formulations. *Pharm. Res.* **2012**, *29*, 695–706. [CrossRef]
272. Killick, R.; Fearnhead, P.; Eckley, I.A. Optimal Detection of Changepoints with a Linear Computational Cost. *J. Am. Stat. Assoc.* **2012**, *107*, 1590–1598. [CrossRef]
273. Kalman, R.E. A New Approach to Linear Filtering and Prediction Problems. *J. Basic Eng.* **1960**, *82*, 35–45. [CrossRef]
274. Nelder, J.A.; Wedderburn, R.W.M. Generalized Linear Models. *R. Stat. Soc. J. Ser. A Gen.* **1972**, *370*, 370–384. [CrossRef]
275. Lawless, J.F. Negative Binomial and Mixed Poisson Regression. *Can. J. Stat.* **1987**, *15*, 209–225. [CrossRef]
276. Lambert, D. Zero-Inflated Poisson Regression, with an Application to Defects in Manufacturing. *Technometrics* **1992**, *34*, 1–14. [CrossRef]
277. Litjens, G.; Kooi, T.; Bejnordi, B.E.; Setio, A.A.A.; Ciompi, F.; Ghafoorian, M.; van der Laak, J.A.W.M.; van Ginneken, B.; Sánchez, C.I. A Survey on Deep Learning in Medical Image Analysis. *Med. Image Anal.* **2017**, *42*, 60–88. [CrossRef] [PubMed]
278. Baddeley, A.; Turner, R. Spatstat: An R Package for Analyzing Spatial Point Patterns. *J. Stat. Softw.* **2005**, *12*, 1–42. [CrossRef]
279. Le, T.C.; Penna, M.; Winkler, D.A.; Yarovsky, I. Quantitative Design Rules for Protein-Resistant Surface Coatings Using Machine Learning. *Sci. Rep.* **2019**, *9*, 265. [CrossRef]
280. Klemm, C.P.; Frömling, T. Machine Learning Assisted Analysis of Equivalent Circuit Usage in Electrochemical Impedance Spectroscopy Applications. *J. Comput. Chem.* **2024**, *45*, 1380–1389. [CrossRef]
281. McDonald, S.M.; Augustine, E.K.; Lanners, Q.; Rudin, C.; Catherine Brinson, L.; Becker, M.L. Applied Machine Learning as a Driver for Polymeric Biomaterials Design. *Nat. Commun.* **2023**, *14*, 4838. [CrossRef]
282. Chen, Y.; Chen, H.; Harker, A.; Liu, Y.; Huang, J. A Supervised Machine Learning Tool to Predict the Bactericidal Efficiency of Nanostructured Surface. *J. Nanobiotechnol.* **2024**, *22*, 748. [CrossRef]
283. Franci, G.; Falanga, A.; Galdiero, S.; Palomba, L.; Rai, M.; Morelli, G.; Galdiero, M. Silver Nanoparticles as Potential Antibacterial Agents. *Molecules* **2015**, *20*, 8856–8874. [CrossRef]
284. Gallo, J.; Holinka, M.; Moucha, C.S. Antibacterial Surface Treatment for Orthopaedic Implants. *Int. J. Mol. Sci.* **2014**, *15*, 13849–13880. [CrossRef]
285. Li, Y.; Rodrigues, J.; Tomás, H. Injectable and Biodegradable Hydrogels: Gelation, Biodegradation and Biomedical Applications. *Chem. Soc. Rev.* **2012**, *41*, 2193–2221. [CrossRef] [PubMed]
286. Robinson, J.; Walsht, F.C. In Situ Synchrotron X-Ray Techniques for Studies of Corrosion of Metals. *Corros. Sci.* **1993**, *35*, 791–800. [CrossRef]
287. Murbach, M.; Gerwe, B.; Dawson-Elli, N.; Tsui, L. Impedance.Py: A Python Package for Electrochemical Impedance Analysis. *J. Open Source Softw.* **2020**, *5*, 2349. [CrossRef]
288. Sadeghi, M.A.; Zhang, R.; Hattrick-Simpers, J. AutoEIS: Automated Equivalent Circuit Modeling from Electrochemical Impedance Spectroscopy Data Using Statistical Machine Learning. *J. Open Source Softw.* **2025**, *10*, 6256. [CrossRef]
289. Yrjänä, V. DearEIS—A GUI Program for Analyzing Impedance Spectra. *J. Open Source Softw.* **2022**, *7*, 4808. [CrossRef]
290. Davidson-Pilon, C. Lifelines: Survival Analysis in Python. *J. Open Source Softw.* **2019**, *4*, 1317. [CrossRef]
291. Pölsterl, S. Scikit-Survival: A Library for Time-to-Event Analysis Built on Top of Scikit-Learn. *J. Mach. Learn. Res.* **2020**, *21*, 1–6.
292. Kvamme, H.; Borgan, Ø.; Scheel, I. Time-to-Event Prediction with Neural Networks and Cox Regression. *J. Mach. Learn. Res.* **2019**, *20*, 1–30.
293. Nagpal, C.; Potosnak, W.; Dubrawski, A. Auton-Survival: An Open-Source Package for Regression, Counterfactual Estimation, Evaluation and Phenotyping with Censored Time-to-Event Data. In Proceedings of the 7th Machine Learning for Healthcare Conference, Durham, NC, USA, 5–6 August 2022; Volume 182.
294. Jackson, C.H. Flexsurv: A Platform for Parametric Survival Modeling in R. *J. Stat. Softw.* **2016**, *70*, 1–33. [CrossRef]
295. Ward, L.; Dunn, A.; Faghaninia, A.; Zimmermann, N.E.R.; Bajaj, S.; Wang, Q.; Montoya, J.; Chen, J.; Bystrom, K.; Dylla, M.; et al. Matminer: An Open Source Toolkit for Materials Data Mining. *Comput. Mater. Sci.* **2018**, *152*, 60–69. [CrossRef]
296. Ong, S.P.; Richards, W.D.; Jain, A.; Hautier, G.; Kocher, M.; Cholia, S.; Gunter, D.; Chevrier, V.L.; Persson, K.A.; Ceder, G. Python Materials Genomics (Pymatgen): A Robust, Open-Source Python Library for Materials Analysis. *Comput. Mater. Sci.* **2013**, *68*, 314–319. [CrossRef]
297. Facebook, M.B.; Facebook, B.K.; Facebook, D.R.J.; Facebook, S.D.; Facebook, B.L.; Wilson, A.G.; Facebook, E.B. BOTORCH: A Framework for Efficient Monte-Carlo Bayesian Optimization. In Proceedings of the Advances in Neural Information Processing Systems 33 (NeurIPS 2020), Virtual, 6–12 December 2020.
298. Herman, J.; Usher, W. SALib: An Open-Source Python Library for Sensitivity Analysis. *J. Open Source Softw.* **2017**, *2*, 97. [CrossRef]
299. Baudin, M.; Dutfoy, A.; Iooss, B.; Popelin, A.-L. OpenTURNS: An Industrial Software for Uncertainty Quantification in Simulation. In *Handbook of Uncertainty Quantification*; Springer International Publishing: Berlin/Heidelberg, Germany, 2015; pp. 1–38. [CrossRef]

300. Van Der Walt, S.; Schönberger, J.L.; Nunez-Iglesias, J.; Boulogne, F.; Warner, J.D.; Yager, N.; Gouillart, E.; Yu, T. Scikit-Image: Image Processing in Python. *PeerJ* **2014**, *2*, e453. [CrossRef]
301. Carpenter, A.E.; Jones, T.R.; Lamprecht, M.R.; Clarke, C.; Kang, I.H.; Friman, O.; Guertin, D.A.; Chang, J.H.; Lindquist, R.A.; Moffat, J.; et al. CellProfiler: Image Analysis Software for Identifying and Quantifying Cell Phenotypes. *Genome Biol.* **2006**, *7*, R100. [CrossRef] [PubMed]
302. Guyer, J.E.; Wheeler, D.; Warren, J.A. FiPy: Partial Differential Equations with Python. *Comput. Sci. Eng.* **2009**, *11*, 6–15. [CrossRef]

**Disclaimer/Publisher's Note:** The statements, opinions and data contained in all publications are solely those of the individual author(s) and contributor(s) and not of MDPI and/or the editor(s). MDPI and/or the editor(s) disclaim responsibility for any injury to people or property resulting from any ideas, methods, instructions or products referred to in the content.